UNIVERSITA' DEGLI STUDI DI MILANO

Dipartimento di Biotecnologie Mediche e Medicina Traslazionale

Scuola di dottorato in Medicina Sperimentale e Biotecnologie Mediche

Ciclo XXIX

THE HUMAN-RESTRICTED DUPLICATED FORM OF THE α7 NICOTINIC ACETYLCHOLINE RECEPTOR, CHRFAM7A: TRANSCRIPTIONAL REGULATION, ROLE IN INFLAMMATION AND POTENTIAL PHARMACOLOGICAL IMPLICATIONS.

Settore disciplinare: Bio/14

Tesi di dottorato di:

Annalisa Maroli

Relatore: Prof.ssa Grazia Pietrini

Coordinatore: Prof. Massimo Locati

Anno accademico: 2016-2017

Contents

Abstract

The α7 nicotine acetylcholine receptor (α7nAChR, CHRNA7) is a homo-pentameric ligand-gated ion channel widely expressed in the Central Nervous System (CNS). Recent evidence has demonstrated its expression also in non-neuronal tissues, including monocytes and macrophages, where it mediates the Cholinergic Anti-Inflammatory Pathway, a neuronal reflex providing the central control of systemic inflammation.

Recently, the human-restricted duplicated gene of the α7nAChR, called CHRFAM7A (α7dup) has been discovered. It is the product of the partial duplication and fusion of exon 5-10 of CHRNA7 gene with the novel exons D, C, B and A belonging to the FAM7A gene, of unknown function. The CHRFAM7A gene is expressed in human immune cells and in the CNS and is translated into two proteins, of 45 kDa and 36 kDa, which are the result of alternative splicing. The α7dup protein assembles with the α7 conventional subunits and exerts a dominant negative regulation on the α7nAChR function. The importance of the α7dup protein in the human inflammatory process has been confirmed by the demonstration of its responsiveness to pro-inflammatory stimuli: indeed, the Lipopolysaccharide (LPS) treatment of THP-1 monocytic cells and of human primary monocytes and macrophages down-regulates CHRFAM7A transcript and protein through a transcriptional mechanism reliant on the NF-κB transcription factor. Moreover, unpublished data demonstrated that LPS has the opposite effect on the α7 transcript in monocytes and macrophages, leading to CHRNA7 up-regulation.

In this study, we have investigated the transcriptional mechanisms leading to CHRFAM7A expression in the THP-1 monocytic cells and in neuroblastoma SH-SY5Y cells and we demonstrate that the CHRFAM7A gene is endowed with several complex transcriptional mechanisms leading to fine expression modulation, including the presence of alternative and tissue-specific Transcription Start Site (TSS), alternative splicing mechanism, tissue-specific transcriptional elements and intronic silencer elements. Moreover, we demonstrated that the CHRFAM7A down-regulation exerted by LPS involve the chromatin remodeling of CHRFAM7A promoter in THP-1 cells.

Increasing evidence has linked CHRNA7 expressional and functional dysregulation to several neurodegenerative disorders, including Alzheimer's disease. The treatment with the acetylcholinesterase inhibitor Donepezil is effective in temporary ameliorating the cognitive symptoms of AD, by increasing the synaptic levels of ACh and counteracting the cholinergic loss, which is characteristic of AD. However, emerging findings sustained that Donepezil can exert its therapeutic effect also by modulating the immune response and potentiating the Cholinergic Anti-Inflammatory Pathway.

So far, the role of CHRFAM7A gene in AD pathogenesis or pharmacological response has not been elucidated. In the present study, we have investigated the expression profile of CHRNA7 and CHRFAM7A genes in human nervous and immune tissues obtained from AD patients, highlighting expressional alterations of both the α7 conventional and duplicated form. Moreover, we have investigated the effect of the AChEI Donepezil on CHRFAM7A and CHRNA7 transcription in THP-1 cells, human primary macrophages and SH-SY5Y cells, collecting new insights about the possible role of the α7dup gene as a pharmacological target in AD therapy.

1. Introduction

1.1. Inflammation

The inflammatory process is the host's physiological response to noxious stimuli or pathogens invasion and is directed to the elimination of the infectious agents and the restoring of the homeostatic condition. Inflammation is mainly triggered by the cells of the innate immune system, such as macrophages or granulocytes, and is sustained by the production of several soluble inflammatory mediators, such as cytokines or chemokines.

Inflammation is scholastically distinguished into an *acute* and *chronic* response: the acute inflammation, once the infectious agent is destroyed, resolves; otherwise, if the triggering stimulus persists, the response could evolve into a chronic process, in which the immunological mechanisms of elimination and repair contribute to exacerbate the tissue damage (Medzhitov, 2008).

1.1.1. Acute inflammation

Acute inflammation is a rapid, stereotyped and non-specific process that could be elicited by any injurious agent, such as a trauma or bacterial or viral infection (**Fig. 1.1**).

The first events during an inflammatory process are vascular changes in flow, caliber and permeability, in order to promote the formation of an exudate, which drive the circulating granulocytes (neutrophils, basophils and eosinophils) to the site of injury, generating a *local inflammatory response*.

Many bacterial components, such as lipoproteins and glycolipids, are able to induce a local inflammation. On the other hand, many different cell types in the host's mucosa and skin respond to the bacterial invasion by producing molecules that control the infection. Among these, the mast cells produce histamine, serotonin, *Tumor Necrosis factor* α (TNFα) and other pro-inflammatory cytokines, such as *Interleukin-1* (IL-1) and

Interleukine-6 (IL-6), which also have a systemic effect (Medzhitov, 2008). The release of pro-inflammatory cytokines and chemokines from the site of invasion has many complementary effects: (i) it induces the activation of the complement cascade, that opsonizes the pathogens and stimulates the phagocytosis; (ii) it recruits the granulocytes, which directly eliminate the pathogens and amplify the inflammatory process by producing pro-inflammatory mediators; (iii) it promotes the recruitment, differentiation and activation of circulating monocytes in macrophages and (iv) activates the tissue-resident macrophages (Turner et al., 2014).

The macrophages, as other immune cells, are provided with specific receptors, called *Pattern Recognition Receptors* (PRR), which recognize particular bacterial structures, defined as *Pathogen-associated Molecular Patterns* (PAMP) (Shi and Palmer, 2011; Davies et al., 2014). Once activated, the macrophages (i) directly eliminate the pathogens by phagocytosis, (ii) release Reactive Oxygen Intermediates (ROS), nitric oxide (NO) and lysosomes enzymes, (iii) sustain the inflammation by producing pro-inflammatory cytokines and (iv) act as *Antigen Presenting Cells* (APC) in order to recruit the acquired immune system (Davies et al., 2014). During inflammation, one of the most important function of macrophages is the production of pro-inflammatory cytokines such as IL-1, IL-6, TNFα, the High Mobility Group Box-1 (HMGB1) and the Interferon γ (INF-γ) (Serbina et al., 2008). All these cytokines act locally by promoting coagulation and increased expression of adhesion molecules by the endothelium, thus supporting the sustainment of the inflammatory process. Moreover, they act back upon macrophages, enhancing the phagocytic activity and chemokines production (Turner et al., 2014).

The cytokines produced by the macrophages exert also systemic effects: when produced in large amount, they promote endocrine functions, inducing fever, cachexia and the production of *Acute Phase Proteins* (APP), such as the fibrinogen and the C-reactive protein (Sica and Mantovani, 2012).

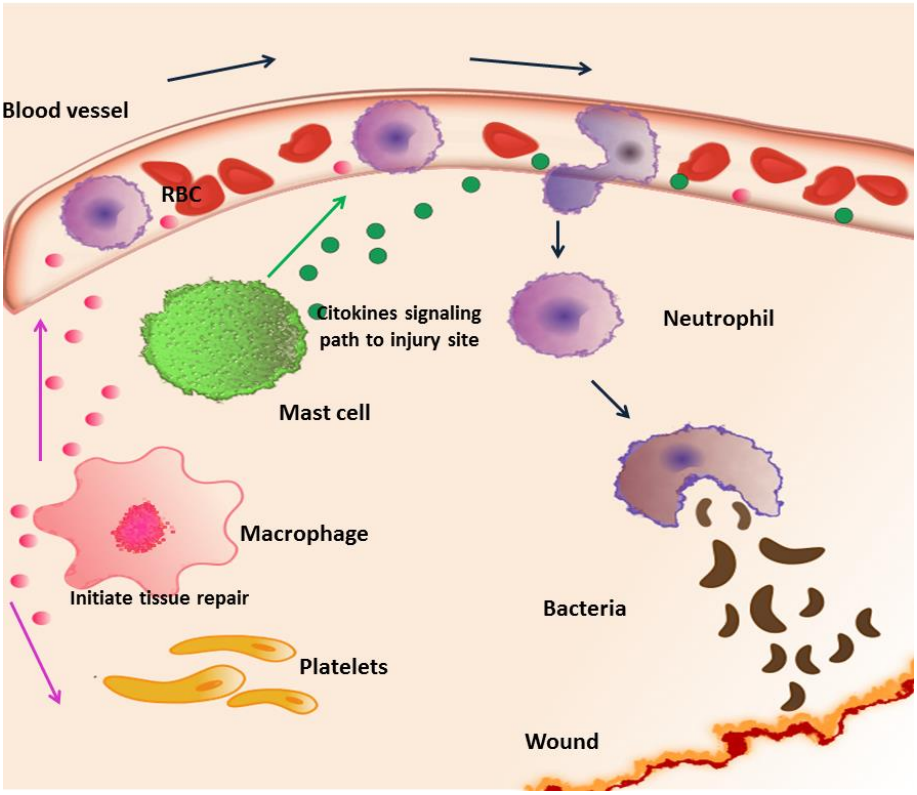

Figure 1.1: **Schematic representation of the inflammatory process**. During inflammation, innate immune cells, such as granulocytes and macrophages are recruited at the site of infection: the concomitant secretion at the infection site of cytokines and chemokines and expression of particular receptors by immune cells result in a complicated process of adhesion and extravasation, which allows the circulating monocytes and granulocytes to reach the inflammation site. The mast cells and macrophages release pro-inflammatory cytokines in order to amplify the inflammatory response. At the same time, macrophages produce also soluble mediators that begin the process of tissue repair.

1.1.2. Molecular mechanisms of acute inflammation

Macrophages are able to distinguish the pathogens by recognizing repetitive molecular structures on their surface, for example the lipotecoic acid of gram-positive bacteria and lipopolysaccharide (LPS) of gram-negative bacteria. The recognition is driven by specific immune receptors, called Pattern Recognition Receptors (PRR). One of the most important classes of PRR is that of the Toll-like receptors (TLRs). Of all TLRs, macrophages express in particular TLR-4, which is able to bind the LPS released in the blood by the gram-negative bacteria. The circulating LPS is bound by a particular soluble molecule, named LPS-Binding-Protein (LBP). The interaction between the complex LPS-LBP and TLR4

occurs with the cooperation of other two receptors, CD14 and MD-2. TLR4 is a key receptor in the innate immune response, because it is able to elicit the Nuclear Factor κB (NF-κB) pathway (Lu et al., 2008).

NF-κB is a crucial transcription factor in the inflammatory process and is involved in the transcriptional regulation of many genes that encode for cytokines and chemokines. It is widely expressed in many tissues and in particular in the immune system. NF-κB can act as homodimer or heterodimer generated from combinations of five Rel family proteins (RelA, or p65, c-Rel, RelB, p50 and p52) (**Fig. 1.2A**).

NF-κB can be involved into two different pathways, the canonical (or classical) pathway and the non-canonical pathway, which differ for the receptors activated and the NF-κB subunits involved: in particular, RelA and p50 are constituents of the canonical NF-κB pathway.

The classical NF-κB pathway is elicited by cytokines, such as IL-1 or TNF-α, or bacterial components such as LPS (Hayden and Gosh, 2004). When inactive, the heterodimer RelA:p50 is retained into the cytoplasm by the interaction with the inhibitor protein IκB, that masks the nuclear import signal. The signalling elicited by cytokines or LPS results in IκB protein ubiquitination and degradation, followed by NF-κB RelA:p50 relocation in the nucleus and binding to particular consensus sequences, named κB sequences, in the promoter of the target genes. The classical NF-κB heterodimer RelA:p50 is generally thought to promote, rather than repress, the transcription, also by recruiting several co-transcription factors or chromatin-remodeling factors, such as p300 or CBP (Pereira and Oakley, 2008; Zhong et al., 2002). Among other genes whose transcription is induced by RelA:p50 there is also IκB, thus providing a robust negative feedback mechanism (Pereira and Oakley, 2008; Wessels et al., 2004). The RelA:p50 function is straight regulated at several levels, including post-translational modifications: it is known, for example, that phosphorylation at Thr435 influences the interaction of RelA with HDAC1 (O'Shea and Perkins, 2010) and phosphorylation at Ser276 increases CBP binding to RelA (Zhong et al., 1998, 2002). On the other hand, the homodimer p50:p50 is generally considered as an inhibitor of transcription, as the p50 subunit lacks the transactivation domain: there is evidence that it is able to bind the promoter sequences and repress transcription either by recruiting HDAC1 or by avoiding the binding of the canonical NF-κB heterodimer

(Elsharkawy et al., 2010). p50:p50 homodimer is able to bind nucleosomes as well as nude DNA (Angelov et al., 2004) and its binding is predominantly observed in "unstimulated" or "resting" cells complexed with HDAC1 and other epigenetic repressors (Kang et al., 1992): after stimulation (LPS, TNF-α), NF-κB dimers, containing phosphorylated p65 and complexed with CBP/p300, are recruited to the DNA, where they displace p50 homodimers and initiate the NF-κB-dependent transcription (Zhong et al., 2002).

The non-canonical pathway, instead, results in the activation of the RelB and p52 NF-κB complex and is activated by alternative receptors, such as CD40. This non-canonical NF-κB pathway relies on a mechanism, which involved the inducible degradation of the precursor of p52, p100. The non-canonical NF-κB pathway is more specific than the canonical one and is thought to regulate important biological functions, such as lymphoid organogenesis, B cell maturation and differentiation and dendritic cell activation (Sun, 2011). The heterodimer composed by RelB and p52 is able to either activate or repress transcription, as p52 lacks the transactivation domain (Hayden and Gosh, 2004) (**Fig. 1.2B**).

During a gram-negative infection, the LPS released from bacteria is primary bound by the CD-14 receptor on the surface of the macrophages and this complex is then recognized by TLR4. TLR4 is involved in two different intra-cellular pathways: the Myd-88-dependent pathway and the Myd-88-indipendent pathway. The Myd-88-dependent pathway is known to activate the NF-κB canonical pathway through the adaptor Myd-88 and the activation of the IKK kinase. Once activated, IKK triggers the phosphorylation and consequent proteasomal degradation of IκB, which binds and sequesters NF-κB in the cytosol. The degradation results in the binding of the canonical complex to the specific binding sequences on the target gene promoters (Fitzgerard et al., 2004) (**Fig. 1.2C**). In addition to the canonical NF-κB pathway, LPS has been described to activate also the NF-κB non-canonical pathway through the activation of TLR4 signaling (Yamamoto et al., 2003). The Myd-88-independent pathway is classically thought to activate the IRF3 transcription factor, but recently it has been also proved that is able to activate the late phase p65:p50 NF-κB subunits (Yamamoto et al., 2003).

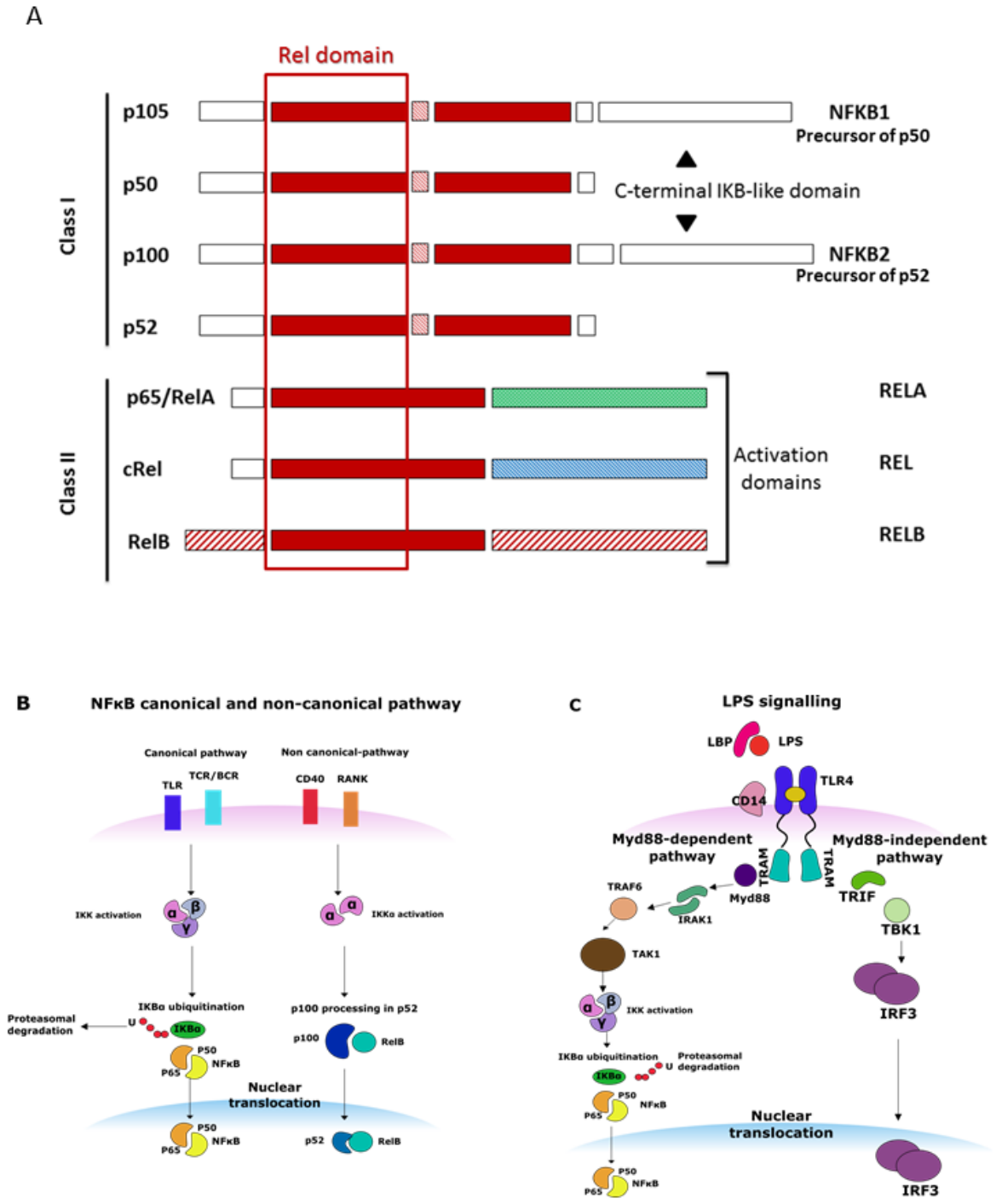

Figure 1.2: Representation of the NF-κB gene family, of the canonical and non-canonical NF-κB pathway, and of the LPS signaling. (A) All five components of NF-κB family are characterized by a conserved Rel domain, highlighted in red, which is responsible of nuclear localization and DNA binding. (B) NF-κB Canonical and Non canonical pathways: the canonical pathway is triggered by several receptors, including TLRs and TCR or BCR receptors and culminates in IKK activation, which phosphorylates and induces the degradation of the inhibitor IKβα, thus leading to the RelA/p50 nuclear translocation; the non-canonical

pathway is instead activated by different receptors, such as CD40 and RANK and is characterized by the activation of IKKα, which promotes the processing of the NF-κB subunit p100 in p52, followed by p52/RelB nuclear translocation. Representation of the NF-κB family proteins. (C) Schematic representation of the LPS-induced signalling. The LPS activates the TLR4 receptor expressed by the innate immunity cells such as monocytes or macrophages, thus activating two different pathways, known as the Myd88-dependend and –independent pathways. The Myd88-dependent pathway leads to the nuclear translocation of the NF-κB transcription factor, while the Myd88-independent pathway induces the activation of IRF3.

1.1.3. Resolution of acute inflammation

Once the infectious agent causing inflammation has been removed, the acute inflammatory process must undergo resolution, in order to avoid tissue damage. Acute inflammation is self-limiting and normally results in tissue restoration and repair.

The first step in resolution of inflammation is neutrophils apoptosis followed by their phagocytosis by other inflammatory cells, such as macrophages (Savill et al., 1989). The mechanisms driving neutrophils apoptosis are still poorly understood: it is known however that macrophages play a key role, by releasing soluble death signals (such as NO) which induce neutrophil apoptosis (Maskrey et al., 2010). The uptake of apoptotic cells stimulates macrophages to release anti-inflammatory cytokines. These cells undergo a functional switch: they quit producing pro-inflammatory cytokines, such as IL-1 and IL-6, and begin producing anti-inflammatory cytokines, such as IL-10 and Transforming Growth Factor β (TGF-β), which has also reparative properties that help the damaged tissues repair. The production of anti-inflammatory cytokines by macrophages and other immune cells is typical of alternatively activated M2 macrophages, which are mainly involved in restoring tissue homeostasis and are weak antigen presenting cells, thus inhibiting Th1 response and supporting the Th2 response (Sica and Mantovani, 2002).

Other important events, that contribute to restore the homeostasis, are the chemokines depletion and the switch of eicosanoids (Ortega-Gómez et al., 2012).

Although the molecular events driving resolution of inflammation are still almost unknown, the current opinion sustains that these mechanisms are switch off during the early onset of inflammation (Serhan and Savill, 2005).

During the resolution of inflammation, the NF-κB transcription factor plays an anti-inflammatory role, by promoting the transcription of anti-inflammatory cytokines and proteins involved in leukocytes apoptosis. Indeed, inhibition of NF-κB during the resolution phase has been shown to protract the inflammatory response and prevent the leukocyte clearance; however, the mechanisms involved in the inflammatory resolution role of NF-κB are still largely unknown (Lawrence and Fong, 2010).

1.1.4. Chronic inflammation

Persistent inflammatory stimuli or dysregulation in the mechanism of resolution of inflammation can result in chronic inflammation, which may last for weeks or even years and is commonly considered as a risk factor for the development of many diseases such as cancer, metabolic diseases, cardiovascular pathologies and neurodegenerative disorders, including Alzheimer's disease.

Chronic inflammation is principally driven by tissue-resident macrophages: indeed, during the acute inflammatory response, these cells physiologically substitute the neutrophils infiltrate at the site of infection. If the intervention of tissue-resident macrophages is still insufficient to eliminate the noxious stimuli, they begin to chronically elaborate low levels of TNF-α and IL-1 (Maskrey et al., 2010), leading to chronic inflammation onset, which may involve the formation of granuloma and tertiary lymphoid tissues (Medzhitov, 2008).

1.2. The Cholinergic Anti-Inflammatory Pathway

The immune system response to pathogens, during the inflammatory process, is regulated by neural reflex circuits (Tracey, 2002).

Inflammation is perceived by the Central Nervous System (CNS) through different routes, including specialized cells in brain vasculature, choroid plexus and circumventricular organs, and through TLRs and cytokines receptors in the brain (Goehler et al., 2000; Tanga et al., 2005; Boettger et al., 2008).

The “inflammatory reflex” is an anti-inflammatory response composed by a sensory arc, represented by the afferent arm of the Vagus nerve, and by an efferent arc, which is represented by the motor arms of the same nerve (Olofosson et al., 2012) (**Fig. 1.3**).

The afferent neurons of the Vagus nerve express IL-1β and prostaglandins receptors (Ek et al., 1998) and transmit the “danger” signals from the periphery to the Nucleus Tractus Solitarius (NTS), which is interconnected with the dorsal motor nucleus, where the majority of efferent Vagus nerve fiber originate. Afferent signals also reach central neurons that project to the hypothalamus: these projections are important for the regulation of the behavioral and hormonal characteristic of inflammation, such as cachexia, fever and the production of glucocorticoid (Goehler et al., 2000).

Once activated, the cholinergic efferent fibers of the cervical Vagus nerve transmit the output signals through the celiac ganglion and splenic nerve to the spleen, which is the principal target organ of the inflammatory reflex (Rosas-Ballina et al., 2008; Huston et al., 2006, 2008). Indeed, both pharmacological and electrical stimulation of the Vagus nerve reduce pro-inflammatory cytokines level and TNF-α production in the red pulp of the spleen (Bororikova et al., 2000).

Each component of the efferent arc of the inflammatory reflex is essential for its anti-inflammatory effect: in fact, the surgical ablation of the cervical Vagus Nerve prevents the systemic TNF-α decrease driven by the motor arc (Bernik et al., 2002), but also the removal of the splenic nerve abolishes the inhibitory effect of Vagus nerve stimulation on splenic TNF-α production (Vida et al., 2011). At the same time, splenectomy reduces the anti-inflammatory signal driven by the splenic nerve (Huston et al., 2006, 2008).

The splenic nerve has catecholaminergic terminations, which release norepinephrine to T-cell-rich areas of the spleen. Indeed, also catecholamine depletion with reserpine results in abrogation of the anti-inflammatory effect of vagal nerve stimulation (Huston et al., 2008).

The norepinephrine released by the catecholaminergic terminations of the splenic nerve interacts with specific β2-adrenergic (β2-AR) receptors expressed by a selective population of T-cells of the red pulp of the spleen. The involvement of β2-AR in mediating the vagal output was demonstrated by the inhibitory effect of β-adrenergic, but not α-

adrenergic, antagonist on TNF-α decrease after Vagus nerve stimulation (Kees et al., 2003).

T-cells can also express the Choline Acetyltransferase (ChAT) enzyme and synthetize acetylcholine (ACh). The ChAT+ T cells represent a small population among the CD4+ cells, covering only 1% of the entire population of the spleen, while in the Peyer's plaque they reach about 10%. When activated, the ChAT+ T cells show a Th2 phenotype, releasing principally IL-10 and attenuating macrophage cytokines production in the spleen (Elenkov et al., 2000). The integrity of the inflammatory reflex also relies on the action of this T-cell population, as T-cells nude mice showed an impaired anti-inflammatory response after Vagus nerve stimulation (Rosas-Ballina et al., 2011).

When the norepinephrine binds the β2-AR, ChAT+ T cells synthetize and release ACh. The ACh exerts an anti-inflammatory effect, decreasing the level of pro-inflammatory cytokines (**Fig. 1.3**).

Because of the involvement of the Vagus nerve and the cholinergic system the inflammatory reflex was named "Cholinergic Anti-Inflammatory Pathway" (Pavlov et al., 2003; Rosas-Ballina and Tracey, 2009).

For long time the link between the release of ACh and the consequent anti-inflammatory response has been missed.

ACh targets both the nicotinic (ionotropic) and muscarinic (metabotropic) receptors. The muscarinic receptors are G protein-coupled receptors further classified in five subtypes (M1-M5) (Caulfield and Birdsell, 1998), while nicotinic receptors are homo- or hetero-pentameric ligand-gated ion channel composed by different subunits (α1- α10; β1-β4; δ, γ and ε) (Lindstrom, 1997). Both muscarinic and nicotinic receptors are widely distributed in the CNS and in immune cells (Pavlov and Tracey, 2004). However, while the agonist of nicotinic receptors, nicotine, determines a strong reduction of TNF-α level in endotoxin-stimulated human primary macrophages, muscarine is less effective (Bororikova et al., 2000), indicating the involvement of the acetylcholine nicotinic receptors.

Few years after the discovery of the expression of the α7 nicotinic acetylcholine receptor (α7nAChR) by human macrophages (Wang et al., 2003), the role of this receptor in mediating the Cholinergic Anti-Inflammatory Pathway was postulated.

This receptor is indeed crucial for the integrity of the inflammatory reflex: in fact, antisense oligonucleotides targeting the α7nAChR abolished the nicotine-induced TNF-α inhibition in endotoxin-stimulated human macrophages (Wang et al., 2003), and knock-out mice for the α7 subunit failed to reduce TNF-α serum level after electric vagal stimulation (Wang et al., 2003). Moreover, the anti-inflammatory effect of acetylcholine can be counteracted by selective α7nAChR antagonists (Tracey, 2002; Wang et al., 2003; Ulloa, 2005), while selective agonists reduce the pro-inflammatory cytokines produced by macrophages in animal models of pancreatitis (van Westerloo et al., 2006), dextran sulfate sodium (DSS)-induced colitis (Ghia et al., 2006) and intestinal ileus (The et al., 2007).

The α7nAChR modulates the levels of another important pro-inflammatory cytokine, HMGB1, which is one of the most promising target molecules for the treatment of several inflammatory diseases, including severe sepsis (Czura et al., 2004). Acetylcholine, and more effectively nicotine, has an inhibitory effect on the release of HMGB1 in endotoxin-stimulated murine macrophages and the inhibition is counteracted by selective nicotinic antagonist (Wang et al., 2004). The α7nAChR decreases HMGB1 levels through a post-translational mechanism, by inhibiting NF-κB function and avoiding HMGB1 translocation from the nucleus to the cytoplasm (Wang et al., 2004).

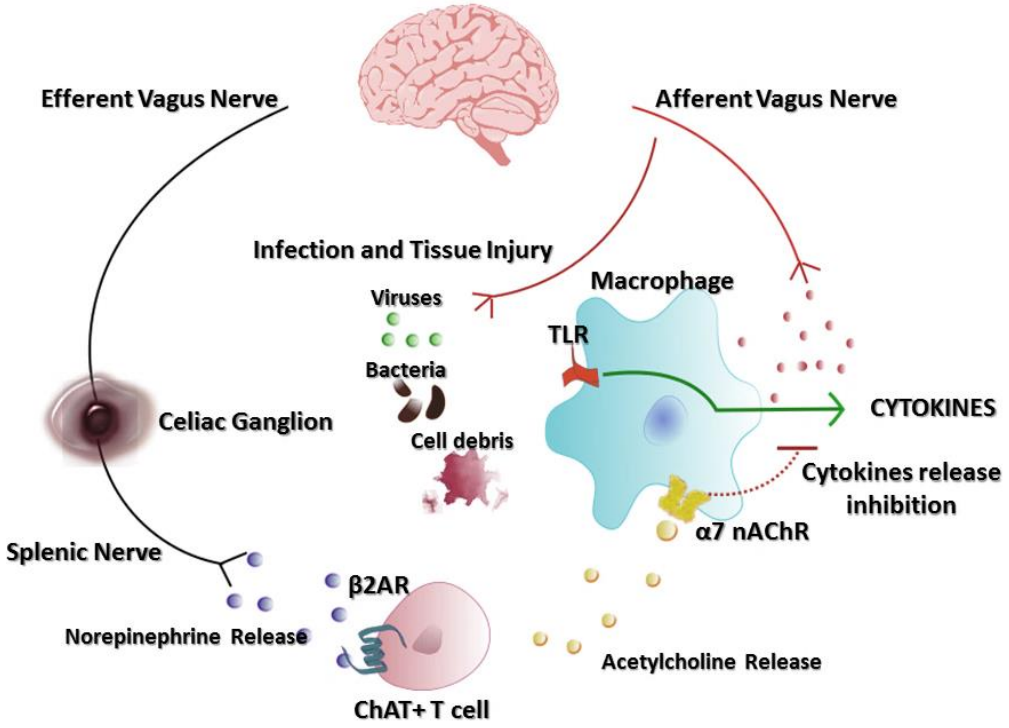

Figure 1.3: The Cholinergic Anti-Inflammatory Pathway. The Cholinergic Anti-Inflammatory Pathway involves the afferent and efferent branches of the Vagus Nerve. The afferent fibers activate the Nucleus Tractus Solitarius, which responds releasing norepinephrine from the vagal splenic terminations. Norepinephrine induces ACh secretion by the T cells in the spleen and ACh binds to the α7nAChR expressed by macrophages, thus inducing an anti-inflammatory response.

1.3. The α7 nicotinic acetylcholine receptor

The nicotinic acetylcholine receptors (nAChRs) are a family of ligand-gated ion channels consisting of five different subunits creating a transmembrane selective cationic pore, expressed both in the CNS and in extra-neuronal tissues. They are sensitive to activation by nicotine but the endogenous ligand is acetylcholine.

The nAChR prototype is the muscle nicotinic receptor, a hetero-pentameric receptor composed of five related but genetically distinctive subunits organized in stoichiometry of two α1 subunits and one each of β1, γ and ε subunits (the embryonic muscular nAChR differ for the presence of the δ subunit in place of the ε). Each subunit is composed of four transmembrane segments, a cytoplasmatic loop between transmembrane 3 and 4, a

long N-terminal extra-cellular domain and an extra-cellular C-terminus loop. The ligand binding domain is localized at the interface between the α subunits and the next subunit (Karlin, 2002) (**Fig. 1.4**).

The neuronal nicotinic receptors have a different subunit composition: they are homo-pentameric or hetero-pentameric receptors composed by the combination of twelve different subunits, nine α (α2-10), and three β (β2-4). The hetero-pentameric receptor has a structure composed by two α subunits and three β subunits, and displays a high affinity for nicotine, while homo-pentameric receptors display low affinity for nicotine. The neuronal nAChRs are expressed in the CNS, in the autonomic ganglia and in the adrenal medulla (**Fig. 1.5**).

The neuronal nAChRs can be classified as α-bungarotoxin (α-BTX)-sensitive or α-bungarotoxin (α-BTX)- non sensitive: generally, the hetero-pentameric nAChR are non-sensitive to α-BTX, whereas the homo-pentameric receptors, including the α7nAChR and the α9nAChR, are classified as α-BTX-sensitive (Karlin, 2002).

Among the nAChRs, the α7nAChR is particular, because it is a homo-pentameric channel composed of five identical α7 subunits, endowed with five ligand binding domain (**Fig. 1.6**).

The α7nAChR is widely expressed in all the CNS areas, both at pre-synaptic terminals, where it modulates neurotransmitter release, and at post-synaptic level, where it triggers the action potential. In the Peripheral Nervous System (PNS) it has been found in autonomic and sensory ganglia (Berg and Conroy, 2002).

Recent evidence demonstrated the expression of the α7nAChR also in extra-neuronal tissues, such as epithelial cells, endothelial cells, keratinocytes, lung fibroblasts and most immune cells, such as monocytes and macrophages (Sharma and Vijayaraghavan, 2002).

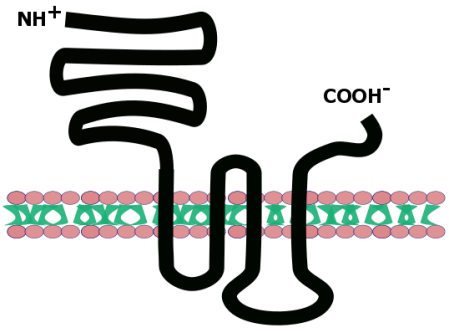

Figure 1.4: **Schematic representation of a general nicotinic acetylcholine subunit**: the figure highlights the presence of a long N-terminal extracellular domain, containing the acetylcholine binding domain and the signal peptide, four transmembrane domains, forming an intra-cellular loop, and a short C-terminal extracellular domain.

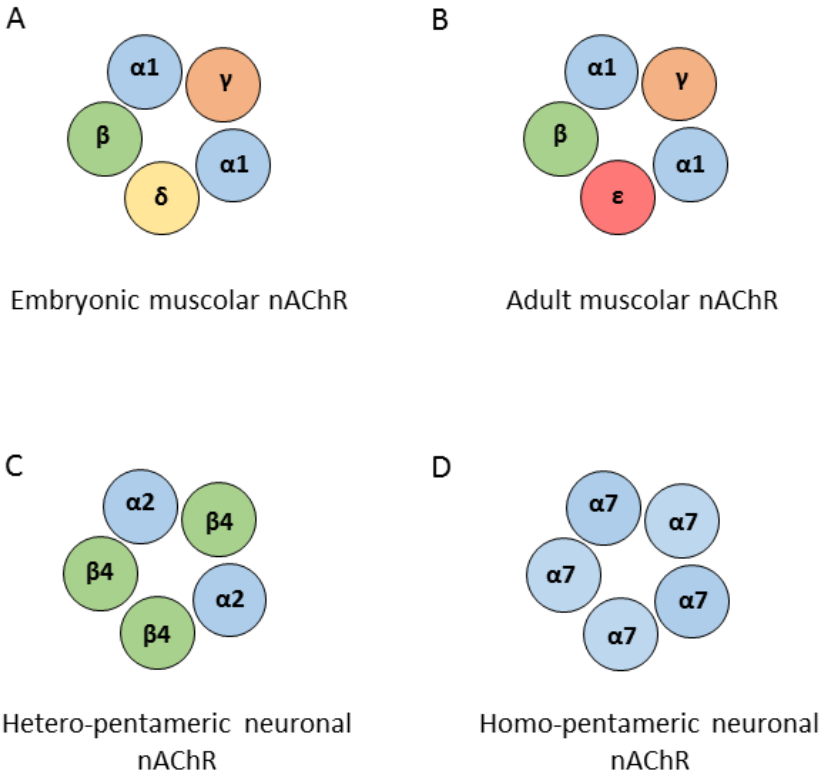

Figure 1.5: **Schematic representation of the structure of nAChRs**. (A) Structure of the embryonic muscular nAChR. (B) Structure of the adult muscular nAChR. (C) Structure of the neuronal hetero-pentameric nAChR. (D) Structure of the neuronal homo-pentameric nAChR.

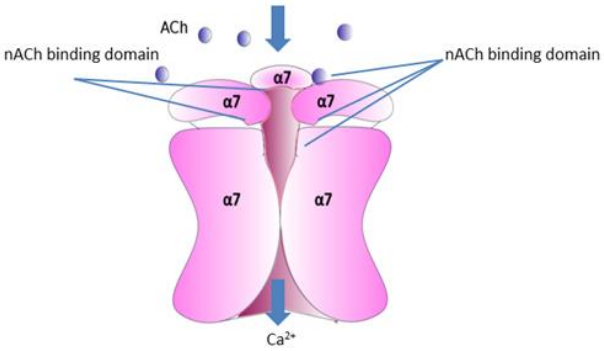

Figure 1.6: The α7nAChR channel. The presence of five identical α7 subunits determines the presence of five ACh binding domains.

1.3.1. The CHRNA7 gene

The α7 subunit is encoded by the CHRNA7 gene, which is a highly evolutionary conserved gene, mapping on chromosome 15 in position 15q13-q14. In contrast to others genes encoding nicotinic acetylcholine subunits, which are composed of at least six exons, the CHRNA7 gene is composed of ten exons, and is located on the positive strand. Exons 1-5 encode the extra-cellular N-terminus domain, including the signal peptide and the acetylcholine binding domain; exons 6-8 encode three of the four transmembrane domains and the long intra-cellular loop, which contributes to forming the cationic pore; exons 9 and 10 encode the last transmembrane domain, and the small extra-cellular C-terminal domain (**Fig. 1.7**).

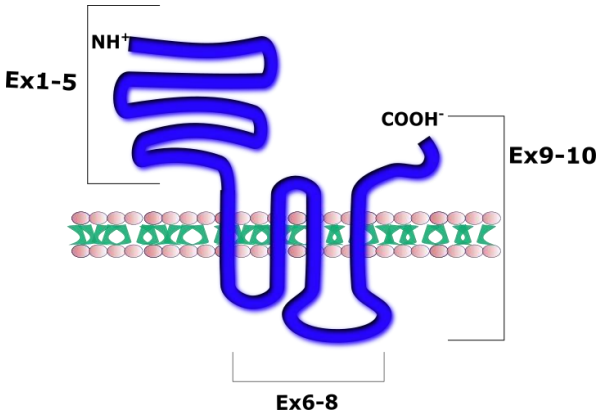

Figure 1.7: Schematic representation of the α7 subunit. The extracellular N-terminal domain is encoded by exons 1-5. Exons 6, 7 and 8 encode the first three transmembrane segments and the intracellular loop responsible of the intracellular signaling elicited in the cholinergic anti-inflammatory pathway, while exons 9 and 10 encode the last transmembrane domain and the extra-cellular C-terminal domain.

As many other genes, the human CHRNA7 undergoes alternative splicing, generating 9 alternative splicing isoforms, only two of which are known to maintain the open reading frame: the first isoform is characterized by the skipping of exon 3, while the second is characterized by the presence of the novel exon 4a (Gault et al., 1998; Severance and Yolken, 2008). A schematic representation of all the alternative isoforms generated from CHRNA7 gene splicing is reported in **Fig. 1.8**.

The full length CHRNA7 transcript gives rise to an α7 subunit of approximately 56 kDa, composed of 502 aa, including the 22 aa N-terminal signal peptide, which is eliminated after the correct subunit localization (Changeaux et al., 1998).

As for other nicotinic receptors, the assembly of the α7nAChR is a slow and inefficient process: the assembly of the entire channel takes place in the endoplasmic reticulum (ER) and involves the action of several chaperones, including the high specific Resistance to Inhibitors of Cholinesterase 3 (RIC 3), whose function is limited to the nAChRs and to 5-hydroxytryptamine type 3 receptor (5-HT_3R) (Millar, 2008).

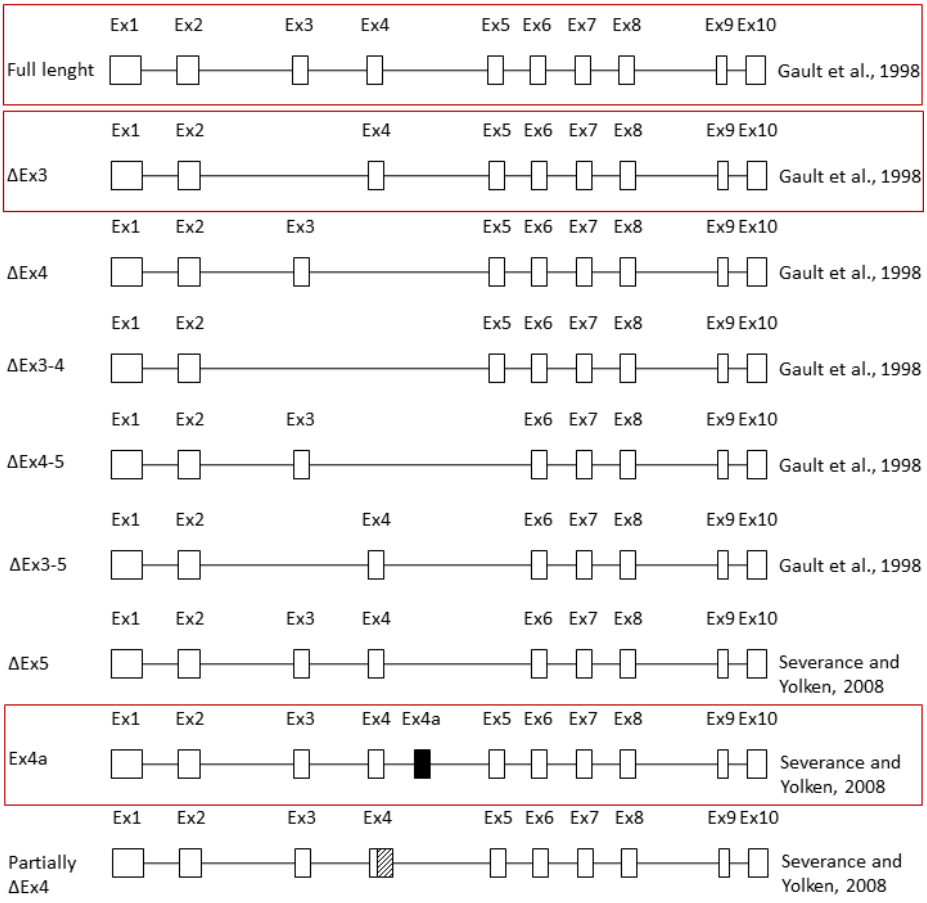

Figure 1.8: **Schematic representation of the splicing isoforms generated from CHRNA7 gene**. Only the full length coding sequence, out of the nine known splicing isoforms, one without exon 3 and the other retaining the novel exon 4a (highlighted in red in the figure), are known to contain a functional open reading frame. The others contain premature stop codons determining the non-sense mediated decay of the mRNA.

1.3.2. α7 nicotinic acetylcholine protein in the nervous system

The α7nAChR is expressed both in the human CNS and PNS. In the CNS, it is expressed in several areas, including the hippocampus, the thalamus and the cerebral cortex, both at pre- and post-synaptic level, but also at peri-synaptic and non-synaptic sites.

Receptors containing the α7 subunit belong to the α-bungarotoxin (α-BTX)-sensitive nicotinic acetylcholine receptor family and are blocked by nanomolar concentrations of

the snake toxin α-BTX. In the chick CNS and PNS there is evidence that the α7 subunit can form hetero-pentamers with the α8 and α5 subunits, and experiments performed on transfected *Xenopus laevis* oocytes, and in human epithelial kidney cells tsA201, demonstrated that it could also associate with the β2 nicotinic receptor. Despite the previous opinion that in mammals α7nAChR is predominantly homomeric ligand-gated ion channel, recent evidence demonstrated the presence of functional α7-β2 receptors in mouse and human basal forebrain (Moretti et al., 2014).

The α7nAChR is activated quickly and its desensitization is fast: when activated by the endogenous ligand acetylcholine, the α7nAChR produces a rapidly decaying inward current that elevates the intracellular levels of calcium in neurons, either directly through the channel or indirectly via depolarization and activation of voltage-gated Ca^{2+} channels, or by inducing the release of the intra-cellular Calcium storage in the ER.

At the pre-synaptic terminals, the α7nAChR has a role in modulating neurotransmitters release, in particular glutamate and norepinephrine, whereas at the post-synaptic level, it is implicated in triggering the action potential and can contribute to the long term potentiation (Berg and Conroy, 2002).

1.3.3. Function of the α7 nicotinic acetylcholine receptor in the immune system

In the extra-neuronal tissues, the α7nAChR plays important roles in proliferation, differentiation, migration, adhesion, cell contact, apoptosis, angiogenesis and tumour progression. In particular, activation of the α7nAChR on monocytes and macrophages by acetylcholine leads to the anti-inflammatory response in the context of the Cholinergic Anti-Inflammatory Pathway (Sharma and Vijayaraghavan, 2002).

Although in extra-neuronal contexts the α7nAChR may act as ion channel, increasing the levels of free intracellular calcium, evidence shows that in immune cells, and in particular in the Cholinergic Anti-Inflammatory Pathway, it mainly functions by triggering intracellular signaling through its intracellular loop. Indeed, human leukocytes treatment with nicotine or acetylcholine generates no detectable membrane currents.

When activated by the endogenous ligand, the α7nAChR expressed by leukocytes induces a rapid increase of intracellular Ca^{2+} concentration, probably due to an increased

release of calcium from the ER induced by the activation of PI3K and Phospholipase C (PLC), rather than to increased calcium influx. The increased concentration of Ca^{2+} activates the protein kinase C (PKC) which in turn activates the MAPK cascade, thus leading to change in gene expression (Villiger et al., 2002).

Moreover, many proteins have been shown to bind the intracellular portion of the α7nAChR and participate to the signal transduction. For example, the α7nAChR activates the Janus Kinase 2 (JAK2)-PI3K-AKT-STAT3 signalling. This signalling has been found to trigger the transactivation of NF-κB, which in turn increases the expression of the anti-apoptotic protein Bcl-2 (Marrero and Bencherif, 2009).

The activation of NF-κB-Bcl-2 has a central pro-inflammatory role but it is also involved in the neuroprotective effect against $A\beta_{1-42}$-dependent apoptosis elicited by nicotine treatment (Marrero et al., 2004).

At the same time, the activation of STAT3 has also anti-inflammatory effects: STAT3 is in fact an anti-inflammatory transcription factor, whose activation results in decreased pro-inflammatory cytokines' gene expression.

α7nAChR-mediated STAT3 activation is important for the anti-inflammatory response induced by acetylcholine: indeed, nicotine or acetylcholine fails to reduce TNF-α production in cells expressing STAT3 mutated in the residues that are phosphorylated or in the DNA-binding domain, and vagal stimulation does not inhibit intestinal inflammation in STAT3 conditional knock-out mice (De Jonge et al., 2005).

On the other hand, the α7nAChR exerts an anti-inflammatory effect also by directly reducing the activity of the NF-κB transcription factor (Shaw et al., 2002; Arredondo et al., 2006). It has been shown that the anti-inflammatory potential of the α7nAChR in macrophages, monocytes and epithelial cells relies upon the direct inhibition of NF-κB: the inhibitory effect may be mediated by counteracting the degradation of IκB and preventing NF-κB translocation (Saeed et al., 2005; Yoshikawa et al., 2006) (**Fig.1.9**).

The signalling elicited by α7nAChR activation involves also other pathways: for example, nicotine up-regulates the cyclooxygenase (COX-2) and increases PGE2 production (Heeschen et al., 2001; Takahashi et al., 2006).

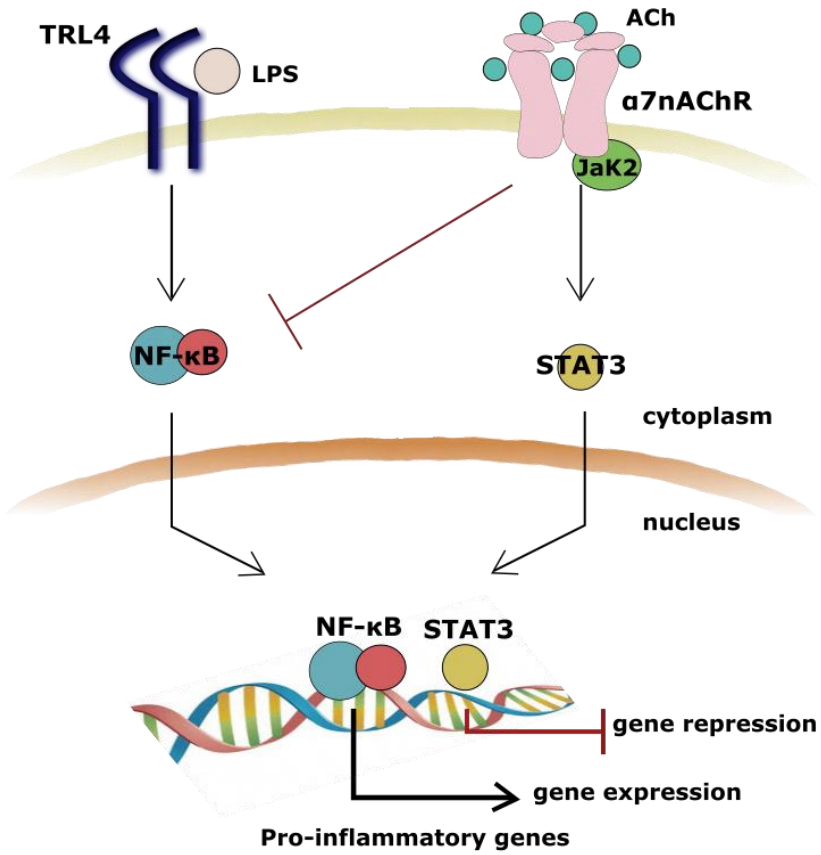

Figure 1.9: The α7nAChR signaling in the immune system. In the immune system, in particular in monocytes and macrophages, the α7nAChR, once activated by ACh, triggers an intra-cellular signalling which culminates with the activation of the anti-inflammatory transcription factor STAT3, that mediates transcriptional repression of pro-inflammatory genes, such as IL-1 and TNF-α. The activation of α7nAChR leads also to the direct inhibition of NF-KB.

1.3.4. α7nAChR-related pathologies

1.3.4.1. Neurological disorders

Mutations in the CHRNA7 gene or alteration of the function of α7nAChR have been linked to several human neurological disorders, such as Alzheimer's disease (AD) and schizophrenia.

It is worth noting that all the neurological diseases involving an altered function of the α7nAChR as causative or contributing factor are known to be associated with an

inflammatory state, generally caused by hyper-activation of the microglia. The α7nAChR is indeed expressed by microglial cells where it plays important roles in controlling microglia activation (Egea et al., 2015).

Accumulating evidence indicates a role of the α7nAChR in the pathogenesis of neurodegenerative diseases as well as in therapeutic strategies for several dementias, including Alzheimer's disease (AD). AD is indeed characterized by the loss of cholinergic neurons due to a selective decrease of nicotinic receptors (Burghaus et al., 2000; Leonard et al., 2000; Guan et al., 2002). Moreover, recent studies have suggested a protective role of nicotine assumption for Alzheimer's and Parkinson diseases and the administration of nicotine to rat hippocampal cultures seemed to exert a neuroprotective effect against glutamate- and β-amyloid-related cytotoxicity (Morens et al., 1995; Brenner et al., 1997; Shimohama, 2009).

Many authors have reported the high affinity association between the α7nAChR and Aβ peptides: the two proteins co-localized not only at the neuronal cell membrane, but also into the β-amyloid plaques found in AD brain samples (Wang et al., 2000). The nature of this association is far from being elucidated: many studies hypothesized an antagonist role of the Aβ peptide (Pettit et al., 2001), while others reported increased pre-synaptical calcium current in response to $A\beta_{42}$- α7nAChR association (Wang et al., 2000).

Specific mutations or polymorphisms in CHRNA7 sequence are associated with an increased or decreased risk of AD development: for example, the combination of two particular SNPs in CHRNA7 5'-UTR and Intron 2 are associated with a decreased risk of AD, while another SNP in CHRNA7 Intron 3 is instead associated with increased risk (Carson et al., 2008). The different genotype at CHRNA7 gene can also alter the pharmacological response to AD treatment: patients carrying rs8024987 (C/G) or rs6494223 (C/T) polymorphisms respond better to AChEi treatment. α7nAChR upregulation induced by Donepezil is higher in lymphocytes from TT subjects than in CC or CT (Russo et al., 2015).

Concerning the pattern of expression of CHRNA7 gene in human AD brain, several studies have been conducted with different and often controversy results: in 2000, Wevers and collaborators reported a marked decrease of α7nAChR protein in AD pre-frontal cortex, while they found no differences in mRNA expression compared to controls. Contrary, in 2007, Counts et al. reported an up-regulation of CHRNA7 mRNA in Nucleus

Basalis neurons (Wevers et al., 2000; Counts et al., 2007). Moreover, Chu and collaborators found a significant up-regulation of α7nAChR protein level in leukocytes obtained from AD patients compared to control: the up-regulation inversely correlated with the Mini-Mental State Examination (MMSE) score, which measures the patient cognitive ability, suggesting that CHRNA7 protein level in blood could be used as a diagnostic marker for AD (Chu et al., 2005). The results provided by Chu were recently confirmed by Conti and collaborators, which measured the level of CHRNA7 mRNA in Peripheral Blood Mononuclear Cells (PBMCs) obtained from healthy controls, AD patients and AD patients treated with the Donepezil. They found a significant increase of CHRNA7 expression in AD and AD-Donepezil samples compared to controls (Conti et al., 2016).

The α7nAChR has a well-characterized role also in several psychiatric disorders, such as schizophrenia. Since 1998, it is known that the α7nAChR is implicated in the P50 auditory gating deficit (Adler et al., 1998) characterizing schizophrenia and rare, though large recurrent microdeletions in CHRNA7 locus are associated with this psychiatric disease (Stefansson et al., 2008). No mutations in the CHRNA7 coding region were reported to be associated with schizophrenia, but several SNPs in its promoter, usually correlated to a decreased CHRNA7 expression, seemed to be associated with schizophrenia and P50 auditory gating deficit (Leonard et al., 2002; Stephens et al., 2009). Interestingly, one of the most characteristic behaviours of schizophrenic patients is heavy smoking, thus suggesting the involvement of cholinergic system in this disease (Olincy et al., 1997).

At the same time, it is worth noting that also schizophrenia has a high component of neuro-inflammation: for example, viral or bacterial infections occurring during pregnancy are thought to increase the risk of schizophrenia and schizophrenic patients show increased levels of circulating pro-inflammatory cytokines (Patterson, 2009).

Emerging evidence suggests that the α7nAChR can be also implicated in other neurological disorders, such as autism (Bacchelli et al., 2015), epilepsy (Damiano et al., 2015), and Tourette syndrome (Melchior et al., 2013).

The Chr15q13.3 locus, which contains CHRNA7 gene together with other five genes, is subjected to Copy Number Variations (CNVs), due to the presence of six Low Copy Repeat (LCR) mediating Non-allelic Homologous Recombination (NAHR), leading to chromosomal microdeletions and duplications. The CNVs at Chr15q13.3 are responsible for various

neuropsychiatric diseases, including autism, learning disabilities and seizures (Szafranski et al., 2000). Recently, it has also been reported the presence of CHRNA7 triplication, segregating in four affected family members in three generations: these patients presented several neuropsychiatric disorders and intellectual disabilities, including anxiety, bipolar disorder, attention deficit and seizures (Soler-Alfonso et al., 2014).

Of great interest is the role of CHRNA7 in Autism Spectrum Disorders (ASD): it is indeed known that the 15q11.2-13.3 region is deleted or duplicated in 1-3% of autism patients (OMIM 209850). This genomic region is under control of the Prader-Willi Syndrome Imprinting Center (PWS IC). In 2011, Yasui and collaborators demonstrated that the expression of CHRNA7 during neuronal development is regulated by the PWS IC through the involvement of the transcriptional silencer MeCp2, whose loss of function is responsible for Rett Syndrome and which can contribute to long range chromatin remodelling (Yasui et al., 2011). This evidence provided a link between CHRNA7 altered expression and development of complex neurological disorders, such as Rett Syndrome, that is characterized by neurodevelopmental regression similar to autism, and by several neurological symptoms, including epilepsy (LaSalle et al., 2009).

1.3.4.2. Immunological disorders

Given the central role of the α7nAChR in the Cholinergic Anti-Inflammatory Pathway, it's not surprising if it has become a promising target for anti-inflammatory therapies.

Several immunological pathologies characterized by uncontrolled production of pro-inflammatory cytokines and systemic inflammatory status could be treated with drugs and compounds that target the α7nAChR and its pathway in extra-neuronal tissues. For example, a particular α7nAChR agonist (TC-7020) is effective in reducing the serum levels of pro-inflammatory cytokines and of glucose level, weight gain and food intake in a mouse model of diabetes type 2 (Marrero et al., 2010).

Other α7nAChR agonists (such as nicotine or acetylcholine) seem to be effective also in asthma (Mishra et al., 2010), arthritis (van Maanen et al., 2009), psoriasis (Mazza et al., 2010), ulcerative colitis (Ghia et al., 2006) and sepsis (van Westerloo et al., 2005).

Sepsis or Systemic Inflammatory Response Syndrome (SIRS) is one of the major causes of death in the western world and is characterized by a systemic inflammation in response to high level of endotoxin (generally LPS), which could result in septic shock or Multiple Organ Dysfunction Syndrome (MODS). The exaggerated response of the innate immune system to bacterial infection is thought to be the leading cause of the high mortality of this syndrome, although the precise molecular mechanisms controlling SIRS are far to be elucidated. However, new evidence suggests that the high rate of mortality could be also due to a state of unresponsiveness of the innate immune cells after prolonged exposures to high levels of endotoxin. This aspect of the sepsis is characterized by the production of high levels of anti-inflammatory cytokines and is generally indicated with the term of endotoxin tolerance or Compensatory Anti-Inflammatory Reaction (CARS) (Bone et al., 1997). Several α7nAChR agonists have been reported to reduce the TNF-α serum level in experimental sepsis, but the anti-inflammatory effect exerted by α7nAChR agonists leads sometimes to an increased lethality rate, due to a decreased bacterial clearance (van Westerloo et al., 2005).

In the last years, several studies have suggested new therapeutic strategies for immunological disorders involving CHRNA7 targeting: between those, a therapeutic approach directed on modulation of miRNAs, involved in the Cholinergic Anti-Inflammatory Pathway, has become more and more interesting. In 2013, Sun and collaborators discovered that nicotine inhibits STAT3 expression through the activation of miRNA-124, via α7nAChR stimulation. This results in a reduced production of pro-inflammatory cytokines IL-6 and TNF- α. Interestingly, the inhibition of TNF- α by miRNA-124 is shown to be mediated by the prevention of TNF-converting enzyme (TACE) translation, which is necessary for the release of the soluble TNF- α. The pre-treatment with miRNA-124 agomir is sufficient to improve the 24 hour survival rate in a murine model of endotoxemia, giving interesting hints for a miRNA-based therapy of inflammatory pathologies (Sun et al., 2013; Ulloa, 2013).

More recently, Liu et al. investigated the role of miRNA-132 in sepsis-induced lung-injury. miRNA-132 is known to be induced after LPS treatment in human primary macrophages and contributes to activate the Cholinergic Anti-Inflammatory Pathway by reducing acetylcholinesterase level (Shaked et al., 2009). Liu and collaborators found that

miRNA-132 is also up-regulated in LPS-treated alveolar macrophages, and this up-regulation determines an anti-inflammatory response by reducing AChE protein level, thus improving ACh anti-inflammatory signaling through α7nAChR activation. Moreover, alveolar macrophages treatment with ACh in the presence of miRNA-132 over-expression resulted in NF-κB nuclear translocation inhibition and STAT3 up-regulation. Overall, the results achieved suggest that miRNA-132 can act as a modulator of inflammation through the recruitment of the Cholinergic Anti-Inflammatory Pathway (Liu et al., 2015).

In the last years, emerging evidence has also highlighted the role of CHRNA7 in the development of HIV-associated Neurocognitive Disorders (HAND). Given that HIV does not directly infect neurons, the finding of neurological symptoms in HIV-infected patients has become an interesting field of research: indeed, different hypotheses have been raised to explain the molecular mechanisms of neurological impairment in HIV infection. First, it is possible that HIV infection could alter the chemokine/cytokine balance, thus inducing a microglial over-activation; alternatively, it has been hypothesized a neuro-toxic effect exerted by soluble HIV proteins, such as gp120. Indeed, it has been demonstrated that in cultured cells the neurotoxic effect is partly due to α7nAChR activation, leading to neuronal death (Ballester et al., 2012).

1.3.5. α7nAChR involvement in AD therapy: the case of Donepezil

The cholinergic system is one of the most promising therapeutic targets in AD: the treatment with Acetylcholinesterase Inhibitors (AChEI) such as Galantamine or Donepezil is indeed effective and ameliorates the cognitive symptoms of AD (Taylor, 1998). In particular, Donepezil, a selective non-competitor AChEI, is one of the most effective drugs used in Alzheimer's disease. As other AChEI, Donepezil overcomes the Blood Brain Barrier and temporary ameliorates the cognitive symptoms of AD by inhibiting the acetylcholinesterase (AChE) enzyme which is responsible for the degradation of ACh. The inhibition of AChE function results in an increased permanence of ACh at nicotinic synapses, thus partly counteracting the nicotinic loss, that is one of the characteristic signs of AD. Moreover, Donepezil treatment determines the up-regulation of α7nAChR protein level in neurons (Takata-Takatori et al., 2008). In addition to its role as AChEI,

Donepezil also binds directly the α7nAChR in neurons, exerting a neuro-protective function by stimulating the receptor activation: on one hand, the α7nAChR activation leads to PI3K-Akt-Bcl-2 signaling pathway, thus providing neuro-protection against β-amyloid neuro-toxicity; on the other hand, α7nAChR stimulation determines the internalization of NMDA functional receptors, thus reducing the glutamate-dependent neuro-toxicity (Shen et al., 2010).

Little is known about the mechanisms of action of Donepezil or other AChEI in the context of the immune response. It is known that several AChEI are also able to inhibit the action of the circulating Butyryl-cholinesterase (BChE) enzymes, while Donepezil effect is limited to the AChE. The inhibition of ACh degradation results in a more effective anti-inflammatory response evoked by ACh, thus improving the Cholinergic Anti-Inflammatory Pathway (Pohanka, 2014). However, Donepezil functions also via AChE-independent pathways, as it exerts anti-inflammatory effects also in the microglia, where AChEs are not expressed (Hwang et al., 2010).

A very recent study by Arikawa and collaborators provided new insights about the anti-inflammatory properties of Donepezil: the pre-treatment with Donepezil before LPS administration was indeed effective in reducing pro-inflammatory cytokines levels in murine macrophages cultures (Arikawa et al., 2016).

Moreover, Donepezil can also exert its anti-inflammatory potential by directly binding the α7nAChR, acting as an agonist (Pohanka, 2014).

Increasing evidence indicates that AChEI treatment also modulates the adaptive inflammatory response, and increasing the antibody-mediated immune response (Reale et al., 2006). Recently, it has been demonstrated that Donepezil treatment provides GATA-3 expression up-regulation through the activation of the α7nAChR. GATA-3 is a key transcription factor involved in the switch of Th1-Th2 response and it has been hypothesized a possible role of the Donepezil-α7nAChR axis in inducing the antibody-mediated response against Aβ peptides (Conti et al., 2016).

There is evidence of alternative pathways activated by Donepezil treatment: an alternative receptor of Donepezil is the σ1 receptor, which is a “receptor chaperone” located in the ER that leads to the stabilization of the inositol 1-4-5-triphosphate receptor in response to low levels of intra-cellular calcium, thus leading to mitochondrial calcium

level increase (Ishikawa and Hashimoto, 2016). Donepezil has been demonstrated to induce a rescue in amyloid-dependent Long Term Potentiation impairment through activation of σ1 receptor (Solntseva et al., 2014), but there is no evidence that Donepezil can bind this receptor also in the immune system.

1.4. The CHRFAM7A gene

Recently during the evolutionary history, the CHRNA7 gene has undergone a partial duplication and fusion, giving rise to a duplicated gene product, named CHRFAM7A.

The CHRFAM7A gene is present only in humans and is characterized by a complex genomic organization. Since its discovery in 1998, many authors have investigated the characteristics and functions of this gene, thus defining new insights about its role in the immune system. Despite the great amount of information obtained about the CHRFAM7A gene, the mechanisms regarding its regulation and expression remain almost unknown.

1.4.1. The CHRFAM7A locus

The CHRFAM7A gene maps on chromosome 15 (15q13-q14) and is the product of the partial duplication and fusion of exons 5-10 of the CHRNA7 gene with the novel exons D, C, B and A, identified by 5'-RACE analysis on hippocampal mRNA. The genetic sequence shared by CHRFAM7A and CHRNA7 (from exon 5 to exon 10) shows more than 99% of homology (Gault et al., 1998).

Exon D belongs to the gene FAM7A, mapping on chromosome 15, whose function is still unknown, while exons C, B and A derive from the Unc-51 Like Kinase 4 (ULK4) gene, mapping on chromosome 3 and encoding a serine/threonine kinase (Riley et al., 2002).

The novel exons D, C, B and A are fused to the CHRNA7-derived exons in frame and the two counterparts of the CHRFAM7A gene are transcribed as a single unit (Gault et al., 1999). In addition to the novel exons D-A, Riley et al. identified also other exons, named E, F and G. Exon E derives from the ULK4 gene, while exons F and G belong to the FAM7A gene (Riley et al., 2002) (**Fig. 1.10**).

The chimeric CHRFAM7A gene maps 1.6 Mb centromeric apart from its parental gene CHRNA7 in inverted orientation (Gault et al., 1998) and is located in a high polymorphic locus: indeed, there is evidence that it could be in hemizygosis or even absent in some populations. Interestingly, Riley and collaborators reported the case of two individuals (father and son) lacking the CHRFAM7A gene in a group of South African Bantu schizophrenic patients, suggesting that the loss of CHRFAM7A gene could be relevant in neuropsychiatric diseases pathogenesis (Riley et al., 2002).

The homozygotic absence of CHRFAM7A gene is rare (1% of individuals), while the hemizygosis is more common (20% of individuals), indicating that the CHRFAM7A gene can be subjected to Copy Number Variation (CNV) (Flomen et al., 2006) (**Fig. 1.11A, Fig. 1.11C**). Moreover, it has been described a 2 base pair deletion polymorphism in exon 6 of CHRFAM7A (but not present in the CHRNA7 gene) (Gault et al., 1998) which correlates with the inversion of CHRFAM7A orientation (Flomen et al., 2008). This polymorphism seems to be more frequent in the Caucasian population rather than in African Americans (Sinkus et al., 2009) (**Fig. 1.11B**).

The 2 base pair deletion polymorphism found in CHRFAM7A exon 6 is less frequent in individuals carrying a particular CHRNA7 promoter mutation and is in linkage disequilibrium with a 3 base pair intronic insertion in CHRNA7 exon 7, which is thought to trigger the alternative splicing of the CHRNA7 gene, generating the exon 3 deleted isoform (Gault et al., 2003; Rozycka et al., 2013).

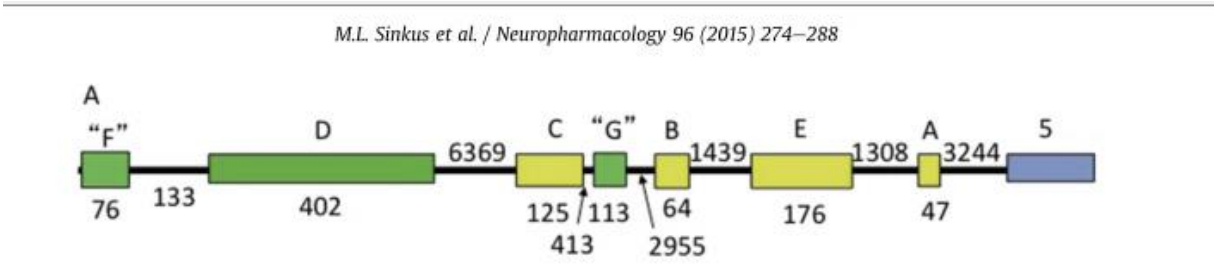

Figure 1.10: **Schematic representation of the order of the upstream exons of CHRFAM7A** (apted from Sinkus et al., 2015).

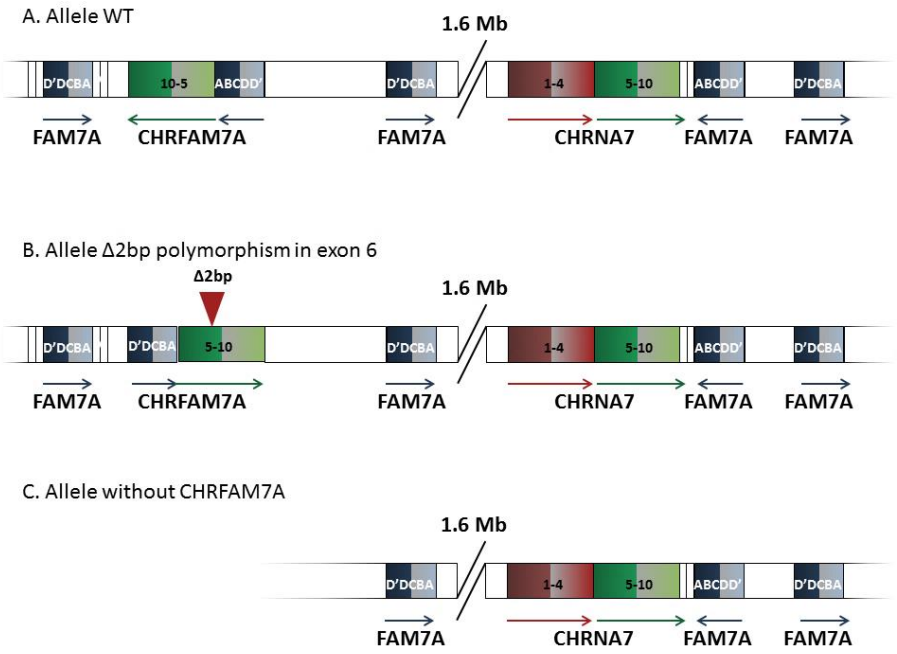

Figure 1.11: Schematic representation of CHRFAM7A alleles. (A) Wild Type (WT) CHRFAM7A locus allele: the CHRFAM7A gene is located 1.6 Mb centromeric with respect to CHRNA7 on opposite strand. (B) Allele carrying the 2 base pair deletion in CHRFAM7A exon 6: the deletion correlates with the gene inversion and CHRFAM7A is located on the same strand with respect to CHRNA7. (C) Allele characterized by the absence of CHRFAM7A gene.

1.4.2. The CHRFAM7A transcript

The first evidence of CHRFAM7A expression in human tissues was reported by Villiger and collaborators in 2002. In this study the authors investigated the expression of CHRNA7 transcript in leukocytes. Despite the high expression level of CHRNA7 transcript in leukocytes, electrophysiological studies failed to reveal ACh or nicotine-evoked current. The authors explained the results hypothesizing that the transcript identified actually corresponded to the CHRFAM7A transcript, earlier characterized by Gault and collaborators in 1998. The CHRFAM7A transcript is indeed translated into a protein, named α7dup, that not containing the ACh binding domain of the α7 conventional subunit is unable to induce Ca^{2+} currents. They corroborated the hypothesis by analysing by RT-PCR the CHRFAM7A sequence encompassing exons C-A, thus demonstrating that

the predominant transcript expressed in leukocytes was the CHRFAM7A. Moreover, while in the CNS the CHRNA7 gene is more expressed than CHRFAM7A, in leukocytes CHRFAM7A has higher expression level compared to CHRNA7 (Villiger et al., 2002). It is now known that CHRFAM7A transcript is expressed in more than 30 human tissues.

The CHRFAM7A gene is transcribed into a mRNA that could be subjected to alternative splicing, generating two different isoforms. The isoform 1 (CHRFAM7A-002) contains all ten exons, eight of which are coding exons and generate a mRNA of 6220 bp, while the isoform 2 (CHRFAM7A-201) is characterized by the skipping of the novel exon B and has nine exons, five of which are coding exons, generating a transcript of 2749 bp.

The analysis of the CHRFAM7A sequence identified two different Open Reading Frames (ORFs) from which the translation could initiate: the first ATG is located in the novel exon B and gives rise to a protein of 46 KDa (412 aa), characterized by the presence of an N-terminus domain of 27 aa which is encoded by the novel exons B and A. The second ATG is located in the CHRNA7-derived exon 6 and when the translation start from this ATG a 35 KDa protein (321 aa) is produced, characterized by the absence of the N-terminus domain, resulting in a truncated form of the α7nAChR conventional subunit and does not contain any FAM-derived sequence (http://www.ensemble.org).

Given the fact that the CHRFAM7A pre-mRNA undergoes alternative splicing, while the isoform 1 (CHRFAM7A-002) can be translated from both the ATG, giving rise to the 35 KDa and 46 KDa proteins, the isoform 2 (CHRFAM7A-201), which lacks the exon B, can be translated only from the ATG in exon 6, giving rise only to the 35 KDa protein (**Fig. 1.12A**).

The translation is further complicated by the presence of the 2 base pair deletion in exon 6: the polymorphism involves a TG dinucleotide and is located upstream the ATG in exon 6 and its presence generates a premature stop codon in the sequence (Gault et al., 1998). Thus, when the polymorphism is present, both the isoform 1 and 2 could be translated only from the ATG in exon 6, generating the shortest isoform (**Fig.1.12B**).

The protein produced by the CHRFAM7A gene, hereon called α7dup, shows many analogies with the α7nAChR conventional subunit, as it is characterized by four transmembrane domains, a long intra-cellular loop and a short extra-cellular C-terminal; however, both the α7dup proteins generated by the CHRFAM7A gene differ from the

α7nAChR for their N-terminus domain, which in particular lacks the α7nAChR signal peptide and the ACh binding domain (Araud et al., 2011) (**Fig. 1.13**).

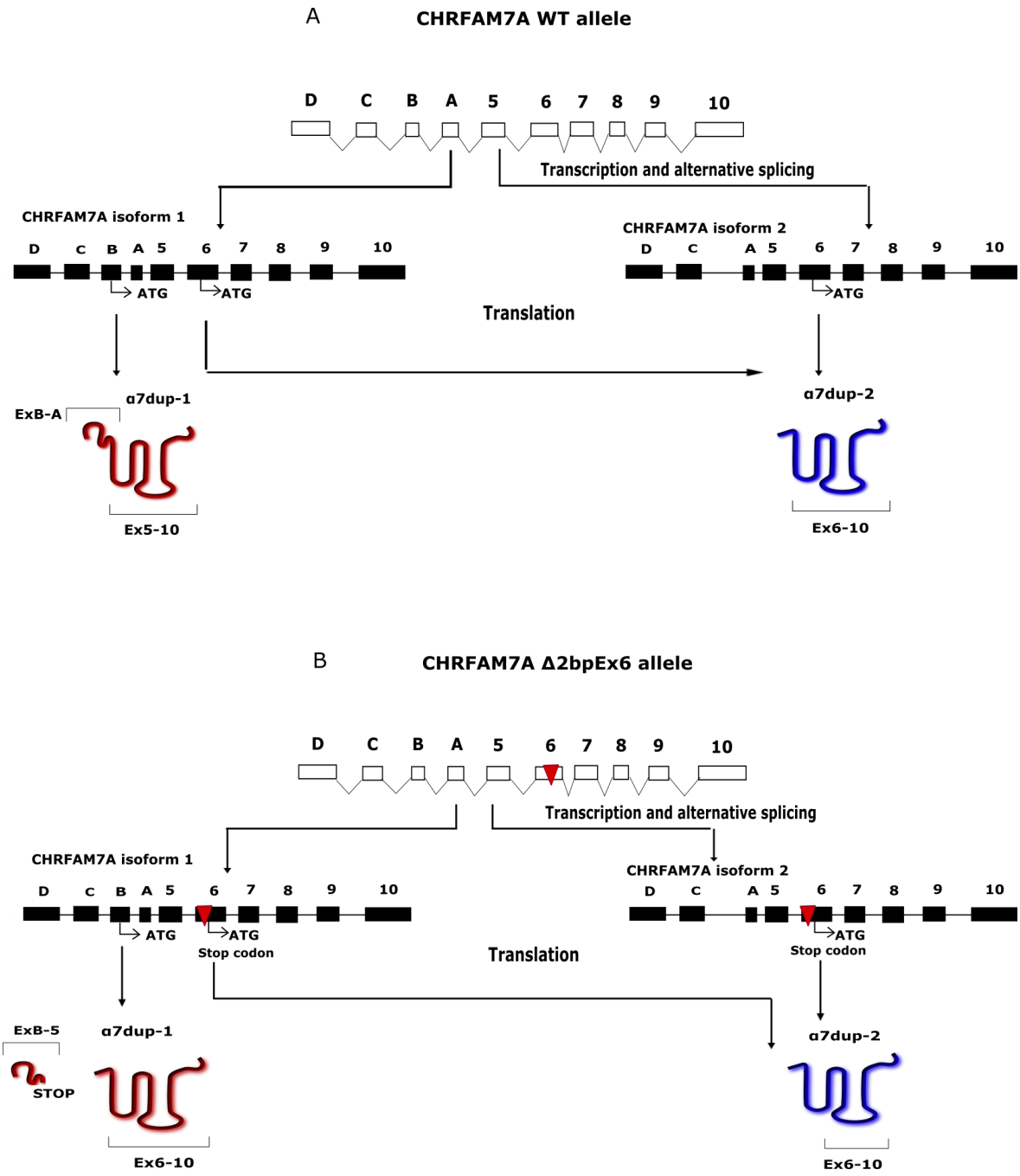

Figure 1.12: Schematic representation of the CHRFAM7A transcription and translation. (A) The WT CHRFAM7A allele is transcribed into two splicing isoforms, the isoform 1, characterized by the presence of all the exons, and the isoform 2, which is characterized by the skipping of exon B. The isoform 1 can be translated from both the ATG in exon B and the in one exon 6, giving rise to two different proteins of 46

KDa and 35 KDa respectively. The isoform 1 is characterized by the presence of a 27 aminoacids N-terminal domain, encoded by the novel exons B and A; the isoform 2 lacks the N-terminal domain but is characterized by the presence of four transmembrane domains and a short C-terminal as the isoform 1. The splicing isoform 2 instead is only translated from the ATG in exon 6, thus giving rise only to the 35 KDa protein. (B) The TG deletion in CHRFAM7A exon 6 maps upstream the ATG and causes the insertion of a premature stop codon: the isoform 1 is then translated from the ATG in exon B but the translation terminates at the premature stop codon inserted by the polymorphism, giving rise to a 40 aminoacids peptide whose fate is unclear. The translation re-starts at the ATG in exon 6 giving rise to the 35 KDa protein. The CHRFAM7A isoform 2 instead is only translated from the ATG in exon 6, giving rise to the shortest isoform.

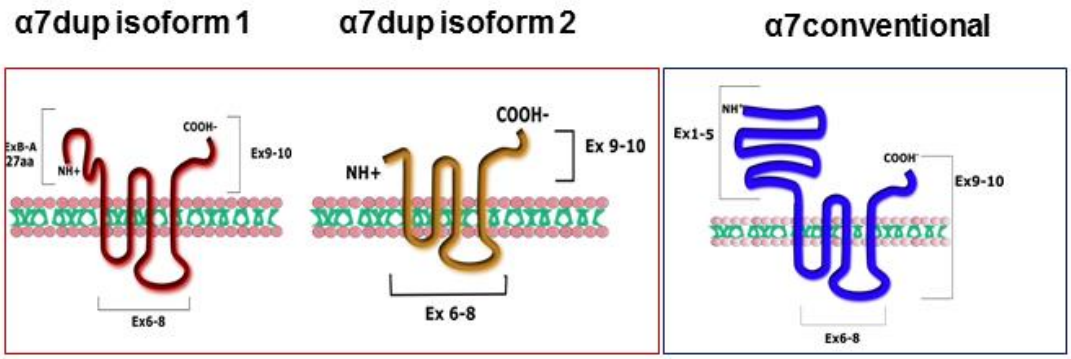

Figure 1.13: **Comparison between the two α7 duplicated proteins and the α7 conventional subunit**: the α7dup proteins, as the α7 conventional subunit, are characterized by the presence of four transmembrane domains and a short C-terminal extracellular loop, but they completely lack the N-terminal domain of the α7 conventional protein, including the signal peptide and the acetylcholine binding domain.

1.4.3. The α7dup protein

The α7dup subunit seems to be unable to form functional receptors, as it lacks the α7nAChR N-terminal domain, normally encoded by exons 1-5, and the portion encoded by the novel exons is thought not to contain any conventional signal peptide. The α7dup also has particular pharmacological properties, as it is not blocked by α-BTX and is not able to evoke inward calcium currents.

In 2011, De Lucas Cerillo et al. reported that the α7dup subunit is able to bind the conventional α7 isoform thus exerting a dominant negative regulation upon the α7 function: indeed, the co-transfection of α7: α7dup subunits in a molar ratio of 1:5 in Xenopus oocytes decreases the nicotine-elicited calcium current (De Lucas Cerillo et al., 2011).

This effect seemed to be due to a reduction of the number of functional α7nAChRs reaching the oocyte's membrane. In this perspective, the α7dup protein can act by sequestering the conventional α7 subunits in the endoplasmic reticulum. These results were confirmed in 2012 by Araud at al. However, the authors also showed an increased potentiation of the allosteric modulator PNU-120596, which interacts with the α7 transmembrane domain, in oocytes transfected with a 1:10 ratio of α7: α7dup. This evidence raised the hypothesis that the α7dup protein can exert its dominant negative effect also by directly binding the conventional α7 subunits in the plasma membrane and reducing the number of ACh binding domains of the receptors (Araud et al., 2012) (**Fig. 1.14**). This speculation is also supported by the observation of a direct interaction between the two subunits by means of FRET analysis in Neuro2A cells and primary rat hippocampal neurons (Wang at al. 2014).

Interestingly, the α7dup protein encoded by the CHRFAM7A gene carrying the 2 base pair deletion polymorphism in exon 6, currently named Δα7dup, seems to exert a more potent dominant negative effect upon the α7 conventional function (Araud et al., 2012).

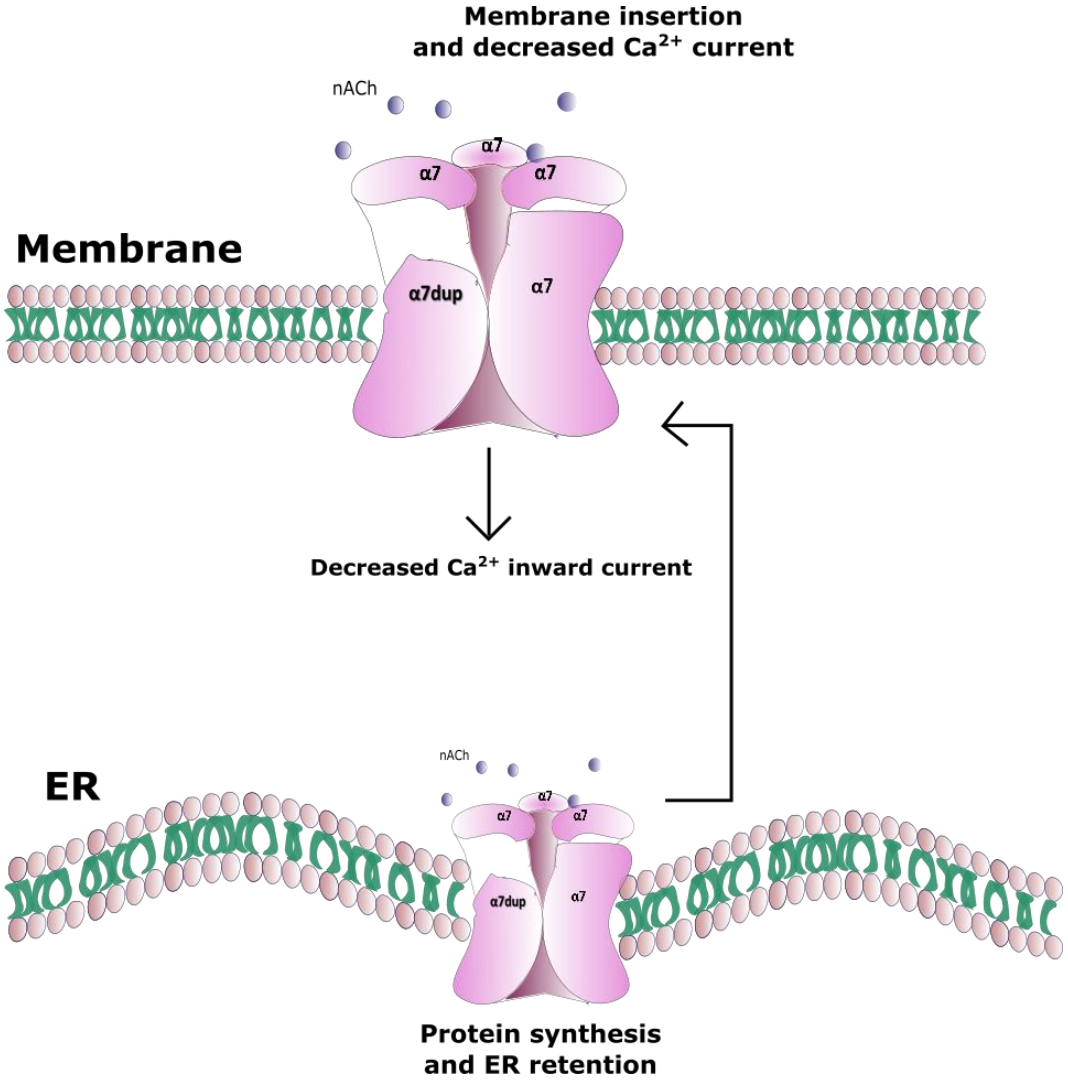

Figure 1.14: Schematic representation of the two principal mechanisms by which the α7dup protein is thought to exert a dominant negative regulatory role on the α7 conventional receptor. The first mechanism relies on the capacity of the α7dup subunit to bind and retain the α7 conventional subunit in the Endoplasmatic Reticulum, given the absence in its sequence of a signal peptide, thus reducing the number of functional receptors in the plasma membrane. In the second mechanism, the α7dup protein binds the α7 conventional subunits and the complex is transported in the plasma membrane: given that the α7dup protein lacks the ACh binding domain, the heteropentamers formed by the α7dup and α7 conventional subunits is characterized by a reduced number of ACh binding domain, thus leading to a reduced ACh-induced Ca^{2+} current.

A functional role of α7dup protein *in vivo* is suggested by its down-regulation in monocytes and macrophages after LPS challenge: the down-regulation, which affects the

CHRFAM7A transcript as well as the protein, is also observed in the leukaemic monocytic cell model THP-1 (Benfante et al., 2011). The THP-1 cells, unlike the primary monocytes and macrophages which are characterized by the expression of both the α7 conventional and α7dup proteins, express only the CHRFAM7A transcript and completely lack CHRNA7 mRNA, even if the CHRNA7 gene is detected in the genome.

The CHRFAM7A down-regulation occurring in THP-1 and in monocytes and macrophages after LPS challenge relies on a transcriptional mechanism directly driven by the NF-κB transcription factor. Indeed, the treatment with the NF-κB inhibitor Parthenolide rescues the CHRFAM7A control level upon LPS challenge (Benfante et al., 2011) (**Fig. 1.15**).

Interestingly, unpublished data show that the LPS treatment on human primary monocytes and macrophages induces the expression of the CHRNA7 gene, suggesting that in these cells heteromeric α7 receptors, consisting of both α7 subunit, could be formed **(Fig. 1.16).** This receptor would have a lower capacity to respond to acetylcholine, because the subunit has no conventional binding site for the ligand. If true, one might speculate that the negative regulation of CHRFAM7A gene may be somehow involved in regulating levels of homomeric α7 nicotinic receptor on the membrane of macrophages and therefore the ability of these immune cells to respond to acetylcholine released from Vagus nerve during an infection. Pro-inflammatory stimuli then would lead to increase of the conventional subunits transcript level on one side, and an inhibition of the duplicated subunits on the other, thus increasing the ability to respond to ACh.

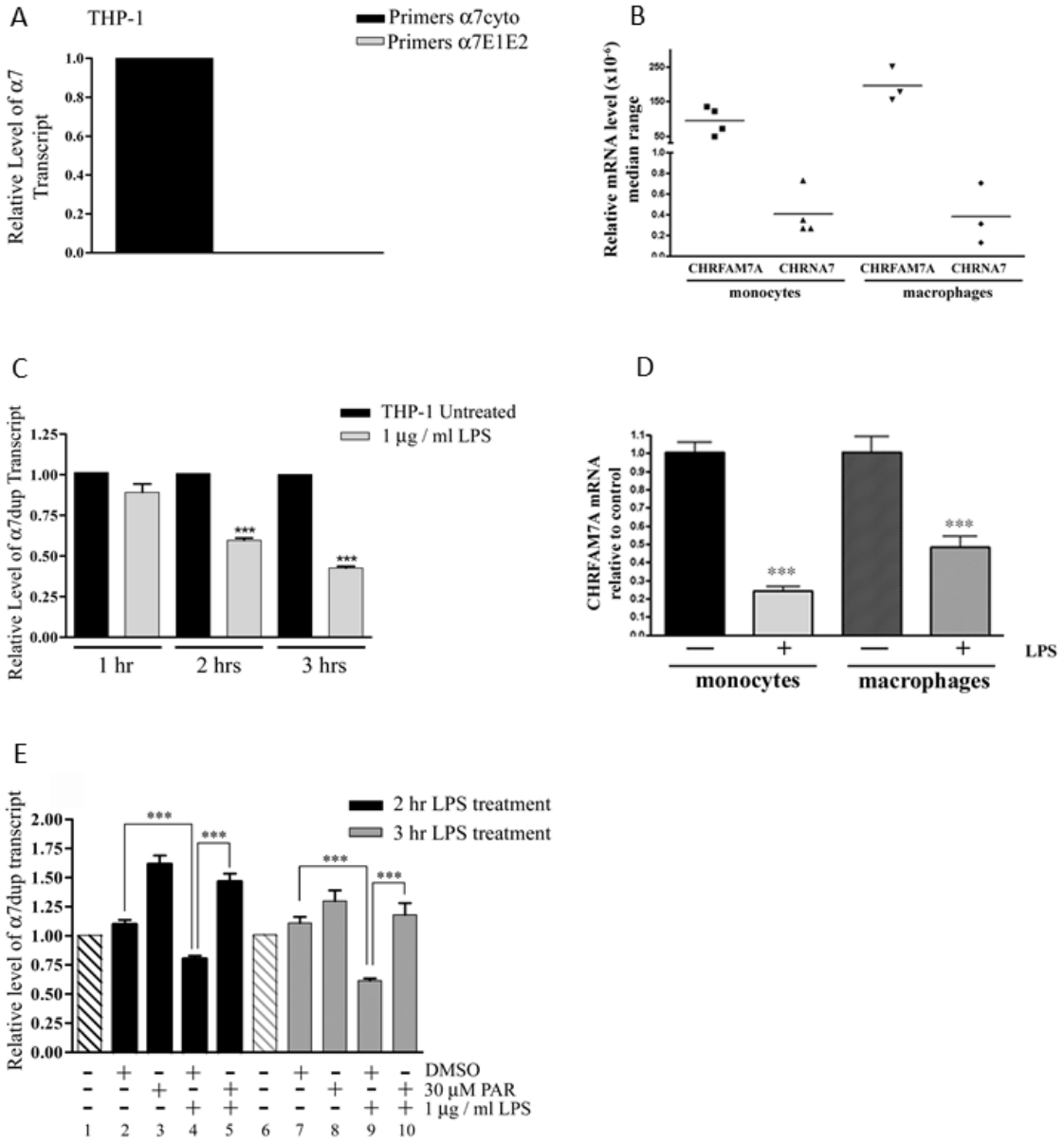

Figure 1.15: CHRFAM7A responsiveness to LPS in THP-1 cell line and human primary monocytes and macrophages. (A) The THP-1 cell line expresses the CHRFAM7A but not the CHRNA7 transcript. Real-Time PCR analysis was performed using different primers: the primers α7cyto amplifies both the α7 conventional and α7dup mRNAs, as they are designed across exon 9 and exon 10; the primers α7E1E2 amplifies only the α7 conventional transcript as they are complementary to a region across exon1 and exon2. While the primers α7cyto give rise to an amplicon, there is no amplification using the specific α7E1E2 primers, thus indicating that the THP-1 cell line express only the α7dup mRNA. (B) Real-Time analysis performed using specific primers for the α7 conventional (α7E1E2 primers) and α7dup (α7EAE5) transcript showed that primary monocytes and macrophages express both the isoforms and that the CHRFAM7A transcript is expressed at higher level compared to CHRNA7. (C) The LPS treatment (1 µg/mL) down-regulates the

CHRFAM7A transcript in THP-1 cell line after 2 hours and 3 hours. (D) The CHRFAM7A transcript down-regulation observed in THP-1 after LPS treatment is detectable also in primary monocytes and macrophages after 3 hours. (E) The down-regulation is a transcription-based mechanism reliant on the NF-κB transcription factor: indeed, the treatment with the NF-κB inhibitor Parthenolide up-regulates CHRFAM7A transcript after 3 hours of LPS treatment recovering the CHRFAM7A mRNA control level (modified from Benfante et al., 2011).

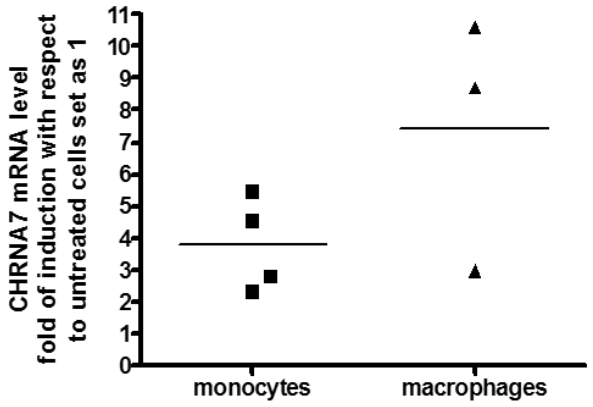

Figure 1.16: CHRNA7 responsiveness to LPS in human primary monocytes and macrophages. 3 hours LPS treatment (1 μg/mL) on primary monocytes and macrophages of respectively four and three healthy donors determines an up-regulation of the CHRNA7 transcript, detected by means of Real-time PCR. The graph shows CHRNA7 mRNA level normalized on GAPDH mRNA of LPS-treated monocytes and macrophages compared to that of the control samples set as 1. The monocytes show an up-regulation of about 4-fold, while macrophages CHRNA7 transcript is up-regulated of about 7.5-fold with respect to the untreated cells.

The LPS treatment causes alterations in CHRFAM7A transcript expression also in other cell models. Dang and collaborators analysed 9 different human gut epithelial cell lines, confirming the expression of both CHRNA7 and CHRFAM7A transcripts. Interestingly, while the LPS treatment does not affect the expression of CHRNA7, the CHRFAM7A mRNA showed a different responsiveness to LPS and is both up- and down-regulated depending on the cell line analysed (Dang et al., 2015). In the same study, the authors also investigated the CHRFAM7A promoter responsiveness to LPS in the gut epithelial cell line FHs. The CHRFAM7A promoter was predicted to encompass about 500 bp of the 5' flanking region from the ATG in exon B, in intron 2 and showed a 3-fold activity compared

to the promoter-less vector in the Luciferase assay. The LPS stimulation, however, determines only a slight increase in CHRFAM7A promoter activity (Dang et al., 2015).

The same CHRFAM7A 5' flanking region was tested to establish its transcriptional activity in THP-1 cell line, resulting in a 4-fold activity compared to the empty vector (Costantini et al., 2015). Moreover, the over-expression of CHRFAM7A transcript in THP-1 cell model alters the cell phenotype and the expression of genes associated with focal adhesion (Costantini et al., 2015).

These results, taken together, suggest that the α7dup protein is biologically active and may have a role in regulating the inflammatory process, adding a further level of complexity in the human resolution of inflammation.

1.4.4. CHRFAM7A involvement in human disease

1.4.4.1. Neurological disorders

The discovery of a new human-restricted gene in a genetic locus known to be involved in several psychiatric disorders has risen new possibilities for the genetic studies of neuropsychiatric diseases.

There are indeed several studies linking CHRFAM7A genotype or expression to schizophrenia. In 2006, Flomen and collaborators found a correlation between CHRFAM7A genotype and psychosis: in particular, the single allelic copy of CHRFAM7A (heterozygous genotype) occurred in 24% of psychosis patients, compared to the 16% of controls (Flomen et al., 2006). However, this correlation is very weak and the same authors were not completely convinced. Moreover, CNVs involving the deletion of 2 Mb in the region containing CHRNA7, CHRFAM7A and other genes, which are very rare in the common population, are otherwise overrepresented in population affected by schizophrenia (Stefansson et al., 2008), autism, neurodevelopmental disorders (Shinawi et al., 2009), intellectual impairment such as the Attention Deficit/Hyperactivity Disorder (ADHD) (Manchia et al., 2010; Wilens and Decker, 2007) and even more by idiopathic generalized epilepsy (Helbing et al., 2009). It has been hypothesized that the correlation between the CNVs and the aforementioned pathologies is more likely due to the absence

of CHRNA7 gene rather than CHRFAM7A and indeed there are also many cases of schizophrenic patients in which the CNV involves the CHRNA7 gene but not the CHRFAM7A gene, leaving the patient with only one copy of CHRNA7 and two copies of the dominant negative regulator (Stone et al., 2008).

A recent work by Kunii and collaborators found a decreased CHRNA7/CHRFAM7A expression level ratio in the prefrontal cortex of schizophrenic patients. Interestingly, decreased CHRNA7/CHRFAM7A ratio is also observed in immature and neonatal prefrontal cortex even in the absence of psychotic disorders, suggesting a neurodevelopmental role for CHRFAM7A (Kunii et al., 2015).

Other evidence supported the possible significance of CHRFAM7A in schizophrenia pathogenesis: in 2009, it was reported the correlation between the presence of the 2 base pair deletion polymorphism in CHRFAM7A gene and schizophrenia both in African Americans and Caucasian samples (Sinkus et al., 2009), and the same polymorphism was correlated to bipolar disorder (Hong et al., 2004), P50 sensory gating deficit (Raux et al., 2002; Flomen et al., 2013) and deficits in episodic memory, another endophenotype proposed for schizophrenia (Dempster et al., 2006).

The presence of the 2 base pair deletion in CHRFAM7A exon 6 was also investigated in idiopathic generalized epilepsy, even though the correlation is controversial, as some authors affirm an inverse correlation between the polymorphism and the pathogenesis (Rozycka et al., 2013) while other authors do not observe any correlation (Damiano et al., 2015).

Giving the numerous studies linking the CHRNA7 gene with dementia pathogenesis, also the CHRFAM7A gene has been investigated. Indeed, the CNV involving CHRFAM7A is overrepresented in Mild Cognitive Impairment (MCI) and late-onset AD patients (Swaminathan et al., 2012). Moreover, a recent work by Fehèr and collaborators investigated a possible correlation between the three different genotypes of CHRFAM7A (genotype 1: two wild type alleles; genotype 2: one wild type allele and one Δ2bp allele; genotype 3: two Δ2bp alleles) and four types of dementia, including Alzheimer's disease (AD), Dementia with Lewys bodies (DLB), Pick's Disease (PiD) and Vascular Dementia (VD). Fehèr et al. demonstrated a higher frequency of the CHRFAM7A genotype 1 (two wild type alleles) in AD, DLB and PiD samples, indicating the presence of the 2 bp

polymorphism in the genetic sequence as a protective factor against the development of these dementia. The authors hypothesized that the expression of the wild type dominant negative regulator reduces the α7nAChR function and increases the risk of neurodegenerative diseases, while the presence of the polymorphism and the consequent production of a truncated form of α7dup protein can result in a more efficient α7nAChR assembly, thus reducing the risk of developing neurological disorders (Fehèr et al., 2009).

1.4.4.2. Immunological disorders

Right now, little is known about a possible role of CHRFAM7A in human immunological disorders, although its high expression level in leukocytes and immune cells and its dominant negative regulatory role towards α7nAChR function makes it a promising marker or therapeutic tool for several immunological diseases.

The α7nAChR seems to be involved in the development of HIV-associated Neurocognitive Disorder (HAND), as it is activated by the HIV glycoprotein gp120 and is implicated in the neurotoxic effect exerted by this viral protein. In 2014, Ramos and collaborators showed that the exposure to increasing concentration of gp120 protein determined a simultaneously dose-dependent up-regulation of CHRNA7 and down-regulation of CHRFAM7A transcript in neuronal cell cultures. This effect was shown to be dependent on gp-120-CXCR4 interaction, as the administration of CXCR4 antagonists abrogated CHRNA7/CHRFAM7A expressional alteration. These results were also confirmed *in vivo*, as the authors found a significant up-regulation of CHRNA7 and a significant down-regulation of CHRFAM7A transcripts in post-mortem basal ganglia samples of HIV-infected patients (Ramos et al., 2014). Given the dominant negative effect of CHRFAM7A towards the α7nAChR functionality, the opposite regulation of the two genes can be partly explained by a toxicity effect exerted by gp120, which induce a dramatic increase in α7nAChR activity, mediating neuronal death (Ballester et al., 2012).

Recently, a study by Baird and collaborators investigated the expression of CHRFAM7A and CHRNA7 in intestine biopsies of individuals affected by Inflammatory Bowel Disease (IBD).

IBD is a complex nosological entity characterized by an inflammatory status of the gut, which include for example Crohn's Disease, Celiac Disease, and Ulcerative Colitis.

The expression analysis revealed an up-regulation of CHRFAM7A transcript in biopsies of Crohn's Disease and Ulcerative Colitis compared to control samples and a concomitant down-regulation of CHRNA7 mRNA (Baird et al., 2016).

2. Aim of the project

The α7nAChR has a pivotal role in regulating the inflammatory process and increasing evidence has reported its importance in the pathogenesis of neurodegenerative and inflammatory diseases. Recently, the CHRFAM7A gene, which is the product of the partial duplication of CHRNA7 gene, has been discovered. This gene has unique characteristics, as it is expressed exclusively in humans and exerts a dominant negative effect towards α7nAChR functions. Since its discovery, the CHRFAM7A gene has rapidly become the point of interest of several studies which have linked its expression and genotypes to different neuropsychiatric diseases. So far, little is known about the expression and biological role of CHRFAM7A in inflammatory diseases, although several studies suggested the involvement of CHRFAM7A altered expression in inflammatory and/or infective pathologies. Interestingly, the acute treatment of human primary monocytes and macrophages with LPS, which is considered a paradigm of acute inflammation, down-regulates CHRFAM7A transcript, by a NF-κB-driven mechanism, and up-regulates CHRNA7 mRNA.

The down-regulation of CHRFAM7A and the up-regulation of CHRNA7 in response to LPS have led us to hypothesize a possible regulatory role for CHRFAM7A in the Cholinergic Anti-Inflammatory Pathway. The protein encoded by CHRFAM7A would indeed act as a sensor protein influenced by the inflammatory status. In the early phase of inflammation, the signalling triggered by LPS-TLR4 down-regulates the expression of CHRFAM7A, reducing the number of dominant negative subunits which counteract the formation of the functional receptors. The concomitant up-regulation of the conventional CHRNA7 results in an increased number of α7nAChR in the membrane and in potentiation of the Cholinergic Anti-Inflammatory Pathway. In this perspective, the CHRFAM7A transcriptional regulation becomes a key step in the resolution of human inflammation.

The mechanisms driving the transcriptional regulation of CHRFAM7A gene are still almost unknown.

In this project, we have investigated the transcriptional mechanisms regulating CHRFAM7A expression in two particular cell models: the human acute monocyitc

leukemia cell line THP-1 and the neuroblastoma cell line SH-SY5Y. Given the high expression levels of CHRFAM7A in the human CNS and leukocytes, we have decided to focus on these two cell lines, in order to explore possible differences in tissue-specific expression patterns and regulatory mechanisms. Our goal was to identify the minimal CHRFAM7A promoter driving its expression and to explore its responsiveness to inflammatory stimuli, such as LPS treatment.

Recent studies have demonstrated the central role of CHRNA7 in the development of neurological disorders, including Alzheimer's disease (AD). Changes in CHRNA7 expression or function can concur to AD development either by altering the normal neuronal function and/or by unbalancing the pro- and anti-inflammatory signal equilibrium. Given the little knowledge regarding the expression and the role of CHRFAM7A gene in AD onset and progression, our aim was to investigate whether altered transcriptional regulation of CHRFAM7A could contribute to AD development. In this context, we focused our attention on the acetylcholinesterase inhibitor Donepezil, which is the leading drug used in AD therapy. We identified a specific effect of Donepezil on the transcription of CHRFAM7A both in monocytic THP-1 cells, and human primary macrophages and Peripheral Blood Mononuclear Cells (PBMCs) of AD patients.

Overall, our findings provide important insights on the molecular mechanisms of Donepezil, supporting its anti-inflammatory potential and suggesting new research lines on AD therapy.

3. Materials and Methods

3.1. Cell Lines

The human acute monocytic leukemia cell line THP-1 and the human neuroblastoma cell line SH-SY5Y were cultured in RPMI 1640 (Lonza) supplemented with 10% fetal bovine serum (FBS), penicillin (100 U/ml), streptomycin (100 µg/ml) and L-glutamine (2 mM) at 37 °C in the presence of 5% CO_2. THP-1 cells were maintained at a recommended density of between $2x10^5$ and 10^6 cells/ml. Primary monocytes and macrophages were obtained as previously described (Benfante et al., 2011). Briefly, blood CD14+ monocytes were obtained from buffy coats of four different healthy donors using Ficoll-Hypaque (Ficoll, Biochrome) and Percoll (Amersham Pharmacia Biotech) gradient centrifugation. The macrophages were obtained from monocytes' differentiation after six days of culturing in standard condition in the presence of ng/mL M-CSF 100.

3.2. Cell treatment

THP-1 cells were counted and seeded at density of 3 x 10^5 cells/mL the day before all treatments. Each experiment was performed with cells at low passage.

The Escherichia Coli 055: B5 strain (Sigma Aldrich Co., St. Louis, MO, USA) was used for the LPS treatment: the cells were challenged for 6 hours at the final concentration of 1 µg/mL LPS.

The treatment with the cholinesterase inhibitor Donepezil was performed using Donepezil hydrochloride monohydrate (Sigma Aldrich Co., St. Louis, MO, USA): the THP-1 cells were treated at the final concentration of 10 µm, 20 µm, 30 µM and 50 µM for 3, 6, 12 and 24 hours. The SH-SY5Y cells were instead treated with 30 µM Donepezil concentration for 3h and 6h.

The transcription arrest studies were performed on THP-1 cells with 3 hours pre-treatment with 30 µM Donepezil followed by treatment with the Polymerase II inhibitor DRB (Sigma Aldrich Co., St. Louis, MO, USA) at 75 µM final concentration. The cells were

collected at 1 hour, 2 hours and 4 hours after DRB challenge. Untreated THP-1 and DMSO-treated (DRB vehicle) THP-1 cells were used as control.
Macrophages were treated with 1 μg/mL of LPS for 1 hour and with 20 μM Donepezil for three hours.

3.3. 5' RACE

5' terminus has been determined by 5' RACE. The *FirstChoice RLM-RACE* kit (AMBION) was used according to the manufacturer's instructions. Briefly, total RNA from THP-1 and SH-SY5Y cells and primary monocytes and macrophages was treated with CIP enzyme (Calf Intestinal Alkaline Phosphatase), at 37 °C for one hour, to remove the 5'-phosphate group from ribosomal RNA, tRNA, degraded mRNA fragment and genomic DNA and a 45 bp long adapter was ligated by T4 RNA ligase, after TAP mediated decapping of mRNA. RNA was collected by centrifugation at 14000 rpm for 20 minutes at 4 °C; the pellet was washed with 0.5 ml of 70% ethanol and resuspended in RNase-free water to proceed with the following step. Adapter-ligated mRNA was reverse transcribed by means of *SuperScript III First-Strand Synthesis System RT-PCR* (Life Technologies), using random hexamers and cDNA was amplified by nested PCR with *GoTaq Flexi* (Promega) used according to the manufacturer's instructions. cDNA was amplified by an initial denaturation step at 95 °C for 3 minutes followed by 40 cycles of 30'' denaturation at 95 °C, 45''annealing at 60 °C, 80" elongation at 72 °C and one cycle of a 5 minutes elongation step at 72 °C. The primers used for the outer PCR reaction are described in **Table 2.1**.

Name	Sequence
Outer FW	5' – GCT GAT GGC GAT GAA TGA ACA CTG - 3'
Ex5 REV	5' – GTT AGT GTG GAA TGT GGC GTC AAA GC - 3'
Ex6 REV	5' – ACA TCG ATG TAG CAG GAA CTC TTG A - 3'
Inner FW	5'- CGC GGA TCC GAA CAC TGC GTT TTG CTG GCT TTG ATG - 3'
ExA REV	5'- GCA GTT TGC AGC TAT CCA CAA AAT GC - 3'
Ex5 REV	5' – TAG TGT GGA ATG TGG CGT CAA AGC G - 3'

Table 2.1: Sequence of the primers used in the 5'-RACE experiment.

3.4. Total RNA Extraction and Reverse Transcription

Total RNA was extracted using the *RNeasy Mini kit* and accompanying *QIAshredder* (Qiagen), according to the manufacturer's instructions. Briefly, a maximum of $9x10^6$ cells was collected by centrifugation and the cells lysed with 600 µl of buffer RLT, previously added with β-mercaptoethanol (10 µl/ml RLT buffer). The lysate was homogenized by means of QIAshredder column centrifuged for 2 minutes at maximum speed.

To avoid DNA contamination, samples were on-column incubated with DNase I for 15 minutes and RNA eluted with 50 µl of RNase-free water. The amount of eluted total RNA was determined by spectrophotometer at 260 nm and its purity was evaluated using the 260/280 ratio; 1 µg per sample was reverse transcribed using the SuperScript™ III First-Strand Synthesis System for RT-PCR (Invitrogen Ltd., Paisley, UK) in accordance with the manufacturer's instructions.

3.5. Standard PCR protocol using GoTaq Flexi (Promega)

The standard PCR protocol was performed with the GoTaq Flexi kit (Promega) following the manufacturer's instruction, using a $MgCl_2$ concentration of 1.5 mM and 0.5 µM primers final concentration. The thermal protocol was performed using an annealing temperature of 55°C-60 °C (depending on the CG contents of the primers) and an extension temperature of 72 °C.

The sequence of the primers used in standard PCR protocol is reported in **Table 2.2**.

Name	Sequence
Promoter 1 FW	5'-CGC GAG TGT GAG GAA GGG A-3'
Promoter 2 FW	5'-CAA GTC CTC GGT GCC CCT T-3'
Promoter RV	5'-AGG TGT CCA CTT GTA ATC TTA ATG T-3'

Table 2.2: Sequence of the primers used in the standard PCR for the identification of the alternative promoters in THP-1 and SH-SY5Y cDNA.

3.6. High Fidelity PCR using Expand High Fidelity PCR System (Roche)

The High Fidelity PCR protocol was performed using the Expand High Fidelity PCR System (Roche) according to the manufacturer's instruction, using the suggested thermal protocol. The sequences of the primers used is reported in **Table 2.3**.

Name	Sequence
Intron 5 -2487 FW	5'-CAC TTA CAC ACA TGC AGG CA-3'
Intron 5 -1037 FW	5'-ATC TGG TTT CCT CCC CTT GG-3'
Intron 5 -610 FW	5'-TTA CGG GCA TGA GAC ACT GT-3'
Ex 6 REV	5'-CCA CTA GGT CCC ATT CTC CAT TG-3'

Table 2.3: Sequence of the primers used in the High Fidelity PCR performed for the identification of a novel TSS in CHRFAM7A Intron 5.

3.7. Quantitative Real-Time PCR

Gene expression analyses were performed by quantitative Real-Time PCR assay using the QuantStudio 5 Thermocycler (Applied Biosystems, CA) and QuantStudio 5 software. The target sequences were amplified from 50 ng of cDNA in the presence of TaqMan® Gene Expression Master Mix Kit (Applied Biosystem, CA).

The TaqMan® primer and probe assays used were human CHRNA7 (ID #Hs01063373_m1), human CHRFAM7A (ID #Hs04189909_m1) and the endogenous control GADPH (ID #Hs99999905_m1) 18S (ID#Hs99999901_s1) and ACTB (ID#Hs01060665_g1). The $2^{-\Delta\Delta CT}$ method was used to calculate the results, thus allowing the normalization of each sample to the endogenous control, and comparison with the calibrator for each experiment (set to a value of 1).

3.8. Absolute quantification by Real-Time RT-PCR

Absolute quantification analysis was performed by quantitative Real-Time PCR assay using the ABI Prism™ 7000 Sequence Detection System (Applied Biosystems, CA) and SDS software version 1.2.3 and the Power SYBR® Green Master Mix (Applied Biosystem, CA), with specific primers for the CHRFAM7A isoform 1 and CHRFAM7A isoform 2 transcripts (**Table 2.4**).

To estimate the number of copies of CHRFAM7A isoform 1 and 2 per ng of total RNA, serial dilutions of plasmid containing CHRFAM7A isoform 1 and 2 fragments were included in the Real-Time PCR assay to obtain a standard curve.

Briefly, the CHRFAM7A isoform 1 and CHRFAM7A isoform 2 Forward and Reverse primers were used in standard PCR assay on THP-1 cDNA in order to obtain an amplicon of 81 bp and of 135 bp, respectively. The fragments were then purified from agarose gel by means of the *NucleoSpin ® Gel and PCR Clean Up* kit (Macherey-Nagel, Neumann-Neander, Germany) and cloned into the empty vector pCR2.1 with the *TOPO-TA-cloning* kit (TermoFisher Scientific), according to the manufacturer's protocol. The identity of the two constructs was confirmed by sequencing.

In order to obtain the standard curve, the two constructs were linearized with NcoI digestion and dephosphorylated with the *T-SAP* enzyme (Euroclone). Their concentration was measured by spectrophotometer at 260 nm.

The number of molecules for ng of plasmid was calculated with the reported formula:

Number of molecules = ng of plasmid / (660 kDa x plasmid length)

Serial dilutions of the two plasmids from 10^5 copies/µL to 10 copies/µL were generated and analysed by means of ABI Prism™ 7000 Sequence Detection System (Applied Biosystems, CA) and SDS software version 1.2.3 and the Power SYBR® Green Master Mix (Applied Biosystem, CA), with CHRFAM7A isoform 1 and 2 Forward and Reverse primers at concentration of respectively 300nM-300nM and 300nM-900nM.

The standard curves were performed in order to obtain a slope comprised between -3.2 and -3.6 and a R^2 >0.98.

The serial dilutions were included in all the Real-Time PCR analysis, together with the cDNA samples.

Data Analysis- The results are expressed as the mean ± standard deviation of three independent experiments. The plasmid serial dilutions allowed to interpolating the Ct values for each cDNA analysed to the calibration curve, returning the number of cDNA molecules/µL as result. The number of molecules for ng of RNA was obtained considering that 1 µL contains cDNA derived by the retrotranscription of 50 ng of total RNA.

Name	Sequence
CHRFAM7A isoform 1 FW	5'-GCA CTC TGA CAA ATA ATG AAA CAA CC-3'
CHRFAM7A isoform 1 REV	5'-TTG GAA CTG AAA ATG CTG GTA GTG-3'
CHRFAM7A isoform 2 FW	5'-AGA TTA CAA GTG GAC ACC TGA GT-3'
CHRFAM7A isoform 2 REV	5'-AAT GTG GAA TTG TCA GAG TGC TTT CT-3'

Table 2.4: Sequence of the primers used in the absolute quantification of the CHRFAM7A-201 and -202 transcripts.

3.9. Plasmid vectors

All of the reporter constructs were obtained by sub-cloning fragments of the human CHRFAM7A gene 5'-flanking region into the pGL4b and pGL4.11 plasmid (pGL4.11, Promega).

CHRFAM7A -2122 bp/-1 bp_pGL4basic: The genomic region including exon D (from -2122bp to -155bp with respect to ATG codon in exon B) was obtained by PCR amplification of THP-1 genomic DNA with *GoTaq Flexi* (Promega) with the primers Forward (5'-ATGACACCAACCATGAGGTCCCA-3') and Reverse (5'-TTGGCCTTGAACCCGGACAT-3'), while the region including exons D, C and B (from -249 bp to -1 bp) was obtained by RT-PCR from the cDNA extracted from THP-1 cell line, with the primers Forward (5'-TCCGGGTTCAAGGCCAAACC-3') and Reverse (5'-CTTAATGTTGCGGTGGGGCG-3'). The two fragments were cloned into the PCRII vector

(ThermoFisher Scientific), according to the manufacturer's instruction, generating the CHRFAM7A -2122 bp/-155 bp_pCRII and a CHRFAM7A -249 bp/-1 bp_pCRII vectors; the genomic fragment was then digested with HindIII and the cohesive end was filled in with the Klenow fragment, followed by Sac II digestion. The cDNA fragment was instead digested with EcoRV and SacII and was cloned into the vector containing the genomic region. The whole fragment was then extracted by digestion with Nco I and subcloned into the pGL4basic (Promega, Madison, USA) vector.

CHRFAM7A -2122 bp/-184 bp_pGL4b: The CHRFAM7A -2122 bp/-1 bp_pGL4b was digested with Eco RV and Sac II in order to exclude the exons C and B. The fragment containing the putative promoting region and exon D (from -2122 bp to -184 bp with respect to ATG in exon B) was blunted with the T4 polymerase (NEB) and cloned into the pGL4basic vector linearized with Eco RV.

CHRFAM7A -2122 bp/-184 bp_pGL4.11: The CHRFAM7A -2122 bp/-1 bp_pGL4b was digested with Eco RV and Sac II in order to exclude the exons C and B. The fragment containing the putative promoting region and exon D (from -2122 bp to -184 bp with respect to ATG in exon B) was blunted with the T4 polymerase (NEB) and cloned into the pGL4.11 vector linearized with Eco RV.

CHRFAM7A -2015 bp/-184 bp_pGL4b: The CHRFAM7A -2122 bp/-184 bp_pGL4b was digested with Eco RV and Avr II and then filled in with the Klenow fragment (NEB), in order to delete 108 bp from the promoter region.

CHRFAM7A -2015 bp/-184 bp_pGL4.11: The region included between -2015 bp and -184 bp with respect to the ATG in exon B was obtained from the CHRFAM7A -2015 bp/-184 bp_pGL4b by digestion with Xho I and Hind III and cloned into pGL4.11.

CHRFAM7A -1819 bp/-184 bp_pGL4.11: The CHRFAM7A -2122 bp/-184 bp_pGL4.11 vector was digested with Eco RV and PflM I, blunted with the T4 polymerase and then ligated.

CHRFAM7A -1459 bp/-184 bp_pGL4.11: The vector CHRFAM7A -2122 bp/-1 bp_pCRII was digested with Nhe I and Nru I and the fragment was filled in with the Klenow fragment. The region extracted (from -1459bp to -735 bp with respect to the ATG in exon B) was then cloned into the CHRFAM7A -2122 bp/-184 bp_pGL4.11 vector digested with Eco RV and Nru I.

CHRFAM7A -1163 bp/-184 bp_pGL4basic: The CHRFAM7A -2122 bp/-184 bp_pGL4basic vector was digested with Spe I and Pvu II and the fragment obtained was filled in with the Klenow fragment and then cloned into the pGL4basic vector digested with Eco RV and Pvu II.

CHRFAM7A -1163 bp/-184 bp_pGL4.11: The CHRFAM7A -1163 bp/-184 bp_pGL4basic was digested with Kpn I and Hind III in order to extract the fragment spanning from -1163 bp to -184 bp with respect to the ATG in the exon B and the fragment was then cloned into the pGL4.11 vector digested with Kpn I and Hind III.

CHRFAM7A -735 bp/-184 bp_pGL4basic: The CHRFAM7A -2122 bp/-184 bp_pGL4b was digested with Nru I and Hind III and the fragment was cloned into the pGL4basic digested with Eco RV and Hind III.

CHRFAM7A -735 bp/-184 bp_pGL4.11: The CHRFAM7A -735 bp/-184 bp_pGL4basic was digested with Kpn I and Hind III in order to extract the fragment, cloned into the pGL4.11 digested with Kpn I and Hind III.

CHRFAM7A -557 bp/-184 bp_pGL4basic: The CHRFAM7A -2122 bp/-184 bp_pGL4b was digested with Eco RV and Eco NI and then ligated.

CHRFAM7A -557 bp/-184 bp_pGL4.11: The CHRFAM7A -2122 bp/-184 bp_pGL4.11 was digested with Kpn I and Hind III and the fragment was cloned into the pGL4.11 vector digested with Kpn I and Hind III.

CHRFAM7A -4280 bp/-184 bp_pGL4.11: The CHRFAM7A -4280 bp/-1 ΔAlu_pGL4basic was digested with Eco RV and PflM I and the fragment was inserted into the CHRFAM7A -2122 bp/-184 bp_pGL4.11 digested with the same enzymes.

CHRFAM7A -2122 bp/-184 bp ΔTSS SH-SY5Y_pGL4basic: In order to generate a construct with a specific deletion in correspondence to the Transcription Start Site (TSS) characteristic of the SH-SY5Y cell line, included between -417bp and -402bp with respect to the ATG in exon B, we have performed a PCR-based strategy. The region between -591 bp and -417 bp was amplified by PCR using the *GoTaq Flexi* (Promega) with the primers forward 5'-GACGAGGACCGGGGC-3' and reverse 5'-GCGGCTGCACCGAGGACTTGGC-3'. At the same way, the region between -402 bp and -184 bp was amplified with the primers forward 5'-CTCGGTGAGCCGCGCTCCCAC-3' and reverse 5'-GGCCTTGCTTGGCAATC-3'. The reverse primer of the second PCR reaction maps on the pGL4basic backbone sequence which contains a HindIII restriction site. The reverse primer of the first PCR reaction and the forward primer of the second PCR reaction contain at 5' end two sequences (underlined) that are complementary to each other. The two PCR products, of 175 bp and 257 bp, were purified from agarose gel and the annealing between the two complementary regions of the forward and reverse primers was allowed by a thermal protocol including 3 minutes at 95°C, and 5 cycles of expansion protocol with an annealing temperature of 30°C. After the annealing cycles, the primers forward of the first PCR reaction and reverse of the second PCR reaction were added and the amplification of the entire fragment was allowed by a standard thermal PCR protocol. After the agarose gel purification, the PCR product of about 431 bp was cloned into the pCRII vector and extracted by Eco NI and Hind III digestion. The fragment of 364 bp was then cloned into the CHRFAM7A -2092 bp/-184 bp_pGL4basic digested with Eco NI and Hind III and its identity was established by sequencing.

CHRFAM7A -735 bp/-184 bp ΔTSS SH-SY5Y_pGL4basic: The CHRFAM7A -2122 bp/-184 bp ΔTSS SH-SY5Y_pGL4basic construct was digested with Nru I and Hind III enzymes and the

fragment of 568 bp were then ligated into the pGL4basic vector digested with Eco RV and Hind III.

CHRFAM7A -735 bp/-184 bp INTRON4-Luc_pGL4.11: The sequence specific of the CHRFAM7A intron 4 was amplified from genomic DNA by standard PCR using *GoTaq Flexi* (Promega) with the primers Forward (5'- CTCGAGGGCAATTTTTATGGGCATTCC -3') and Reverse (5'-CTCGAGGACCCACACTTGGTTTGTGCTTC-3') carrying at the 5' ends the restriction site for the XhoI enzyme (underlined). The PCR product was purified from agarose gel, cloned into the pCRII vector and then excided with Xho I. The digestion product was then cloned into the CHRFAM7A -735 bp/-184 bp_ pGL4.11 construct digested with Sal I, in order to insert the intron 4 fragment at the 3' end of the Luciferase gene.

CHRFAM7A -735 bp/-184 bp INTRON4 ΔAlu-Luc_pGL4.11: The intron 4 sequence from -3281 bp to -1400 bp from the first nucleotide in exon A was amplified using the Forward primer (5'- CTCGAGGGCAATTTTTATGGGCATTCC -3') and the Reverse primer (5'-CTCGAGACTGCCTTCTACCCATTTGTTC -3') with the Xho I site at the 5' end (underlined) with *GoTaq Flexi* (Promega). The PCR product was purified from agarose gel and cloned into the pCRII vector. The fragment was then digested with Xho I and cloned into the -735 bp/-184 bp_ pGL4.11 construct digested with Sal I, in order to insert the intron 4 fragment at the 3' end of the Luciferase gene.

CHRFAM7A -2122 bp/-557 bp_pGL4.11: The CHRFAM7A -2122 bp/-184 bp_pGL4.11 was digested with Hind III and Eco NI and the fragment of 1570 bp was blunted by Klenow fragment treatment and cloned into the pGL4.11 vector digested with Eco RV.

CHRFAM7A -447 bp/-184 bp_pGL4.11: The pCRII vector containing the sequence from -447 bp to exon 5 amplified during the 5'-RACE protocol was digested with Eco RV and Sac II and the 250 bp long fragment was blunted with T4 polymerase and cloned into the pGL4.11 vector digested with Eco RV.

3.10. Transient transfection and luciferase assay

THP-1 cells and SH-SY5Y cells were transfected by means of a lipid based method (DREAMFECT Gold, Li Star Fish and Fugene HD, Promega, respectively). The day before transfection, 1x 10^6 THP-1 and 2.5 x 10^5 SH-SY5Y cells were plated in 2 ml complete RPMI medium in a 6-well plate. The day of transfection, 50 µl of plain RPMI medium were mixed with 2 µg of plasmid DNA (Mix 1), with the *Firefly* and *Renilla* containing construct in a 1:1 molar ratio; in another tube 50 µl plain RPMI medium were mixed with 8 µl DREAMFECT gold or Fugene HD (Mix 2), in order to have a 1: 4 DNA/lipid ratio.

Mix 2 was added to Mix 1, gently mixed and left for 20 minutes at room temperature, to allow for the formation of the lipid-DNA complexes that were added drop-wise to the cells. All of the transfections were performed in duplicate, and each construct was tested in at least three independent experiments using different batches of plasmid preparation.

The activity of the CHRFAM7A constructs was evaluated 24 hours after transfection by means of the commercial kit Dual-Luciferase Reporter Assay System (Promega), that allows to measure the bioluminescence produced by the two luciferase genes (*Firefly* and *Renilla* luciferase) independently. The activity of Luciferase was measured using a GloMAx Discovery Luminometer (Promega).

3.11. Data analysis

For each construct, the values of *Firefly* luciferase obtained in the different experiments (expressed as relative luminescence units, RLU) were plotted against the corresponding values of *Renilla* luciferase (also expressed as RLU). Linear regressions were obtained with correlation coefficients ranging from 0.75 to 0.99. The transcriptional activity of each construct was defined as the slope of the straight line and expressed as the fold increase over the transcriptional activity of the promoter-less plasmid pGL4.11. The results are given as the mean values ± standard deviation (SEM) of at least three independent experiments. The data were analysed by means of one-way ANOVA, Tukey's test using GraphPad Prism 5 Software (GraphPad Software, Inc.); p values <0.05 were considered significant.

3.12. Chromatin Immunoprecipitation

The day before treatment, THP-1 cells were plated in petri dishes with a density of 5 x 10^5/mL. After 24 hours, the cells were treated with 1µg/mL LPS for 1 hour and 30 minutes. Treated and untreated cells were then collected in order to have 2 x 10^6 cells for sample and the Chromatin Immunoprecipitation protocol was then performed as described below.

1 x 10^7 of treated and untreated THP-1 cells were cross-linked with 1% formaldeyde for 10 minutes and neutralized with 0.125 M glycine for 5 minutes. The cells were then washed with PBS 1X and centrifuged, resuspended in 1 mL of Cell Lysis Buffer (Hepes 5 mM, KCl 85 mM, Triton X-100 0.5%) added with 1 mM PMSF, centrifuged and resuspended in 1 mL of Nuclei Lysis Buffer (Tris HCl pH 8 50 mM, EDTA 10 mM, SDS 1%) added with 1 mM PMSF. The lysate was sonicated in order to obtain chromatin fragments of about 200 nucleotides. 500 µL of sonicated lysate were then pre-cleared for 2 hours with 500 µL of *Novex rProtein G Agarose* beads (Life Technologies) in 4 mL of ChIP Dilution Buffer (SDS 0.01%, Triton X-100 1.1%, EDTA 1.2 mM, Tris HCl pH 8 16.7 mM, NaCl 167 mM), while 100 µL were conserved as Input. 1 mL of the pre-cleared chromatin was added in 1.5 mL tubes together with 5 µg of antibodies specific for the NF-κB subunit p65 (Santa Cruz, Oregon, USA), or p50 (Santa Cruz, Oregon, USA), or c-Rel (Santa Cruz, Oregon, USA), or with the antibody for the Acetylation of Histone 4 (Millipore), or with the Rabbit IgG (Santa Cruz, Oregon, USA). The chromatin and the antibodies were then incubated over night at 4°C.

In order to promote the antibody-beads binding, we used pre-coated beads, incubated over night with CBB buffer added with 10% of BSA (NEB).

40 µL of pre-coated beads were added to the chromatin samples and incubated for 3 hours at 4 °C. The following steps consisted in 5 washes of 10 minutes with Wash Buffer High Salt (SDS 0,1%, EDTA 2 mM, Triton X-100 1%, Tris HCl pH8 20 mM, NaCl 500 mM), Wash Buffer Low Salt (SDS 0,1%, EDTA 2 mM, Triton X-100 1%, Tris HCl pH8 20 mM, NaCl 150 mM) and LiCL Buffer (LiCl 250 mM, NP-40 1%, EDTA 1 mM, Tris HCl pH8 10 mM). The

beads were then eluted in 150 µL of Elution Buffer (Tris HCl pH8 50 mM, EDTA 10 mM, SDS 1%) and DNA de-crosslinked by over-night incubation at 65°C.

The DNA was then purified using the *Chromatin IP DNA Purification* kit (Active Motif).

The DNA obtained from the ChIP protocol was analyzed by means of standard PCR assay using primers specific for the IL-6 and CHRFAM7A promoter (**Table 2.5**).

Name	Sequence
IL-6 promoter FW	5'-GCC TCA ATG ACC ACC TAA GC-3'
IL-6 promoter REV	5'-GAG CCT CAG ACA TCT CCA GTC-3'
CHRFAM7A promoter FW	5'-CCC TGT TGG AGA CCT GGC CA-3'
CHRFAM7A promoter REV	5'-TAC TTT GCC GTG TTC CCT GGT G-3'

Table 2.5: Sequence of the primers used in the standard PCR protocol on ChIP samples.

3.13. Electrophoresis Mobility Shift Assay

Nuclear extracts were prepared from untreated and LPS-treated (1h, 1 µg/mL) THP-1 cells. Briefly, the cell pellet was resuspended and centrifuged twice in buffer A (Hepes 10 mM, $MgCl_2$ 1.5 mM, KCl 10 mM, PMSF 0.2 mM, DTT 0.5 mM), centrifuged and resuspended in buffer C (Hepes 20 mM, glycerol 25%, EDTA 0.2 mM, PMSF 0.2 mM, DTT 0.5 mM).

The double-stranded oligonucleotides, whose sequence is reported in **Table 2.6**, were marked with the filling-in method, by incubating 1-2 ρmoles of oligonucleotides for 20 minutes at 25°C in the presence of 330 µM dNTPs, 40 µCi of α^{32}P dCTP, 1000 U of Klenow fragment and Buffer 10X. 5 ρg of untreated and LPS-treated THP-1 nuclear extract were then incubated in the presence of 2 µg of poly(dI-dC) (Sigma Aldrich), 100 mM NaCl/KCl and binding buffer 2X (Ficoll 4%, Hepes 20 mM, MgCl2 1 mM, DTT 0.5 mM). 10,000-20,000 cpm of marked oligonucleotide (1 fmol) or cold oligonucleotide were then added with or without the specific antibodies against NF-κB p65 (Santa Cruz, Oregon, USA), p50 (Santa Cruz, Oregon, USA), or c-Rel (Santa Cruz, Oregon, USA), and the reactions were incubated in ice for 30 minutes. Products were electrophoresed at 30 mAfor 3 h on 4.8%

polyacrylamide gels in high ionic strength buffer (50 mM Tris, 380 mM glycine, 2 mM EDTA, pH -8.5) and dried gels analysed by autoradiography.

Name	Sequence
CHRFAM7A NF-κB WT FW	5'-GGC CCT TGT CCT GGG AGG CCC ATG CAC CAA CA-3'
CHRFAM7A NF-κB WT REV	5'-GGT GTT GGT GCA TGG GCC TCC CAG GAC AAG GG-3'
CHRFAM7A NF-κB mut FW	5'-GGC CCT TGT CCT TTC TGG GCC CAT GCA CCA CA-5'
CHRFAM7A NF-κB mut REV	5'-GGT GTT GGT GCA TGG GCC CAG AAG GAC AAG GG-3'
Consensus NF-κB FW	5'-GGA GTT GAG GGG GAC TTT CCC AGG C-3'
Consensus NF-κB REV	5'-GGG CCT GGG AAA GTC CCC CTC AAC T-3'

Table 2.6: Sequence of the oligonucleotides used in the EMSA protocol.

3.14. Human biological samples

The RNA of different human brain areas, including hippocampus, thalamus, caudatum, cerebellum, Girus Frontalis Superior (GFS), Girus Temporalis Superior (GTS) and Lobus Parietalis Superior was kindly donated by Dr. Carlo Sala of Istitituto di Neuroscienze (IN), Consiglio Nazionale delle Ricerche (CNR), Milano.

The RNA of human post-mortem hippocampal tissue of control individuals and Alzheimer's disease patients was kindly donated by Prof. Marco Venturin of Università degli Studi di Milano.

The RNA extracted from human PBMCs obtained by healthy individuals, Alzheimer's disease patients and Alzheimer's disease patients treated with Donepezil was kindly donated by Prof. Carlo Ferraresi of the Università di Milano Bicocca. The healthy controls were demonstrated not to have any personal or familial of neurological or psychiatric disorders. Alzheimer's disease patients were diagnosed according to the National Institute of Neurological and Communicative Disorders and Stroke and the Alzheimer's Disease and Related Disorders Association criteria (McKhann et al., 1984), and alternative diagnoses were excluded by brain imaging and an extensive neuropsychological test

battery. Alzheimer's disease patients undergoing Donepezil treatment were treated with 10 ng Donepezil o.d. for at least six months.

4. Results

4.1. Characterization of CHRFAM7A transcriptional regulation

4.1.1. Identification of the CHRFAM7A regulatory region

CHRNA7 and its duplicated form CHRFAM7A are located on Chr.15, 1.6 Mb apart, making unlikely that the same regulatory region can control the expression of both genes.

In silico analysis by means of ENSEMBL and NCBI database, showed that CHRFAM7A is encoded by a ten exons gene (a hybrid of exons D-A and 5-10 from CHRNA7), whose transcription gives raise to two alternative spliced mRNA that differ for the presence of exon B. These two transcripts contain an open reading frame due to the presence of two ATG codons, one in exon B and one in exon 6, giving raise to two proteins of 46.22 kDa and of 35.48 kDa, respectively (**Fig. 4.1.1A**). The EST (Expressed Sequence Tag) analysis of CHRFAM7A gene predicted that the start of transcription is located 566 bp upstream the ATG codon in exon B, defining a 410 base pairs length for exon D and a length for 5'UTR specifying region of 566 bp in the case of the mRNA encoding the isoform 1, and 919 bp, in the case of the isoform 2 (ORF starting from exon 6).

An *in silico* analysis of a region spanning 2600 bp of CHRFAM7A 5' flanking region, by means of the MatInspector database (http://www.genomatix.de), a databank of known regulatory element for transcription factors, identified a number of sites for Sp1 factor, the Aryl hydrocarbon receptor (AhR), the Kruppel-like family transcription factors, STAT3 transcription factor and a binding site for NF-κB. The latter is crucial in the regulation of CHRFAM7A gene, as it could be the site through which NF-kB negatively regulates the the expression of the α7 duplicated gene in response to LPS (**Fig. 4.1.1B**).

The presence of consensus sequences of known transcription factors suggested that this region could be a good candidate for driving the expression of CHRFAM7A gene. The *in silico* sequence analysis allowed us to map an Alu sequence located between 560 and

260 bp upstream the putative transcriptional start site (- 1185 bp/- 851 bp with respect to the ATG codon in exon B), as predicted by EST analysis. This sequence, typically 300 bp long, is highly repeated in the human genome, with an associated negative role on gene expression (Ebihara et al., 2002).

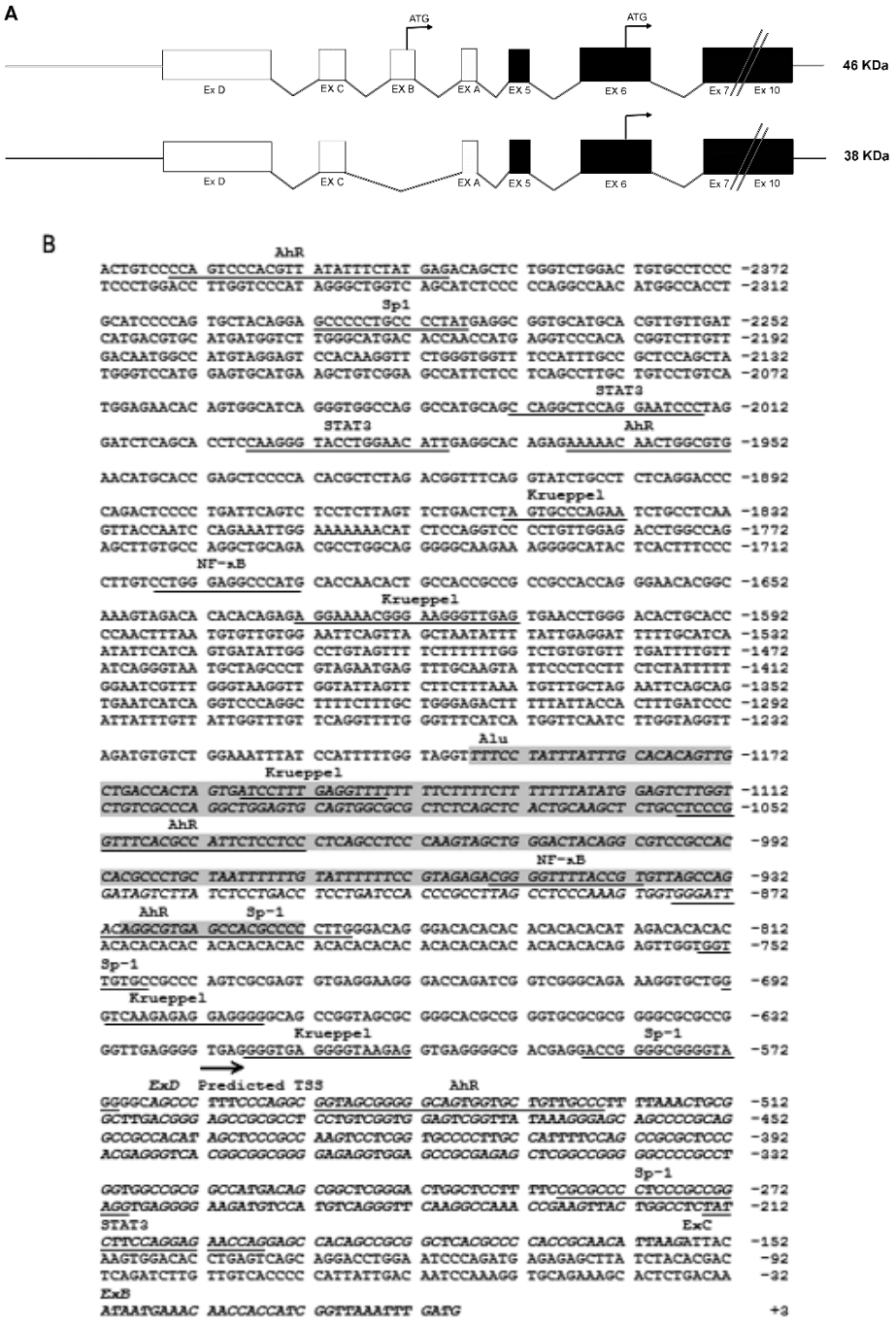

Figure 4.1.1: **In silico analysis of the CHRFAM7A regulatory region**. (A) Schematic representation of the two splicing isoform generated from the CHRFAM7A gene: the isoform 1 is characterized by the presence of all

the exons and two functional Open Reading Frames (ORFs) located in exon B and exon 6, respectively. Isoform 1, which is translated from the ATG in exon B, gives rise either to the longest protein, of about 46 KDa, which is characterized by a 27 amminoacides N-terminal domain encoded by the exons B and A, or to the shortest protein, of about 35 KDa, lacking the N-terminal domain. The isoform 2 is characterized by the skipping of exon B and is translated only by the ATG in exon 6, giving rise only to the shortest protein. (B) Bioinformatic analysis of a region of about 2400 bp upstream the exon B of the CHRFAM7A gene with the online tool MatInspector (hhtp://www.Genomatix.de). The analysis reveals the presence of several consensus sequences for transcription factors involved in immune cells differentiation and maturation but also for neuro-specific transcription factors (underlined in the test). In particular, the analysis highlights the presence of a NF-κB consensus sequence, located at -1717 bp from the ATG in exon B, a AhR consensus sequence and several STAT3 consensus sequences. The EST analysis predicted the start of transcription at -566 bp from the ATG in exon B (black arrow), in correspondence with the first nucleotide of exon D. The UCSC (University of California Santa Cruz) genome browser (http://genome.ucsc.edu) highlighted an Alu sequence in CHRFAM7A 5' flanking region encompassing - 1185 bp/- 851 bp with respect to the ATG codon in exon B (grey box).

4.1.2. Identification of multiple Transcription Start Sites (TSS) in monocytic cell line, primary human macrophages and neuroblastoma cell model

In order to map and functionally characterize the CHRFAM7A gene regulatory region in different cell subtypes, we conducted experiments to determine whether the mRNA start of transcription predicted by the genome project was confirmed. Total RNA extracted from THP-1, SH-SY5Y and primary cultures of human macrophages was analyzed by 5'-RACE, which allows the amplification of 5' mRNA region and the identification of the TSS.

THP-1 cell line do not express CHRNA7 gene, while SH-SY5Y cells express both the CHRNA7 and CHRFAM7A genes, which have 99% of sequence homology in the region encompassing exons 5-10: for this reason, the strategy of 5'-RACE was different for the THP-1 and SH-SY5Y cell line.

In THP-1 cell line, after ligation of the adapter and the retro-transcription of adapter-bound mRNA, the first cDNA strand was amplified by a nested PCR strategy. The first round of amplification was performed by using, as a specific reverse primer, an oligonucleotide complementary to a region of exon 5 (EX5 primer), which would guarantee the amplification of CHRFAM7A gene (5' OUTER primer). The second

amplification (nested-PCR) was carried out with a reverse oligonucleotide complementary to a region of exon A (EXA primer, 5'-RACE INNER primer) (**Fig. 4.1.2A**).

A 500 bp product generated by 5 '-RACE inner PCR was obtained, and eight positive clones out of twelve analysed transformants colonies have been identified. The cloned product was sequenced and the identity, as CHRFAM7A cDNA, confirmed by BLAST analysis (http://ncbi.nlm.nih.gov). To map the exact mRNA TSS we aligned, by means of the Alignment function of Vector NTI software (Invitrogen), the sequence obtained by nested PCR with approximately 2000 bp spanning 5' flanking region of the CHRFAM7A gene and cDNA sequence up to exon B, present in the database. This analysis showed that the first nucleotide maps within exon D, 120 bp downstream of the site predicted by the analysis of EST (**Fig. 4.1.2D**), and 447 bp upstream the ATG codon in exon B (referred as + 1). In addition, this transcript corresponds to isoform 2, as exon B is not present.

However, THP-1 cells express both isoform 1 and 2 (Benfante et al., 2011). To confirm the presence of a transcript encoding isoform 1, which should retain exon B, we repeated the PCR amplification under less stringent conditions. A major band 400 bp long was amplified under these conditions, along with the 500 bp fragment. Ten transformants colonies were analysed and the different products were sequenced, which enabled us to confirm that the 500 bp fragment corresponds to the previously identified mRNA starting 447 bp upstream the ATG codon in exon B. The 400 bp fragment identifies an alternative transcript, missing the region between - 208 and - 703, with a transcription start site mapping 771 base pairs upstream the ATG codon in exon B and corresponding to isoform 1, since it retained exon B (**Fig. 4.1.2C**).

The THP-1 cell line represents a valid experimental model of monocytes/ macrophages. Given the nature of immortalized cells, we wanted to determine whether the transcripts identified in THP-1 cells represented the physiological one in human Peripheral Blood Mononuclear Cells (PBMCs)-derived monocytes/macrophages. For this purpose, total RNA extracted from human macrophages, isolated from peripheral blood, was subjected to 5'-RACE analysis. Oligonucleotides used for amplification were the same as those used in the previous experiments. Only the sequence of one clone, out of 13 colonies, was compatible with the alternative transcripts identified in THP-1, missing region - 703/- 208 of exon D, with the start of transcription at -771 bp and corresponding

to isoform 1 (exon B retained) (**Fig. 4.1.2E**). Five clones, whose fragment was about 350 bp long, show 100% homology to the clone containing the 500 bp fragment, but missing exon B (**Fig. 4.1.2F**).

The expression of the gene encoding CHRFAM7A was also confirmed in a neuronal cell model, the neuroblastoma SH-SY5Y cell line, along with the CHRNA7 gene. Compared to macrophages, where CHRFAM7A turns out to be the mainly expressed gene, here the relative CHRNA7/CHRFAM7A expression level is 2:1 (data not shown). We therefore decided to investigate, by 5'-RACE, the existence of alternative transcripts that could predict for the existence of tissue-specific promoters, responsible for a different regulation of the CHRFAM7A receptor subunit in neuronal cells compared to cells of the innate immunity lineage. To be sure to amplify either the transcript encoding CHRNA7 or CHRFAM7A, we designed two new oligonucleotides, one complementary to a region of exon 6 (primer EX 6), used as an outer primer in the first round of amplification, and a second oligonucleotide, used as inner primer, complementary to a different region of exon 5 with respect to that used in previous experiments (EX 5 new primers), in the second PCR amplification. The nested PCR amplification protocol gave raise to two bands, respectively, 550 and 400 bp long (**Fig. 4.1.2B**). Three positive clones have been selected for sequencing analysis. The BLAST analysis of the sequence corresponding to the 400 bp fragment confirmed that it corresponds to the CHRNA7 gene cDNA, starting from the predicted TSS. The 550 bp long fragment corresponds to the CHRFAM7A cDNA encoding isoform 1, with the transcription start site located 415 base pairs upstream the ATG codon in exon B (**Fig. 4.1.2G**).

The 5'-RACE analysis showed the presence of two alternative TSS in the THP-1 cell model, which may predict the existence of two different alternative promoters. Moreover, in SH-SY5Y cell model, the 5'-RACE analysis revealed the presence of a different TSS and detected the expression of the sole CHRFAM7A isoform 1, retaining exon B. These results suggested that CHRFAM7A isoform 2 (exon B skipped) expression was restricted to the THP-1 cell model, and that CHRFAM7A gene is indeed subjected to alternative tissue-specific splicing. For this reason, we applied an absolute qPCR protocol, in order to specifically and quantitatively detect CHRFAM7A isoform 1 and 2 in THP-1 and SH-SY5Y cDNA, to confirm the presence of tissue-specific isoforms.

The absolute qPCR protocol was performed using primers designed to specifically amplify the two isoforms, avoiding the amplification of genomic DNA: the forward primer for isoform 1 was designed on the exon junction between exon C and B and the reverse primer was designed on the exon junction between exon B and A, giving rise to a PCR product of 81 bp; the forward primer for isoform 2 was designed on the exon junction between exon D and C, and the reverse primer was designed on the exon junction between exon C and A, giving rise to a fragment of 135 bp (**Fig. 4.1.2H**). The primers were initially tested on THP-1 and SH-SY5Y cDNA by means of standard PCR and allowed the amplification of two PCR products of the predicted molecular weights, indicating the expression of the two isoforms in both the cell models (**Fig. 4.1.2I**).

In order to quantify the expression of the two transcripts we performed a Real-Time PCR protocol generating a standard curve with serial dilutions of the two PCR fragment as described in Materials and Methods. This method allowed us to determine the number of copies/ ng RNA of the two transcripts in order to compare their expression levels.

The analysis showed that both in THP-1 cell line and SH-SY5Y cell line the isoform 1 is more expressed than isoform 2 (THP-1: 1476 copies/ng RNA vs 344 copies/ng RNA; SH-SY5Y: 1967 copies/ng RNA vs 819 copies/ng RNA) (**Fig. 4.1.2L**).

These results indicate that isoform 1 and 2 are both expressed in the two cell models, excluding the mechanism of tissue-specific alternative splicing.

Given the expression of both the isoforms in SH-SY5Y cells, we decided to evaluate also the expression of the alternative transcripts, whose transcription is directed by the different TSS: the transcript 1, starting at -771 bp from the ATG in exon B and lacking the region encompassing -703 bp and 208 bp (**Fig. 4.1.2C**) and transcript 2, starting at -447 bp and skipping exon B (**Fig. 4.1.2D**).

In order to confirm the expression of these two transcripts we performed a standard PCR protocol on THP-1 and SH-SY5Y cDNA using primers that could guarantee the selective amplification of transcript 1 (**Fig. 4.1.2C**) and transcript 2 (**Fig. 4.1.2D**).

The amplification of transcript 1 was performed using a Forward primer complementary to the region included between -771 bp and -703 bp and a Reverse primer designed on the exon junction between exon D and exon C, in order to avoid amplification of genomic DNA.

The amplification of transcript 2 was performed using a Forward primer between -447 bp and -415 bp and the same Reverse primer of the transcript 1 amplification (the sequences of the primers are reported in Table 1 of Materials and Methods).

The PCR on transcript 1 amplified a fragment of about 104 bp both in THP-1 and SH-SY5Y cDNA. The molecular weight of the fragment was in accordance with the length of transcript 1, starting at -771 bp from the ATG in exon B and lacked the region between -703 bp and -208 bp (**Fig. 4.1.2M**).

The PCR product resulting from the PCR on transcript 2 was of about 293 bp and was expressed both in THP-1 and SH-SY5Y cDNA (**Fig. 4.1.2N**). In both cases the control samples (which are the result of the reverse transcription in the absence of the retro-transcriptase enzyme) showed no amplification, further confirming the specificity of the amplification product.

The analysis showed that both THP-1 and SH-SY5Y express the alternative transcripts 1 and 2, suggesting that the transcription in both the cell lines could initiate from both -771 bp and -447 bp from the ATG in exon B.

It is worth noting that the expression of transcripts 1 and 2 in SH-SY5Y cells does not exclude that the CHRFAM7A gene in SH-SY5Y could be also transcribed from -415 bp with respect to the ATG in exon B, as predicted by 5'-RACE analysis.

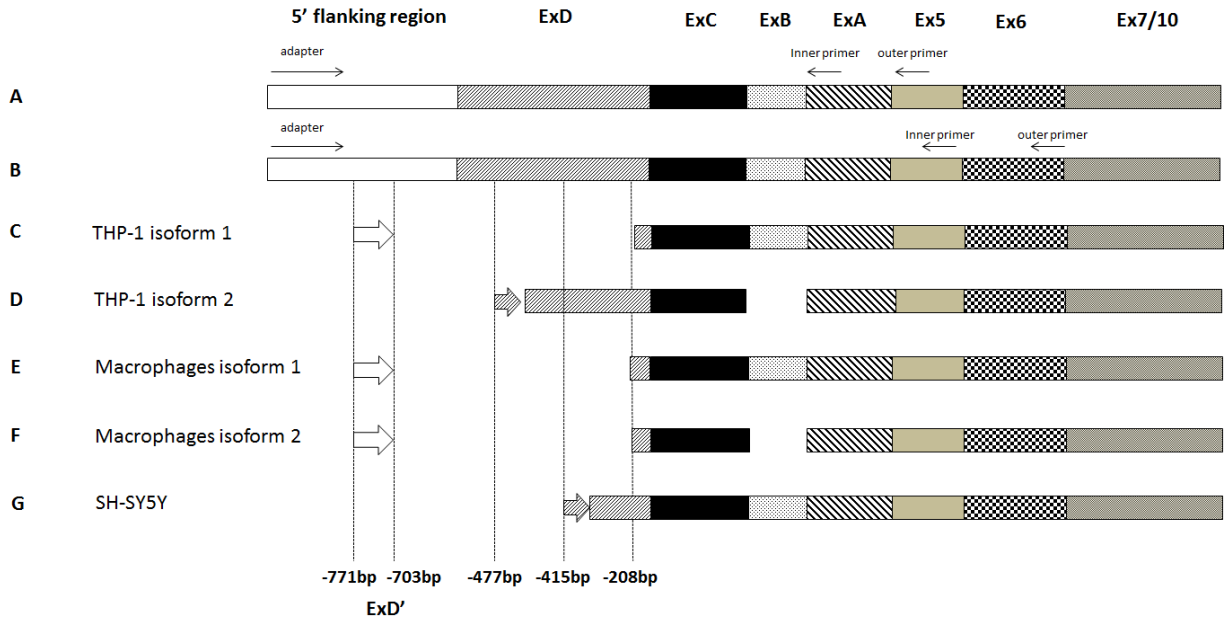

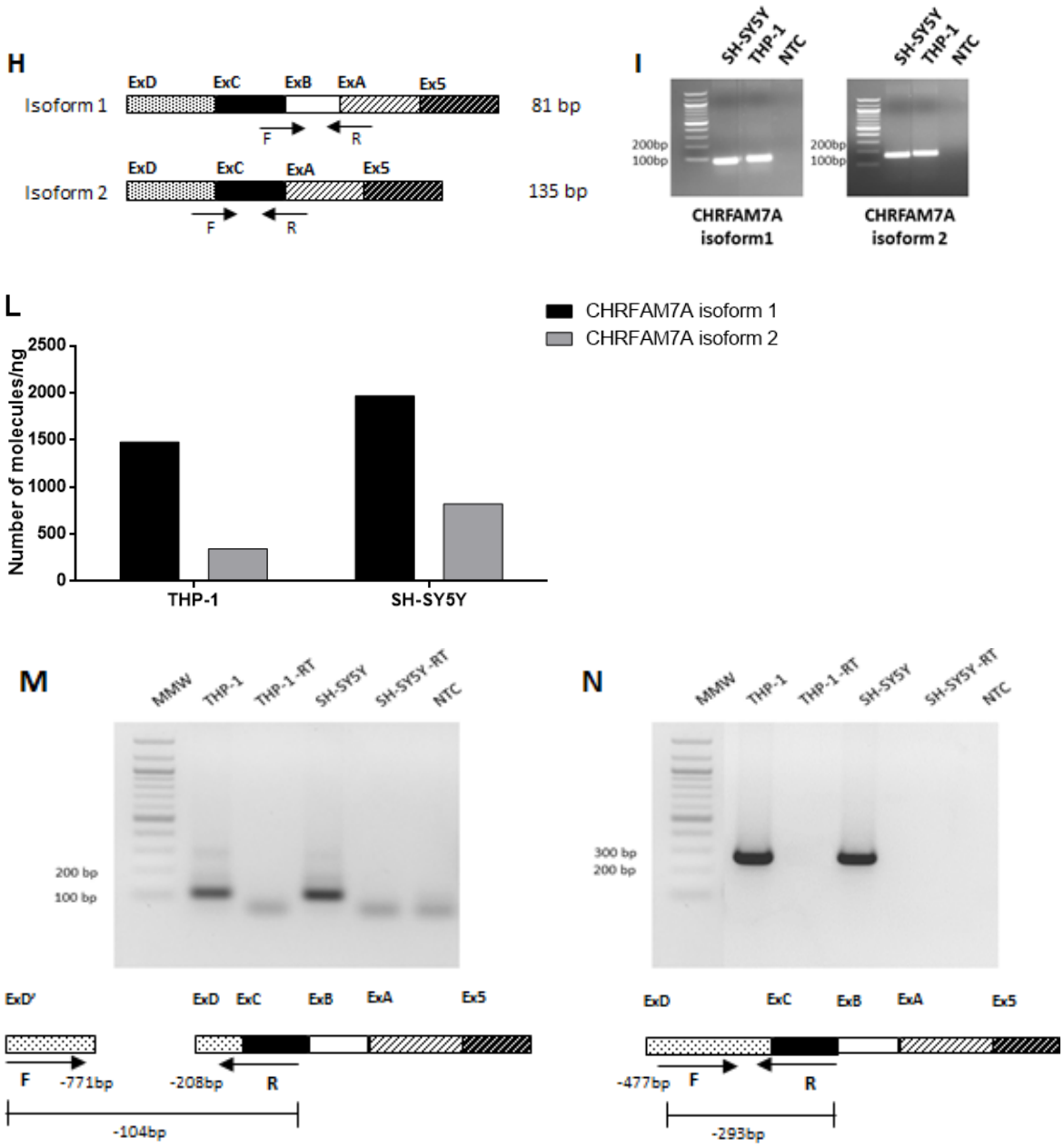

Figure 4.1.2: **Identification of CHRFAM7A Transcription Start Site**. (A) 5'RACE analysis of CHRFAM7A gene in THP-1 cell line was performed using as specific outer primer an oligonucleotide complementary to the CHRFAM7A exon 5 and an inner primer complementary to exon A. (B) In SH-SY5Y cell line both CHRNA7 and CHRFAM7A transcripts are expressed, so the 5'-RACE strategy was differently performed: as outer reverse primer was used a sequence complementary to exon 6, while the inner reverse primer was designed on exon 5. (C) The analysis on THP-1 cells identified two different TSS, one at -771 bp with respect to the ATG in the exon B, and (D) one at -447 bb, respectively. These alternative TSS identify two different alternative promoters. (E,F) The 5'RACE in primary macrophages were designed with the same primers and recognizes a unique TSS for both the spliced isoforms, at -771 bp. (G) The analysis on SH-SY5Y cells showed a unique TSS, located at -415 bp, which seems to give rise only to isoform 201. (H) Schematic representation of the

primer design for the specific amplification of CHRFAM7A isoform 1 and CHRFAM7A isoform 2. (I) Standard PCR on THP-1 and SH-SY5Y cDNA for the detection of the two CHRFAM7A splicing isoforms. (L) Absolute quantification by Real-Time PCR of CHRFAM7A isoform 1 and 2 in THP-1 and SH-SY5Y cDNA samples. The results are expressed as molecules for ng RNA. (M) A standard PCR protocol was used to specifically amplify the promoter 1 in THP-1 and SH-SY5Y cDNA, in order to determine the presence of the TSS located at -771 bp from the ATG in exon B: a forward primer located in region encompassing -771 bp and -703 bp and a reverse primer spanning exon D and exon C were used. The primers should amplify a region of 104 bp, giving the absence of the region between -703 bp and -208 bp. The promoter 1 is expressed not only in THP-1 cell model, but also in SH-SY5Y. (N) In order to verify the expression of promoter 2 in THP-1 and SH-SY5Y cDNA, a primer forward located between -447 bp and -415 bp and a reverse primer spanning econ D and exon C were used in a standard PCR protocol. Both THP-1 cell model and SH-SY5Y cell model express promoter 2, indicating the presence of the TSS located at -447 bp.

4.1.3. Functional analysis of the CHRFAM7A regulatory sequence in THP-1 and SH-SY5Y cell line

5' -RACE experiments have identified, in different cell lines, alternative transcripts, characterized by different transcription start site and the presence/ absence of some regions of exon D and exon B. The identification of the region containing the promoter was based on these data, which led us to hypothesize that the regulatory sequence can be located in the 5'-flanking region of the identified mRNA. In order to test this hypothesis, a construct containing a fragment 2100 bases in length and including part of exon B (up to ATG codon), exon C, exon D and part of the 5’ genomic region into pGL4 basic vector, upstream of the *Firefly* luciferase reporter gene was generated (CHRFAM7A -2122 bp/-1 bp_pGL4b).

To determine whether this region contained functional elements able to sustain the transcription of the reporter gene, transient transfection experiments were conducted in THP-1 monocyte cell line and in SH-SY5Y neuroblastoma cell line. The full-length construct showed a lower activity than a promoterless construct (pGL4.11), taken as a reference of baseline activity, both in THP-1 and SH-SY5Y cell model (data not shown).

This result could suggest that the sequence we cloned actually did not contain the functional elements necessary for CHRFAM7A gene transcription or that a strong negative element was present in this region. In particular, the construct retained the exons D, C

and B and the presence of these exons, without the corresponding intronic sequences, might interfere with the luciferase transactivation. A more thorough *in silico* analysis of the 2000 bp region has also showed the presence of an Alu sequence, between -1083 and -830 base pairs upstream the ATG codon, that could have a negative effect on gene transcription (Levine and Manley, 1989; Ebihara et al., 2002).

Moreover, 5'-RACE experiments showed that the region -208 bp/-703 bp was always absent in transcripts identified in the macrophage lineage, and the same mRNA is co-expressed together with another transcript in THP-1 cell line. This data suggested us that this region could represent an intron, retained in the alternative transcript expressed in THP-1 cells. Its presence, together with the Alu sequence, might have a negative effect on the expression of our reporter constructs in transient transfection experiments.

To address the role of these regions, we generated a series of construct in which the region encompassing the exons C and B was deleted (CHRFAM7A -2122 bp/-184 bp_pGL4.11), as described in Materials and Methods (**Fig. 4.1.3A**).

These constructs retain the TSS identified in macrophages and THP-1 cell model located at -771 bp with respect to ATG codon in exon B, the TSS identified in THP-1 cell line at -477 bp and the TSS identified in SH-SY5Y cell line, and lack most of the putative 5' UTR-specifying region.

The plasmid vectors containing the different portion of the CHRFAM7A genomic region were tested by means of transient transfection of THP-1 and SH-SY5Y cell line. Promoter activity was measured as *Firefly* luciferase values fold changes compared to the empty pGL4.11 or pGL4b vector (**Fig. 4.1.3B, Fig. 4.1.3C**). The deletion of exons C and B increased the activity of the reporter by 17-fold ± 0.78 over pGL4.11 in THP-1 cell line, while in SH-SY5Y cell line it showed a lower activity compared to the empty vector.

Interestingly, the construct -4280 bp/-184 bp, which retains a longer 5' region of CHRFAM7A promoter, had a lower activity in THP-1 cells compared to the -2122 bp/-184 bp (6.16-fold ± 0.39 over pGL4.11 vs 17-fold ± 0.78 over pGL4.11), indicating the presence of negative regulatory elements.

All the deletion constructs had a statistically significant activity compared to the empty vector in THP-1 cell line: in particular, the -735 bp/-184 bp construct, which retains the TSS at -477 bp and lacks the Alu sequence, showed a 33-fold ± 1.86 activity compared to

the empty pGL4.11, indicating also the presence of several and strong positive elements which are sufficient to drive a robust CHRFAM7A expression in monocytic cell line.

Also the -557 bp/-184 bp had a statistically significant higher activity than the promoter-less vector (19.5-fold ± 0.9 over pGL4.11), even though the TSS at -771 bp from the ATG in exon B is deleted. On the other hand, the -447 bp/-184 bp construct, which retains only the TSS identified in SH-SY5Y cells, showed a lower activity compared to the pGL4.11 vector, indicating the -557 bp/-184 bp fragment as the minimal CHRFAM7A promoter (data not shown).

On the contrary, in SH-SY5Y cell line all the deletion constructs retaining the Alu sequence and the entire upstream region showed a lower activity with respect of the empty vector pGL4b (data not shown).

Only the CHRFAM7A -735 bp/-184 bp and the -557 bp/-184 bp constructs showed a higher expression compared to the pGL4b vector, with respectively 1.7-fold ± 0.056 and 1.3-fold ± 0.026 increase. Although the increase in activity of these constructs over the promoter-less vector is statistically significant, it is not high enough to indicate the presence of a neuro-specific promoter.

This result indicated the absence of neuro-specific sequences in the region analysed or the presence of strong negative tissue-specific elements. Moreover, the specific deletion of the SH-SY5Y transcription start site in the -735 bp/-184 bp construct did not decrease the transcriptional activity (-735 bp/-184 bp: 1.7-fold ± 0.056; -735 bp/-184 bp ΔSH-SY5Y TSS: 2-fold ± 0.003), thus suggesting the existence of other elements cooperating in CHRFAM7A expression in neuroblastoma cell model.

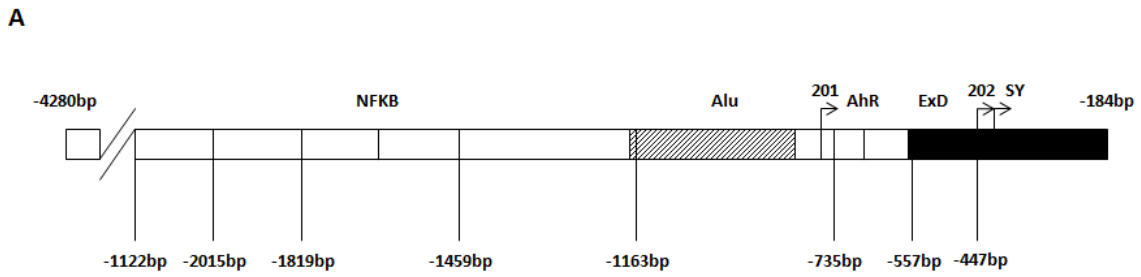

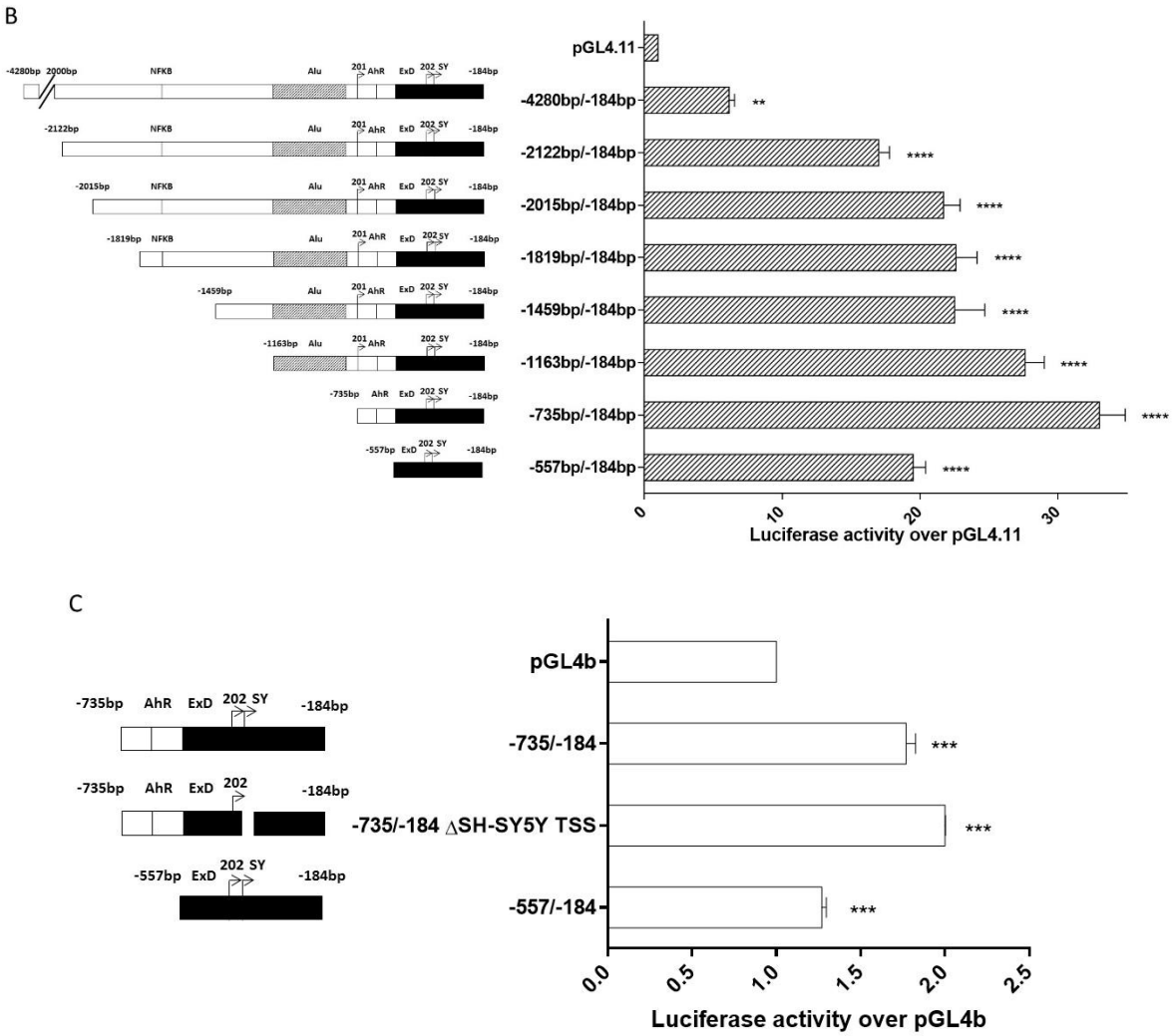

Figure 4.1.3: Functional analysis of CHRFAM7A promoter region in THP-1 and SH-SY5Y cell lines. (A) Schematic representation of the CHRFAM7A 5' flanking region analysed by Luciferase assay. (B) Transient transfection and Luciferase assay on THP-1 cells transfected with several CHRFAM7A promoter deletion constructs: the full length construct (-2122 bp/-184 bp) retains the NF-κB consensus sequence at -1717 bp, the Alu element, all three detected TSS and exon D. All the plasmids analyzed showed a significant activity in THP-1 cells. The results are expressed as fold increase over the promoterless vector, pGL4.11, and are the means ± standard error of three independent transfections performed in duplicate. The data were analysed by means of one-way ANOVA, Tukey's test using GraphPad Prism 5 Software (GraphPad Software, Inc.); p values <0.05 were considered significant. (C) Transient transfection and Luciferase assay on SH-SY5Y cells transfected with several CHRFAM7A promoter deletion constructs. The full length construct (-1122 bp/-184 bp) showed a lower activity with respect to the empty vector. The only constructs that displayed a higher activity compared to pGL4b vector is -735 bp/-184 bp and -557 bp/-184 bp, suggesting the presence of strong neuro-specific negative elements or the absence of necessary neuro-specific elements in the region analysed. The results are expressed as fold increase over the promoterless vector, pGL4b, and are the mean

± standard error of two independent transfections performed in duplicate. The data were analysed by means of one-way ANOVA, Tukey's test using GraphPad Prism 5 Software (GraphPad Software, Inc.); p values <0.05 were considered significant.

4.1.4. The CHRFAM7A Intron 4 reduces the transcriptional activity in THP-1 but not in SH-SY5Y cell model

While in monocytic cell model the CHRFAM7A promoter sequence showed a strong transcriptional activity, in neuroblastoma cell line the activity was very low, even if SH-SY5Y expresses the CHRFAM7A transcript. In line with this evidence, we hypothesized the presence of a neuro-specific enhancer sequence in the genomic region encompassing the CHRFAM7A gene.

In 2005, Stefan et al. reported the presence of a neuronal enhancer sequence into the murine *Chrna7* intron 4, which is critical for the neuronal expression of the gene (Stefan et al., 2005).

In humans, the translocation event involving the CHRNA7 and FAM7A genes occurred into the CHRNA7 intron 4, that, in CHRFAM7A gene, separates the FAM7A-derived exon A from CHRNA7-derived exon 5. In order to identify the position of the recombination point we aligned the CHRNA7 intron 4 sequence compared to the CHRFAM7A intron 4 sequence by means of the alignment tool of the VectorNTI™ software (**Fig. 4.1.4A**): the recombination point maps at -468 bp from the first nucleotide of exon A, referred as +1, at the end of an AluY element of 231 nucleotides predicted by UCSC genome browser (**Fig. 4.1.4B**). The presence of an Alu sequence in CHRFAM7A intron 4 and in CHRNA7 intron 4, exactly at the edge of recombination point suggested that the genetic fusion was driven by the repeated sequences.

We cloned the CHRFAM7A intron 4 sequence at the 3'-end of the Luciferase gene in the -735 bp/-184 bp_pGL4.11 construct and we tested it in THP-1 and SH-SY5Y cell models, in order to verify the presence of a tissue-specific enhancer element.

The -735 bp/-184 bp Intron4 construct was transiently transfected and its transcriptional activity was compared to that of the -735 bp/-184 bp construct. While in THP-1 cell model, the presence of the Intron 4 significantly reduced the transcriptional

activity of about 20%, in SH-SY5Y cell line its presence at the 3'-end of the Luciferase gene did not modify the activity of the -735 bp/-184 bp fragment (**Fig. 4.1.4C**).

The presence of the Alu sequence in the Intron 4 region led us to hypothesize a possible tissue-specific repressive effect exerted by the repeat. In order to investigate the role of the Alu in Intron 4 in modulating the promoter activity, we generated a -735 bp/-184 bp construct carrying at 3'-end of the Luciferase gene the Intron 4 sequence deleted of the Alu element. This sequence corresponds to the FAM7A-derived portion of the CHRFAM7A intron 4.

In THP-1 cell line the -735 bp/-184 bp Intron 4 ΔAlu construct showed a partial recovery of the -735 bp/-184 bp transcriptional activity with respect to the -735 bp/-184 bp Intron4 construct; however, no statistically significant difference was highlighted between the -735 bp/-184 bp Intron 4 and the -735 bp/-184 bp Intron 4 ΔAlu constructs. These results suggested that the Alu repeat in CHRFAM7A intron 4 had a corollary role in reducing the promoter transcriptional activity, but its deletion did not completely counteract the inhibitory effect of the intronic sequence.

In SH-SY5Y cells, the -735 bp/-184 bp Intron 4 ΔAlu construct showed no statistically significant different activity compared to the -735 bp/-184 bp and -735 bp/-184 bp Intron 4 constructs, suggesting that no enhancer elements were present in the FAM7A-derived intron 4 region (**Fig. 4.1.4C**).

A

```
Seq_1  41339 GTGAAACCCCCGTCTCTACTAAAAATACAAAAAAATTAACCAGGTGTGGTGGTGTGCACC  41398

Seq_2  2771  ------------------------------------------------------------  2770


Seq_1  41399 TGTAGTCCCAGCTACTCGGGAAGCTGAGGCAGGAGGATGACATGAACCCAGGAGGTGGAG  41458

Seq_2  2771  ------------------------------------------------------------  2770


Seq_1  41459 CTTGCAGTGAGCCGAGATCATGCCACTGCACTCTAGCCTGGGCAACACAGCAAGACTCTG  41518

Seq_2  2771  ------------------------------------------------------------  2770


Seq_1  41519 TCTCAAAAAAAAAAAAAAAAAGATATATATGTGAAGCACAAACCAAGTGTGGGTCCGCTT  41578
                                   ||||||||||||||||||||||||||||||||||||||
Seq_2  2771  ---------------------gatatatatgtgaagcacaaaccaagtgtgggtccgctt  2809


Seq_1  41579 CAAGAGGCTGGAACTAGAGCTTTGGACACAGCGAGTGAAAACCCTGCCCCATGAGGCTCA  41638
             ||||||||||||||||||||||||||||||||||||||||||||||||||||||||||||
Seq_2  2810  caagaggctggaactagagctttggacacagcgagtgaaaaccctgccccatgaggctca  2869


Seq_1  41639 CAGGGTGGCAGCGTGCCTCACCCACCCTCTGTTCTTCTAGACACCATGAAAATGTCACAT  41698
             |||||||||||||||||||||||||||||||||| ||||||||||||||||||||||
Seq_2  2870  cagggtggcagcgtgcctcacccaccctctgttcttctggacaccatgaaaatgtcacat  2929


Seq_1  41699 CTGCCGATGTCCTCCAGAGTTGTTTACAGGTTTCATTTGGTTAAGAGCTTGGTTTTATAT  41758
             ||||||||||||||||||||||||||||||||||||||||||||||||||||||||||||
Seq_2  2930  ctgccgatgtcctccagagttgtttacaggtttcatttggttaagagcttggttttatat  2989


Seq_1  41759 ACATTGTGAGAAAAATCACCAGTTCGGTGTGAAAATTGAAATGGGGGTAGACACTGGCCC  41818
             ||||||||||||||||||||||||||||||||||||||||||||||||||||||||||||
Seq_2  2990  acattgtgagaaaaatcaccagttcggtgtgaaaattgaaatgggggtagacactggccc  3049


Seq_1  41819 TTCCAAGCTGTGCCCGGGGAAGACCTCCCAGGCCAGTCCCAGTGGTGCTCTCAGGCAGCG  41878
             ||||||||||||||||||||||||||||||||||||||||||||||||||||||||||||
Seq_2  3050  ttccaagctgtgcccggggaagacctcccaggccagtcccagtggtgctctcaggcagcg  3109


Seq_1  41879 TGTGGGGTTGTGAGGACAGACAGGGGCCCCTCTCAAGGTCTTTGCTGCTCCATCAAAGAC  41938
             ||||||||||||||||||||||||||||||||||||||||||||||||||||||||||||
Seq_2  3110  tgtggggttgtgaggacagacaggggcccctctcaaggtctttgctgctccatcaaagac  3169


Seq_1  41939 AGACCCCAGGGCTTCGGGAAATCCACAGCCTGGTGGCACTGGCTCATGCAGTCCTTTTCC  41998
             ||||||||||||||||||||||||||||||||||||||||||||||||||||||||||||
Seq_2  3170  agaccccagggcttcgggaaatccacagcctggtggcactggctcatgcagtcctttcc  3229


Seq_1  41999 TGTTTCTAG----------  42007
             |||||||||
Seq_2  3230  tgtttctagTGCTGATGAG  3248
```

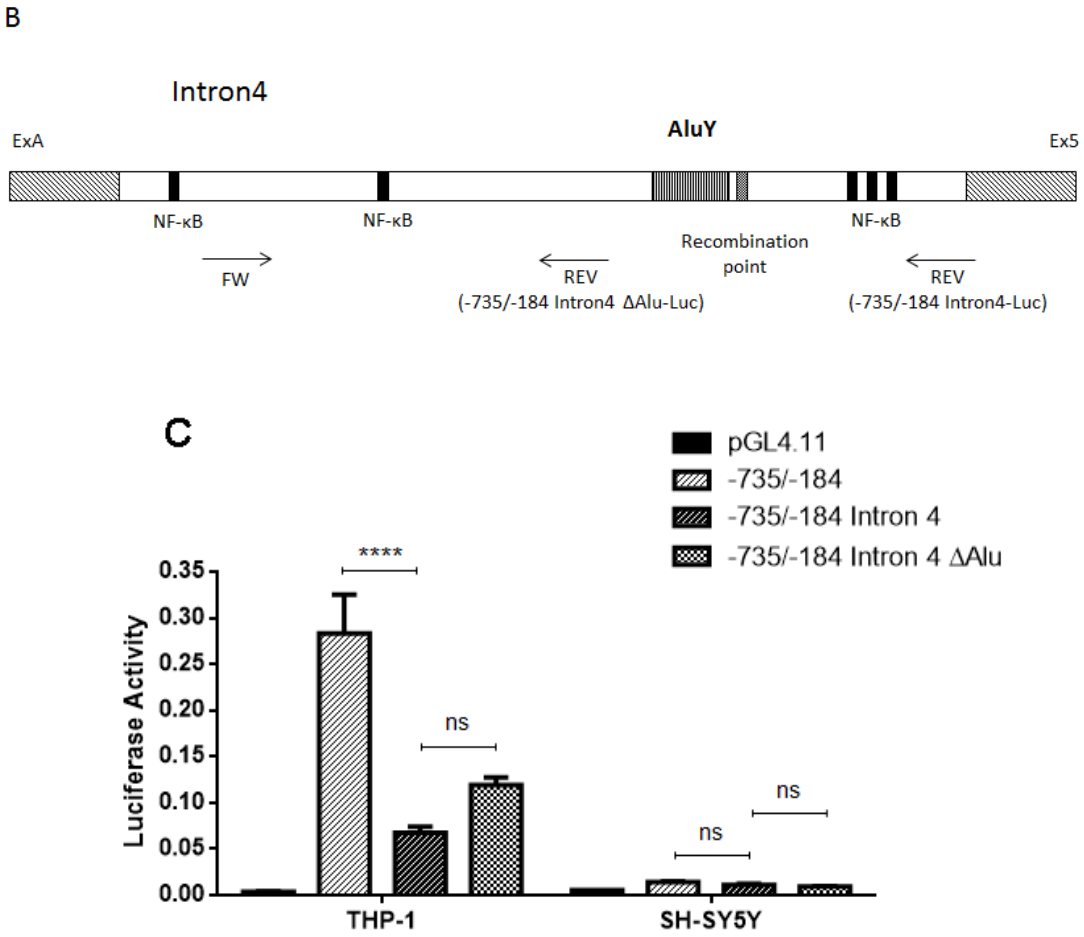

Figure 4.1.4: **In silico and functional analysis of CHRFAM7A Intron 4 region**. (A) The alignment of CHRNA7 Intron 4 (Seq_1) and CHRFAM7A Intron 4 (Seq_2) sequences with the align tool of VectorNTI identifies the point of recombination, which is located 468 bp from the first nucleotide in exon 5. (B) Schematic representation of the CHRFAM7A intron 4: in the scheme the point of recombination, the AluY element, several NF-κB consensus sequences predicted by MatInspector and the primers used for the Luc-intron 4 construct are highlighted. (C) Luciferase assay on THP-1 and SH-SY5Y cells transiently transfected with Luc-intron 4 construct shows that the presence of Intron 4 significantly reduces CHRFAM7A promoter activity in THP-1 but not in SH-SY5Y. The deletion of the intron 4 Alu sequence, in THP-1 cells increase the -735 bp/-184 bp construct activity compared to the -735 bp/-184 bp Intron 4 construct but the difference is not statistically significant. In SH-SY5Y cells the -735 bp/-184 bp Intron 4 ΔAlu shows no statistically significant activity differences with the other constructs. The results are expressed as the mean ± standard error of each deletion construct and are the mean of at least three independent experiments. The data were analysed by means of one-way ANOVA, Tukey's test using GraphPad Prism 5 Software (GraphPad Software, Inc.); p values <0.05 were considered significant.

4.1.5. Identification of a novel CHRFAM7A Transcription Start Site in intron 5

The analysis of CHRFAM7A gene sequence with the online tool PHANTOM5 (http://fantom.gsc.riken.jp/zenbu) revealed the presence of a putative Transcription Start Site in intron 5. The CHRFAM7A intron 5 separates exon 5 from exon 6, in which the second ORF of the CHRFAM7A gene is located. The TSS is predicted at -3022 bp from the ATG in exon 6 (where the A is referred as +1), defining a 5'-UTR of about 3000 bp.

We aligned by means of the alignment tool of VectorNTI™ software the sequences of the CHRNA7 and CHRFAM7A intron 5 obtained from the Ensemble genome browser: the two sequences differ for the presence of 279 additional nucleotides in CHRFAM7A intron 5 constituted by a AC dinucleotide repeat, included between -3037 bp and -2739 bp. The alignment showed that the putative TSS is located into the region specific of CHRFAM7A intron 5 (**Fig. 4.1.5A, B**).

Given the high repetitive feature of the region in analysis, we found several difficulties in performing a 5'-RACE analysis, thus we decided to proceed with a standard PCR protocol on THP-1 and SH-SY5Y cDNA, in order to verify the presence of a putative transcript starting in intron 5.

The standard PCR protocol was performed using a proofreading Taq enzyme (Expand High Fidelity PCR System, Roche) on THP-1 and SH-SY5Y cDNA. Briefly, the PCR was performed using three different Forward primers located at -610 bp, -1037 bp and -2487 bp from the ATG in exon 6, respectively. As common reverse primer, an oligonucleotide complementary to a sequence in exon 6 was used (all the oligonucleotides sequences are reported in Table 2 in Materials and Methods).

The three different PCR gave rise to three different amplification products of respectively 730 bp, 1156 bp and 2607 bp, while the control samples (which are the product of the reverse transcription in the absence of the retro-transcriptase enzyme) showed no amplification (**Fig. 4.1.5C, D, E**), suggesting the presence of a TSS upstream the -2487 bp forward primer. A further PCR assay using a forward primer and a reverse primer located at -2899 bp and -2440 bp from the first nucleotide of exon 6 failed to amplify a specific fragment in the cDNA samples, suggesting the presence of a TSS in the region between -2487 bp and -2899 bp (data not shown).

The *in silico* analysis of the intron 5 region up-stream the predicted TSS by means of the online tool MatInspector, revealed the presence of a CAAT box and a TATA box located at -2810 bp from the first nucleotide of exon 6, suggesting the presence of a functional promoter.

A

```
Seq_1  781   CCTAACTACCACTCACACATACGACTCACACACACACCACTCACAACCACTCACACACAG  840
              ||||||||||||||||||||||||||||||||||||||||||||||||||||||||    |
Seq_2  781   CCTAACTACCACTCACACATACGACTCACACACACACCACTCACAACCACTCACA----G  836

Seq_1  841   CCACTCACACATACCACACACCACTCACCCCTCACACACACCACTCACACACA--T----  894
              ||||||||||||||||||||||||||||||||||||||||||||||||||||||||  |
Seq_2  837   CCACTCACACATACCACACACCACTCACCCCTCACACACACCACTCACACACACCTCACA  896

Seq_1  895   ------------------------------------------------------------  894

Seq_2  897   CACACACACCACTCAGTACTCACACACACCACTCACACCACTCACACTACTCACACCACT  956

Seq_1  895   ------------------------------------------------------------  894

Seq_2  957   CATACACACCACCCACACACACTGTTCACACAACACACACACCACTCACAATCACACACA  1016

Seq_1  895   -------------CACTCACATACCACCCAC-----------------------------  912
                          ||||||||||||||||||
Seq_2  1017  CCACTCACACAACCACTCACATACCACCCACGACTCAACACACACACCACTCACACAACC  1076

Seq_1  913   ------------------------------------------------------------  912

Seq_2  1077  ACTCACATACCACCCACACGACTCAACACACACACCACTCACACAACCACTCACATACCA  1136

Seq_1  913   ------------------------------------------------------ACGACTC  919
                                                                     |||||||
Seq_2  1137  CCCACACGACTCAACACACACACCACTCACACAACCACTCACATACCACCCACACGACTC  1196

Seq_1  920   AACACTCACACACCACTCACACAACCACTCACATACCACCCACACGACTCAACACTCACA  979
              ||||||||||||||||||||||||||||||||||||||||||||||||||||||||||||
Seq_2  1197  AACACTCACACACCACTCACACAACCACTCACATACCACCCACACGACTCAACACTCACA  1256

Seq_1  980   CACCACTCACACAAATATACCACCCACACACCACTCACCACTCCACACATACCACTCACA  1039
              ||||||||||||||||||||||||||||||||||||||||||||||||||||||||||||
Seq_2  1257  CACCACTCACACAAATATACCACCCACACACCACTCACCACTCCACACATACCACTCACA  1316

Seq_1  1040  CAAACCACTCAAACCACCAACACACACACACCAGACACACACACACCCCTCACACACACC  1099
              ||||||||||||||||||||||||||||||||||||||||||||||||||||||||||||
Seq_2  1317  CAAACCACTCAAACCACCAACACACACACACCAGACACACACACACCCCTCACACACACC  1376

Seq_1  1100  ACTTACACACCACTCTCACACACCATACACACCACTCACACACGACTCACAACCCTCACA  1159
              ||||||||||||||||||||||||||||||||||||||||||||||||||||||||||||
Seq_2  1377  ACTTACACACCACTCTCACACACCATACACACCACTCACACACGACTCACAACCCTCACA  1436

Seq_1  1160  CACACCACTTACACACATGCAGGCATGCACTCTCAAACCAGATACACTATTCACACCACT  1219
              ||||||||||||||||||||||||||||||||||||||||||||||||||||||||||||
Seq_2  1437  CACACCACTTACACACATGCAGGCATGCACTCTCAAACCAGATACACTATTCACACCACT  1496

Seq_1  1220  CACATACCACACATACTGGCTGTGCCTTCTCGGTTGCTGTCTGAGTGCCTTCCCTGTCAG  1279
              ||||||||||||||||||||||||||||||||||||||||||| ||||||||||||||||
Seq_2  1497  CACATACCACACATACTGGCTGTGCCTTCTCGGTTGCTGTCTGTGTGCCTTCCCTGTCAG  1556
```

B

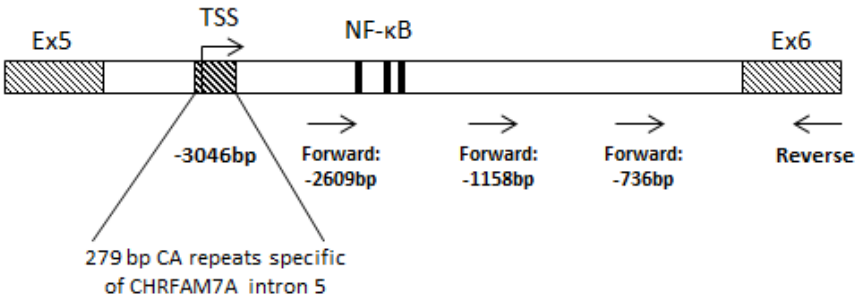

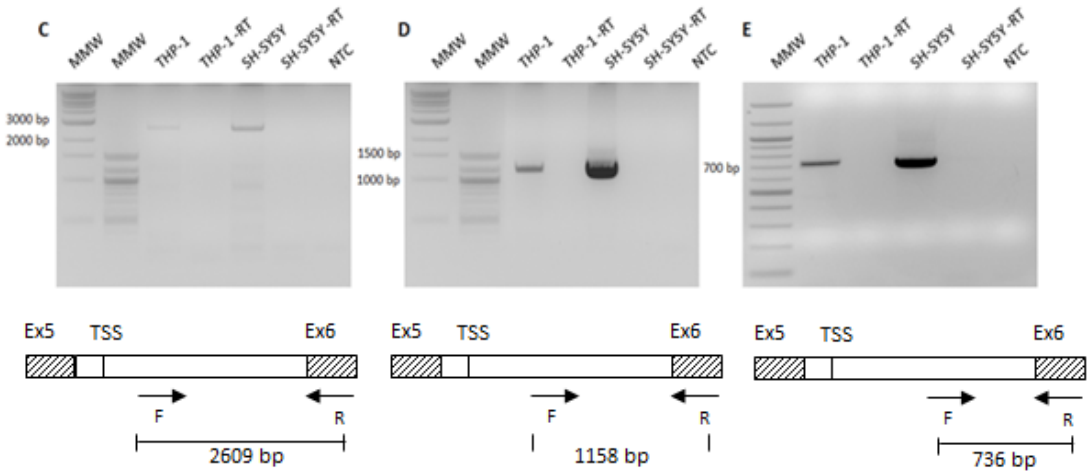

Figure 4.1.5: **Identification of a new Transcription Start Site in CHRFAM7A intron 5**. (A) Alignment of the intron 5 sequences of CHRNA7 gene (Seq_1) and CHRFAM7A gene (Seq_2) obtained from the Ensemble genome browser by means of the Align tool of VectorNTI™ software. The figure highlights the intron 5 sequence from 781 bp from the first nucleotide of intron 5 to 2497 bp. The two genes differ for the presence of additional 279 bp in CHRFAM7A intron 5 characterized by a high repetitive sequence. The TSS predicted by Phantom5 software maps into the CHRFAM7A specific high repetitive sequence (highlighted in the box). (B) Schematic representation of the CHRFAM7A intron 5: the figure shows the position of the three forward primers used for the PCR amplification on THP-1 and SH-SY5Y cDNA. In the figure three NF-κB consensus sequences predicted by the MatInspector tool, the CHRFAM7A high repetitive sequence and the predicted TSS, located at -3022 bp from the ATG in exon 6 are also highlighted. (C, D, E) A standard PCR protocol was used to determine the presence of the putative TSS in intron 5: three different forward primers (located respectively at -2487 bp, -1037 bp and -610 bp from the ATG in exon 6) and a common reverse primer located in exon 6 were used, resulting in three different PCR product of respectively 2607 bp, 1156 bp and 730 bp.

4.1.6. LPS treatment causes chromatin remodelling at the CHRFAM7A promoter

The CHRFAM7A mRNA down-regulation occurring in THP-1 cell line is a transcription-based mechanism driven by the direct intervention of the NF-κB transcription factor (Benfante et al., 2011).

In order to determine whether the LPS challenge could induce alteration in the epigenetic marks of CHRFAM7A promoter, we performed a Chromatin Immunoprecipitation (ChIP) assay on control and LPS-treated THP-1, followed by standard PCR protocol on a particular CHRFAM7A region (encompassing -1714 bp and -1514 bp)

containing the NF-κB consensus sequence predicted by the MatInspector online tool. The PCR analysis was performed using primers designed to amplify a region of 147 bp around the predicted sequence (**Fig. 4.1.6A**).

After 6 hours of LPS challenge a reduction in Histone 4 acetylation (aH4), which is a well-characterized mark of opened chromatin, is visible (**Fig. 4.1.6B**). The deacetylation of the promoter sequence correlates with the observed transcript down-regulation, and indicates that transcriptional repression is also mediated by epigenetic modifications. However, no p65, p50 or c-Rel NF-κB subunits binding was observed (data not shown), suggesting that NF-κB recruitment at CHRFAM7A promoter occurred at another cognate sequence.

As control, the same chromatin samples were analysed for the Interleukin-6 (IL-6) promoter amplification, which is known to undergo transcriptional up-regulation by NF-κB activation after LPS challenge (Libermann and Baltimore, 1990). The LPS treatment results in a marked IL-6 promoter acetylation along with an apparent reduction of p65 signal and an apparent increase in p50 signal, supporting the evidence reported by Libermann and Baltimore in 1990 (**Fig. 4.1.6C**).

In order to definitively exclude that NF-κB could exert its function by binding to the over mentioned sequence, we performed an Electrophoresis Mobility Shift Analysis (EMSA) assay using a synthetic radiolabeled oligonucleotide containing the -1707 bp/-1697 bp CHRFAM7A NF-κB sequence on nuclear extract of LPS-treated THP-1.

The LPS treatment induced the formation of five complexes (indicated in red in **Fig. 4.6D**), which were not detectable in untreated extracts. In particular, the complexes 2 and 4 were more visible in extracts incubated with the mutant oligonucleotide (lane 4) and in extracts incubated in the presence of p50 (lane 6) and c-Rel (lane 7) specific antibodies. The significance of these complexes formation is not clear, but it might indicate that LPS treatment is able to activate THP-1 cells.

However, the EMSA assay did not show competition with an excess of cold oligonucleotide (lane 3) and no specific super-shift was detected in the presence of specific antibody against p65 (lane 5), p50 (lane 6) and c-Rel (lane 7) subunits. These results clearly indicated that NF-κB p65, p50 and c-Rel subunits did not bind the analysed sequence.

On the contrary, the control NF-κB consensus oligonucleotide determined the formation of specific complex (lane 14), which was subjected to competition by increased concentration of cold oligo (lane 15, 16) and showed a specific supershift in the presence of p50 antibody (lane 18) (**Fig. 4.1.6D, E**). The formation of specific complex in the presence of the control NF-κB consensus oligonucleotide supported the validity of the experimental design and further confirmed that NF-κB do not bind the CHRFAM7A -1714 bp/ -1514 bp predicted sequence.

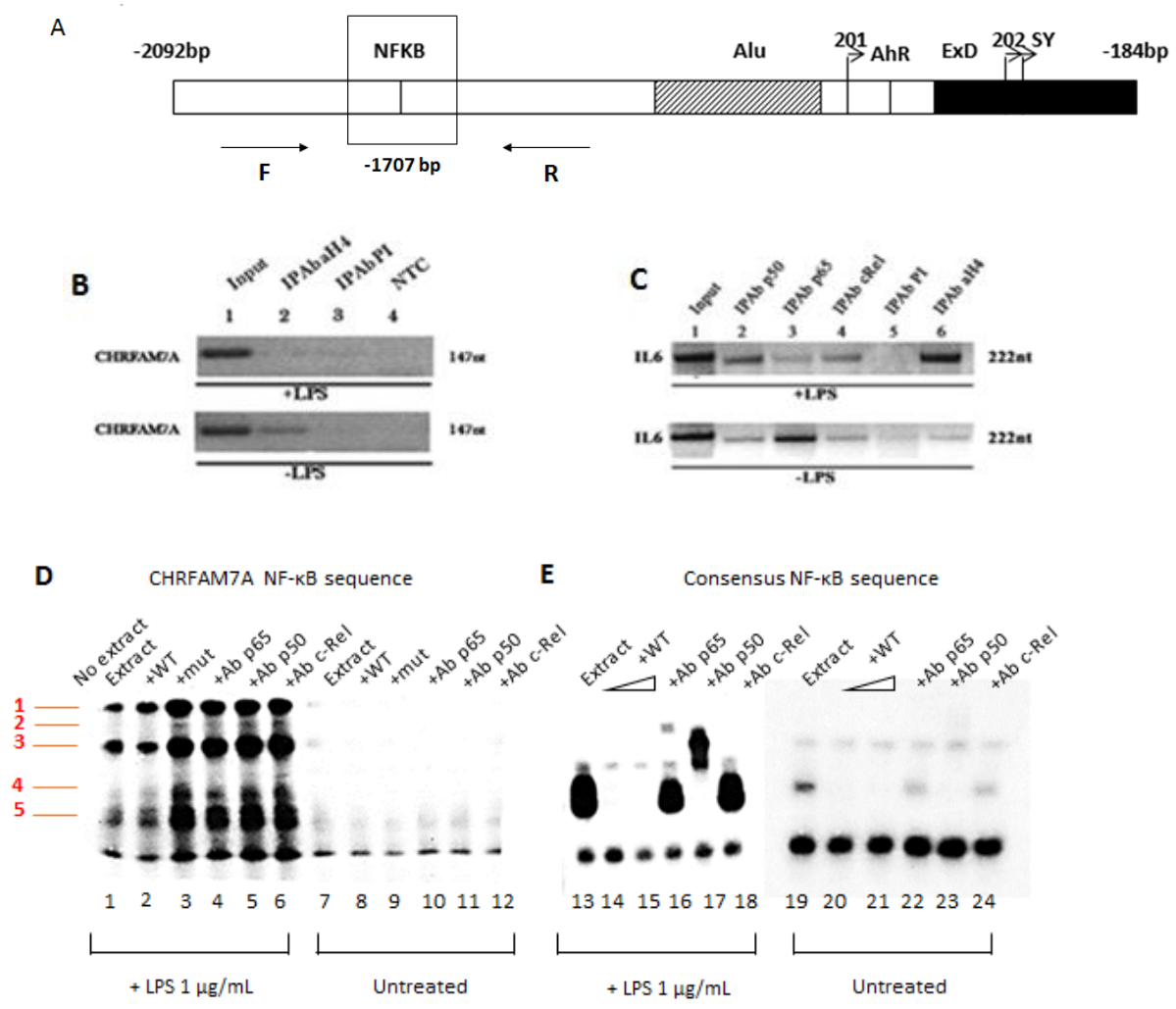

Figure 4.1.6: **CHRFAM7A Chromatin remodelling identification after LPS treatment in THP-1 cell line**. (A) Schematic representation of the region analysed by Chromatin Immunoprecipitation (ChIP): the NF-κB consensus sequence predicted by MatInspector maps at -1707 bp from the ATG in exon B. In the figure the

primers used for the ChIP protocol are highlighted. (B) The ChIP analysis followed by standard PCR on CHRFAM7A reveals a reduction in the aH4 level after LPS treatment, in accordance with the transcript down-regulation. (C) The control IL-6 promoter showed that the LPS challenge on THP-1 cells induces an increase in p50 NF-κB subunit binding and a decrease in p65 NF-κB subunit signal, with a reduction in the Histone 4 acetylation (aH4). (D) EMSA assay performed with a radiolabeled oligonucleotide complementary to the CHRFAM7A NF-κB sequence on LPS-treated and untreated THP-1: the LPS treatment induces the formation of seven complexes (indicated in red), but no specific supershift in the presence of specific antibody against NF-κB subunits could be observed. (E) EMSA assay performed with a radiolabeled NF-κB consensus sequence on LPS-treated and untreated THP-1: the LPS challenge induces the formation of a specific complex which undergoes a supershift in the presence of the NF-κB p50 antibody.

4.1.7. LPS treatment decreases CHRFAM7A promoter activity

Chromatin Immunoprecipitation analysis performed on CHRFAM7A promoter revealed that, after LPS stimulation on THP-1 cells, no p50, p65 or c-Rel binding at the NF-κB sequence located at -1707 bp from the ATG in exon B could be observed. However, many evidence, including the reduction of aH4 level, suggested that the down-regulation of CHRFAM7A expression after LPS treatment is driven by a transcriptional mechanism.

These observations might indicate that NF-κB binds to another promoter region.

In order to map the NF-κB binding sequence driving transcriptional repression upon LPS treatment, we decided to perform a transfection experiment using different CHRFAM7A promoter deletion constructs. Five hours after the transfection the cell medium was changed and the following day the cells were treated with 1 µg/mL LPS for six hours: given that the down-regulation relies on a transcriptional mechanism, the LPS treatment should induce a decrease in the promoter activity, detectable by a reduction of the reporter gene transcription, in all the deletion constructs carrying the NF-κB cognate sequence.

We tested three different deletion constructs: the full length construct -2122 bp/-184 bp, the -1458 bp/-184 bp, which starts downstream with respect to the NF-κB predicted sequence and the shortest construct, the -557 bp/-184 bp, that corresponds to the minimal CHRFAM7A promoter region.

All the constructs showed a statistically significant decreased activity of about 35% after LPS treatment, thus indicating the presence of NF-κB binding in the region encompassing -557 bp and -184 bp from the ATG in exon B (**Fig. 4.1.7A**).

To confirm the results, we also generated a control deletion construct carrying only the promoter region from -2122 bp to -557 bp: if the NF-κB responsive sequence is indeed included between -557 bp and -184 bp, this construct should not respond to LPS.

As expected, although the -2122 bp/-557 bp construct showed lower activity with respect to the full length construct, indicating the presence of important positive elements in the deleted region, it undergoes a slight down-regulation after LPS challenge, but this difference is not statistically significant, confirming that the -557 bp/-184 bp region does contain a LPS-responsive element.

The MatInspector online tool does not predict any NF-κB binding sequence in the region between -557 bp and -184 bp, but highlights the presence of several consensus sequences for transcription factor known to interact with NF-κB (**Fig. 4.1.7B**). For example, it has been demonstrated that NF-κB binds to a non-classical consensus sequence for CREB on IL-1β promoter (Cogswell et al., 1994) and that c-Rel and RelB are able to repress INFβ transcription through the involvement of YY1 as result of a signaling induced by TLR-3 (Siednienko et al., 2011).

On the other hand, different prediction software for transcription factor binding sites, such as TFBIND (http//: www.tfbind.it), revealed the presence of several consensus sequences for NF-κB.

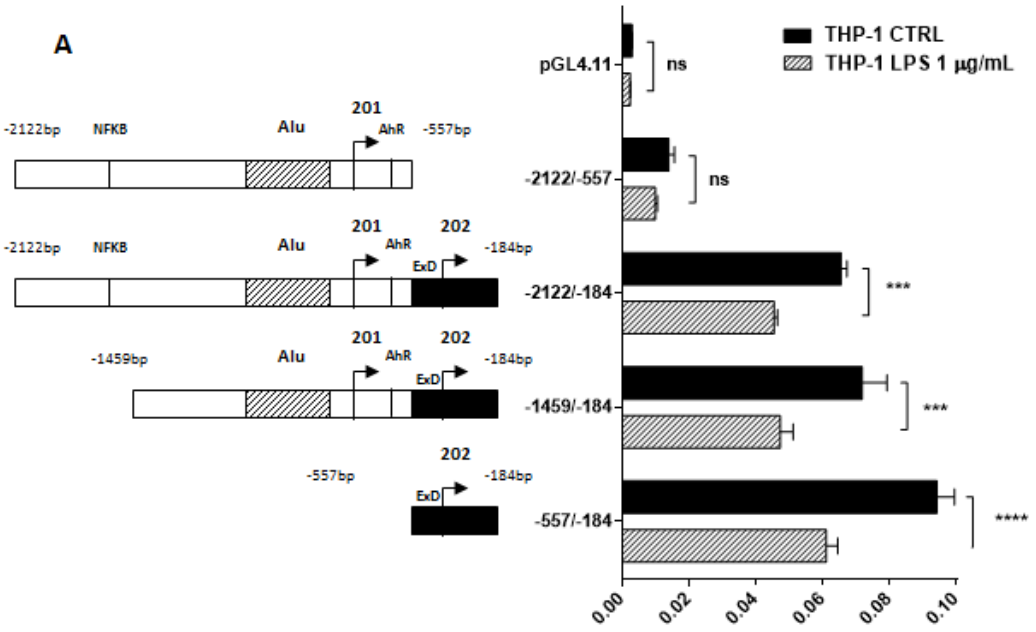

B

```
ExD     -557
AGCCCTTTCC CAGGCGGTAG CGGGGGCAGT GGTGCTGTTG CCCTTTTAAA CTGCGGCTTG  -506
   NF-xB                                    NF-xB
ACGGGAGCCG CGCCTCCTGT CGGTGGAGTC GGTTATAAAG GGAGCAGCCC CGCAGGCCGC  -446
 TSS -447                          TSS -415 NF-xB
CACATAGCTC CCGCCAAGTC CTCGGTGCCC CTTGCCATTT TCCAGCCGCG CTCCCACGAG  -386
                        NF-xB                    NF-xB
GGTCACGGCG GCGGGGAGAG GTGGAGCCGC GAGAGCTCGG CCGGGGGCCC CGCCTGGTGG  -326
CCGCGGCCAT GACAGCGGCT CGGGACTGGC TCCTTTTCCG CGCCCCTCCC GCCGGAGGTG  -266
                                                      STAT3
AGGGGAAGAT GTCCATGTCA GGGTTCAAGG CCAAACCGAA GTTACTGGCC TCTATCTTCC  -206
                         -184                         ExC
AGGAGAACCA GGAGCCACAG CCGCGGCTCA CGCCCCACCG CAACATTAAG ATTACAAGTG  -146
GACACCTGAG TCAGCAGGAC CTGGAATCCC AGATGAGAGA GCTTATCTAC ACGACTCAGA   -86
                                                      ExB
TCTTGTTGTC ACCCCCATTA TTGACAATCC AAAGGTGCAG AAAGCACTCT GACAATAATG   -26
AAACAACCAC CATCGGTTAA ATTTGATG                                      +3
```

Figure 4.1.7: **Identification of the LPS-responsive region in CHRFAM7A promoter**. (A) Transient transfection of THP-1 cells with -2122 bp/-557 bp, -2122 bp/-184 bp, -1459 bp/-184 bp and -557 bp/-184 bp CHRFAM7A promoter deletion constructs reveals a transcriptional activity decreased of the Luciferase reporter gene after 6 hours of LPS treatment for the constructs carrying the -557 bp/-184 bp region, while the reporter construct deleted for this region is not responsive to LPS. The results are expressed as mean ± standard error of each construct and are the mean of at least three independent experiments. The statistical analysis was performed using the one-way ANOVA analysis followed by Tukey's test with GraphPad Prism 5 Software (GraphPad Software, Inc.) and p values <0.05 were considered significant. (B) Schematic representation of the CHRFAM7A 5' flanking region: in the figure, the -557 bp/-184 bp region is

delimited and GCF2, Egr1, CREB and YY1 consensus sequences predicted by MatInspector are highlighted. In the scheme also the NF-κB sequences predicted by the online tool TFBIND.

4.1.8. Summary

Overall, the results obtained in this part of the project highlighted the complexity of the transcription of the human-restricted CHRFAM7A gene. We have investigated the transcriptional mechanisms of the gene in two different cell lines, the monocytic cell line THP-1 and the neuroblastoma cell line SH-SY5Y and we have concluded that:

- The CHRFAM7A gene has different alternative and tissue-specific TSS, and both the splicing isoforms generated from the CHRFAM7A gene are expressed in THP-1 cells and SH-SY5Y cells.
- The CHRFAM7A gene is characterized by the presence of tissue-specific regulatory elements: we have identified the minimal promoter driving its expression in THP-1 cells, while we have not yet identified the neuro-specific elements driving its expression in SH-SY5Y cells.
- The CHRFAM7A intron 4 contains an immune-specific silencer able to overthrow CHRFAM7A expression in THP-1 cells.
- CHRFAM7A intron 5 contains a TSS.
- The LPS treatment down-regulates the CHRFAM7A expression in THP-1 cells through a transcriptional mechanism involving chromatin remodelling.
- The CHRFAM7A LPS-responsive promoter region is located between -557 bp and -447 bp from the ATG in exon B.

4.2. CHRFAM7A as pharmacological target in Alzheimer's disease: a report of Donepezil effect

4.2.1. CHRNA7 and CHRFAM7A expression levels in hippocampus of AD patients

In the last years, many authors have reported a link between nAChRs functional dysregulation and development of Alzheimer's disease (AD). Indeed, cholinergic neurons

loss is a key feature of AD and is probably responsible of most of the neurological symptoms (Burghaus et al., 2000).

The expression pattern of CHRNA7 transcript in AD human brain has been investigated by different authors with different and often controversy results (Wevers et al., 2000; Counts et al., 2007): these differences are probably accountable to the different brain areas analysed.

As the discovery of CHRFAM7A gene is more recent, less evidence has been achieved about the possible role of this gene in AD development. However, given the CHRFAM7A regulatory role of CHRNA7 function, it could be of great interest to investigate CHRFAM7A expression and function in human AD pathogenesis.

For this reason, we first evaluated the expression of CHRNA7 and CHRFAM7A transcripts in different human brain areas, including hippocampus, thalamus and cerebellum: as already reported in literature, both the transcripts are expressed in all the brain areas analysed (Villiger et al., 2002). The expression level, which we compared to that detected in SH-SY5Y neuroblastoma cell line, changed depending on the sample, but the CHRNA7 expression level was always higher compared to that of CHRFAM7A (**Fig. 4.2.1A**).

We then decided to evaluate CHRFAM7A expression in RNA samples obtained from human post-mortem hippocampus of healthy control and AD patients, kindly donated by Prof. Marco Venturin of the Università degli Studi di Milano. We analysed 4 controls samples and 11 AD samples.

Interestingly, our results disagreed with those reported in literature, as we found a significant CHRNA7 transcript down-regulation in AD samples compared to controls.

The CHRFAM7A transcript was instead up-regulated in AD hippocampus compared to controls (Fig. **4.2.1B**). The CHRFAM7A up-regulation observed is not statistically significant, probably because CHRFAM7A transcript expression pattern displayed a great variability among the different samples, compared to that of CHRNA7 transcript, which is more uniform. This is probably due to the high genetic heterogeneity of CHRFAM7A gene, which is present in homozygosis, hemizygosis or is even absent in the population.

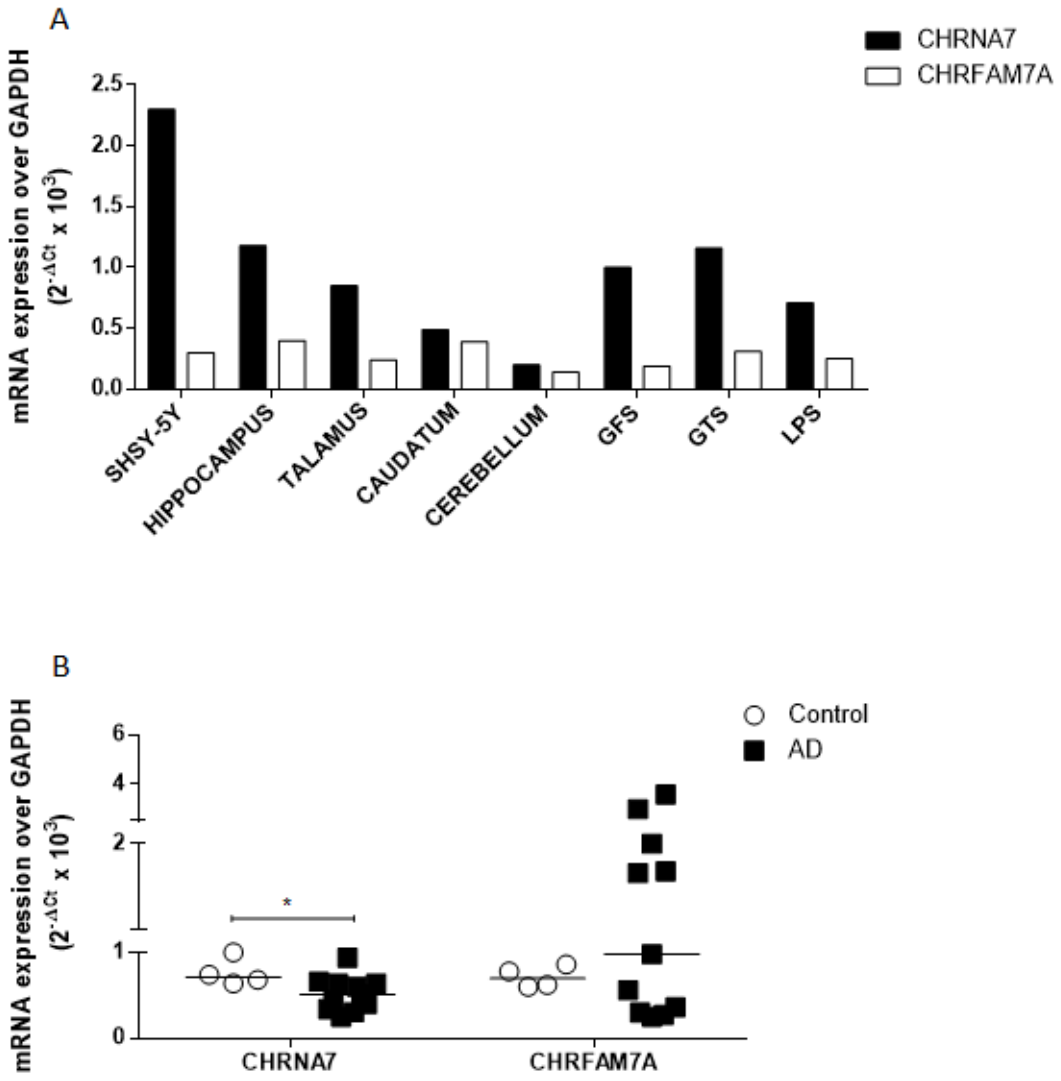

Figure 4.2.1: **CHRNA7 and CHRFAM7A expression in human CNS areas and human AD hippocampal tissue**. (A) CHRNA7 and CHRFAM7A mRNA expression level in different human brain areas. The results are compared to CHRNA7 and CHRFAM7A level of expression detected in SH-SY5Y. The data are obtained after normalization over the internal standard GAPDH and are expressed as $2^{-\Delta Ct}$ x 10^3. (B) CHRNA7 and CHRFAM7A expression level in control (white dots) and AD (black squares) RNA obtained from human hippocampal tissue. The data are obtained after normalization over the internal standard GAPDH and are expressed as $2^{-\Delta Ct}$ x 10^3. Each point represents a single donor and black line represent the median value. Statistical analysis was performed using non-parametric T-test and $p<0.005$ were considered significant.

4.2.2. CHRNA7 and CHRFAM7A expression level in human PBMCs of AD untreated and Donepezil treated patients

The pathogenic mechanisms leading to Alzheimer's disease development are very complex and have not been already completely characterized. It's a common opinion that, beside the neuronal damage mechanisms, including cholinergic loss, tau phosphorylation or amyloid plaques formation, the onset of a systemic mild inflammatory status, could contribute to AD development and progression. In this perspective, several efforts have been taken on to investigate the role of inflammation in AD.

Given the central role of CHRNA7 and CHRFAM7A in the regulation of human immune response, it become of great importance to investigate the expression of these two genes in the immune system of AD patients.

In collaboration with the laboratory of Prof. Carlo Ferraresi of the Università Milano Bicocca, we have analysed CHRNA7 and CHRFAM7A expression pattern in human Peripheral Blood Mononuclear Cells (PBMCs) of healthy controls, AD untreated patients and Donepezil treated AD patients.

Donepezil is a selective non-competitor acetyl-cholinesterase inhibitor (AChEI) frequently used in the therapy for AD. As other AChEI, Donepezil ameliorates the cognitive symptoms of AD by inhibiting AChE activity and increasing the permanence of ACh at the cholinergic synapses. However, increasing evidence indicates that it could act also as a modulator of the innate immune system, probably by directly binding the α7nAChR and activating the Cholinergic Anti-Inflammatory Pathway (Hwang et al., 2010).

We analysed 9 control samples, 8 AD samples and 10 AD-Donepezil samples.

The CHRNA7 transcript is not subjected to marked changes in expression among the different experimental groups.

The CHRFAM7A transcript is up-regulated in AD group and AD-Donepezil group compared to controls. Moreover, CHRFAM7A is down-regulated in AD-Donepezil group compared to AD group. However, the differences in CHRFAM7A transcript expression among the different groups are not statistically significant, probably due to the high heterogeneity in CHRFAM7A expression (**Fig. 4.2.2**).

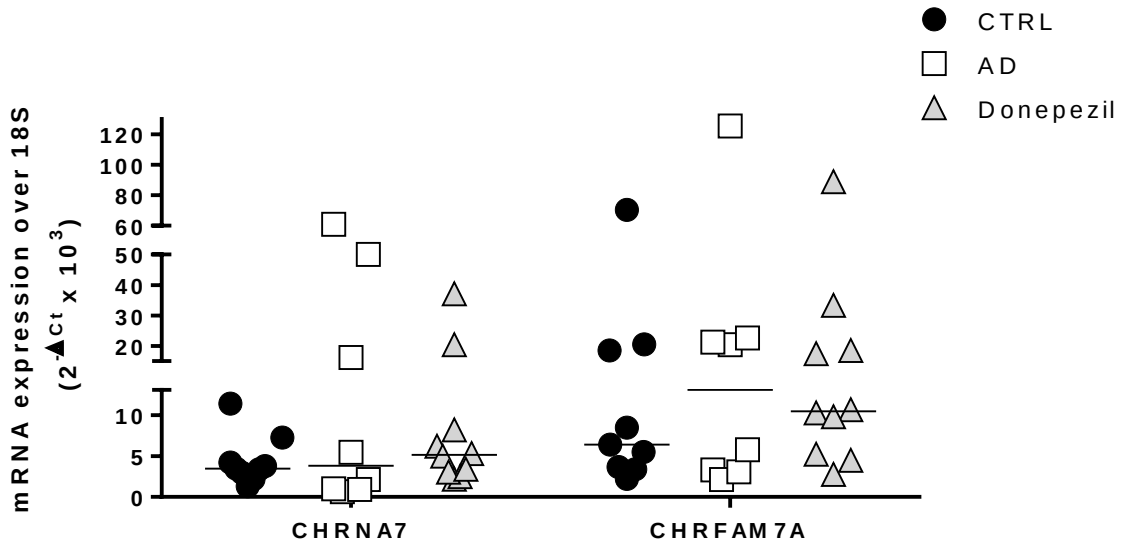

Figure 4.2.2: CHRNA7 and CHRFAM7A mRNA expression level in control (black dots), AD (white squares) and AD-Donepezil treated (grey triangles) human PBMCs samples. The data are obtained after normalization over the internal standard 18S and are expressed as $2^{-\Delta Ct} \times 10^3$. Each point represent a single donor and black line represent the median value. Statistical analysis was performed using non-parametric T-test and $p<0.005$ were considered significant.

4.2.3. Donepezil up-regulates CHRFAM7A transcript in THP-1 cell model

The qPCR analysis performed on RNA samples obtained from human PBMCs of controls, AD and Donepezil-treated AD individuals revealed a possible Donepezil effect on CHRFAM7A transcript expression. In order to better characterize the drug mechanism of action, we decided to move to an immune cell model, represented by the THP-1 cell line.

We treated THP-1 monocytic cell line with increasing concentration of Donepezil at different time in order to analyse its possible effect on CHRFAM7A expression regulation. Interestingly, the treatment with increasing concentrations of Donepezil (10 µM, 20 µM, 30 µM and 50 µM) determined an up-regulation of CHRFAM7A transcript both at 3 hours and 6 hours. The up-regulation is in line with the increasing concentration of the drug (**Fig. 4.2.3.1A**). A time course analysis with 30 µM and 50 µM Donepezil concentration (3h, 6h, 12h and 24h) showed that the CHRFAM7A mRNA up-regulation reaches a maximum at 3 and 6 hours, and remain constant until 24 hours (**Fig. 4.2.3.1B**).

Repeated experiments at 3 and 6 hours with 30 µM Donepezil confirmed the statistically significant CHRFAM7A transcript up-regulation in THP-1 cell model (**Fig. 4.2.3.1C**: hatched grey bars).

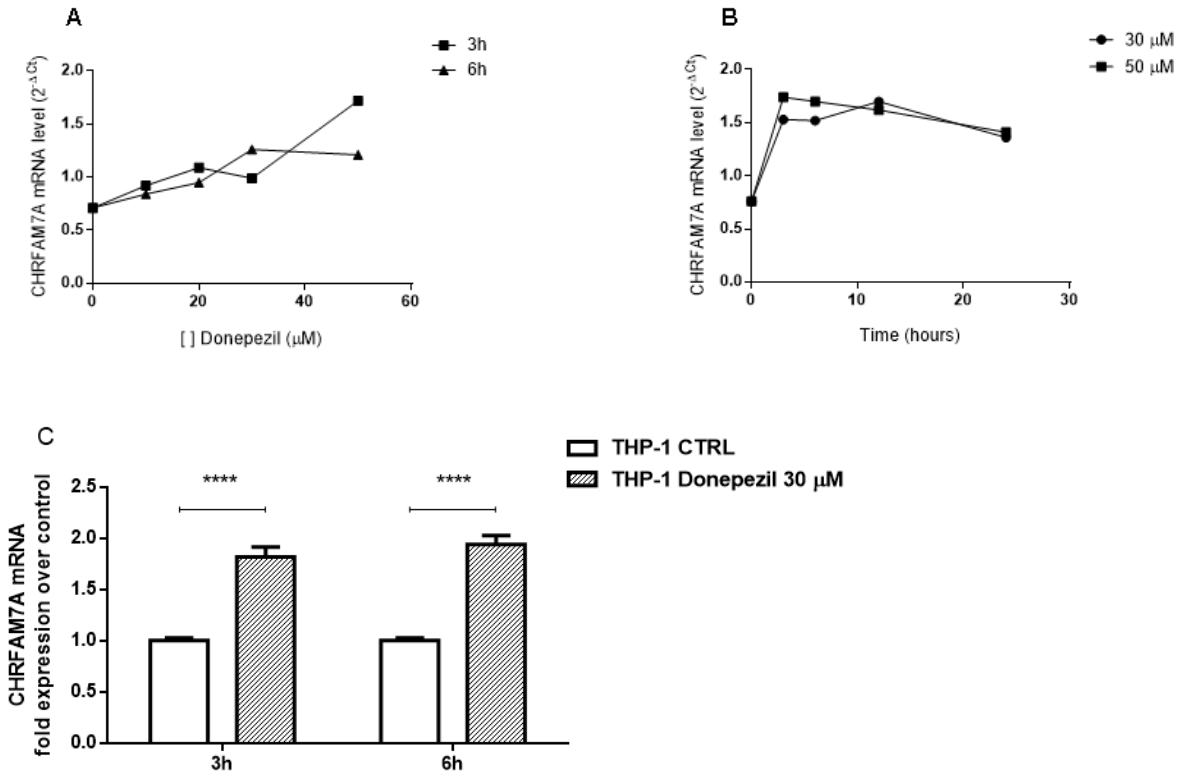

Figure 4.2.3.1: **Donepezil effect on CHRFAM7A expression in THP-1 cells**. (A) Dose-response of Donepezil (10 µM, 20 µM, 30 µM and 50 µM) at 3h (black square) and 6h (black triangle) determines the linear up-regulation of CHRFAM7A transcript in THP-1 cells. (B) Time-course experiment with 30 µM (black dot) and 50 Mm (black square) Donepezil showed a maximal up-regulation of CHRFAM7A transcript in THP-1 cells at 3h and 6h. results are expressed as relative CHRFAM7A mRNA level normalized to that of endogenous GAPDH gene, according to the $2^{-\Delta Ct}$ method. (C) Repeated experiments on THP-1 cells with Donepezil 30 µM at 3h and 6h showed a statistically significant up-regulation of CHRFAM7A transcript (grey bars) versus control cells (white bars). Results are expressed as fold expression over the untreated sample (white bar) ± standard deviations, and are the mean of at least three independent experiments. The statistical analysis was performed using ordinary One-way ANOVA followed by Tukey's test; ****p values<0.0001.

We decided to verify if Donepezil effect on CHRFAM7A transcript could counteract the down-regulation exerted by LPS treatment; for this purpose, we followed the protocol reported in **Fig. 4.2.3.2A**: cells were treated with 30 µM Donepezil for 1h, followed by 1

µg/ mL LPS challenge for 3h. At the end of experiment Donepezil treatment lasted 4 hours.

As expected, LPS treatment determined a statistical significant transcript down-regulation (**Fig. 4.2.3.2B**: dark grey bar vs white bar) while Donepezil treatment induced a significant CHRFAM7A transcript up-regulation (**Fig. 4.2.3.2B**: hatched grey bar vs white bar).

The Donepezil treatment followed by LPS challenge resulted in significant CHRFAM7A transcript up-regulation (**Fig. 4.2.3.2B**: black bar vs white bar), which is however statistically significant lower compared to the up-regulation induced by the sole Donepezil treatment (**Fig. 4.2.3.2B:** black bar vs hatched grey bar).

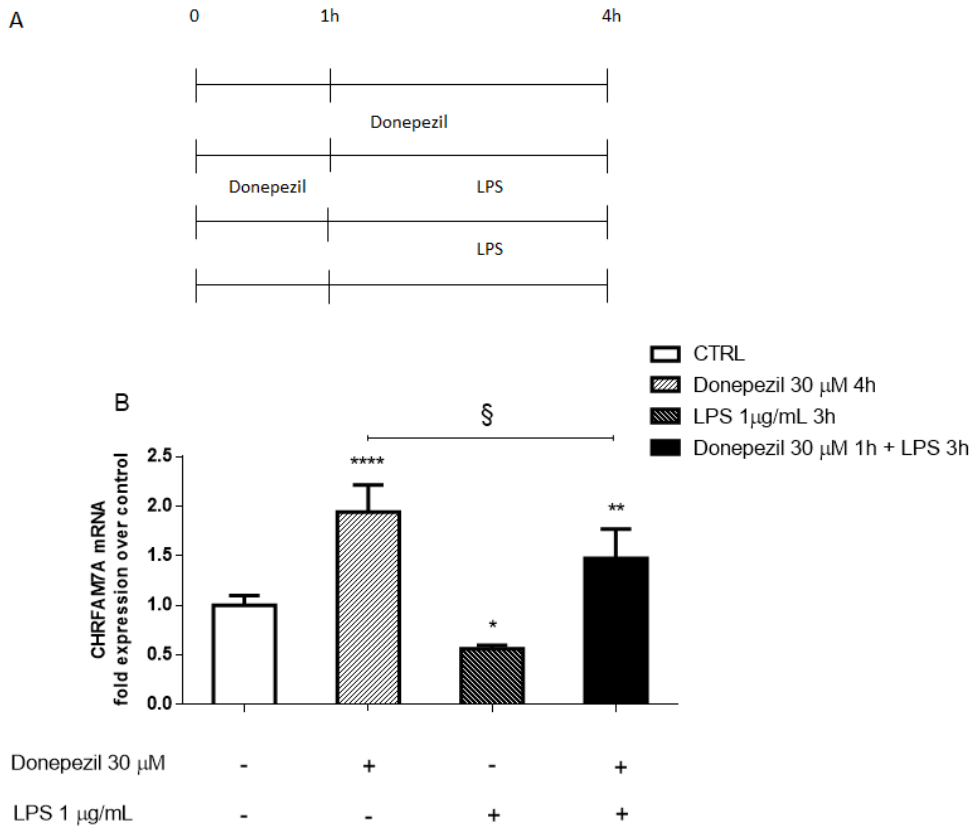

Figure 4.2.3.2: **CHRFAM7A modulation after Donepezil-LPS co-treatment in THP-1 cells**. (A) Experimental design of the Donepezil/LPS analysis. (B) The pre-treatment of THP-1 cells with 1h of Donepezil 30 µM followed by 3h of LPS 1 µg/mL challenge showed that Donepezil counteracts the CHRFAM7A transcript down-regulation induced by LPS (black bar vs dark grey bar). Results are expressed as fold expression over the untreated sample (white bar) ± standard deviations, and are the mean of at least three independent

experiments. The statistical analysis was performed using ordinary One-way ANOVA followed by Tukey's test; p values<0.005 were considered significant. *statistical significant compared to control (white bar). § statistical significant compared to Donepezil treated cells (hatched grey bar).

To simulate the drug administration in the presence of an already sustained inflammatory process, we performed the opposite experiment, by pre-treating THP-1 cells with 1 µg/mL LPS for 2h followed by two additional hours in the presence of 30 µM Donepezil, as reported in **Fig. 4.2.3.3A**. In this case, Donepezil treatment lasted two hours and LPS four hours.

As expected, LPS treatment significantly down-regulated CHRFAM7A transcript (**Fig. 4.2.3.3B**: dark grey bar vs white bar), while Donepezil treatment alone significantly up-regulated it (**Fig. 4.2.3.3B**: hatched grey bar vs white bar). The combination of the two treatments (black bar) determined again a significant up-regulation of CHRFAM7A over the control (**Fig. 4.2.3.3B**: black bar vs white bar), although significantly lower with respect to that induced by the Donepezil treatment alone (**Fig. 4.2.3.3B**: black bar vs hatched grey bar), as observed in the previous experiment. These data led us to conclude that Donepezil either if added after or previous a pro-inflammatory stimulus, is capable of counteracting CHRFAM7A down-regulation, due to LPS treatment.

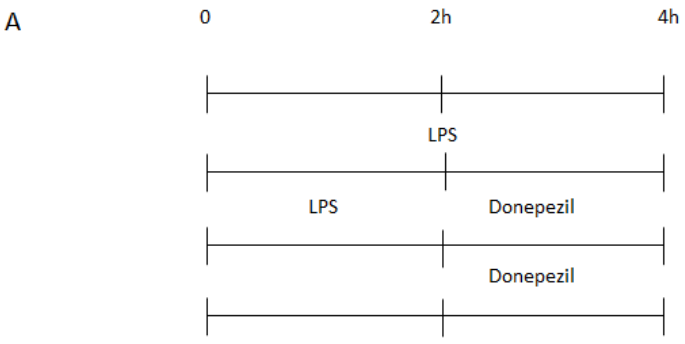

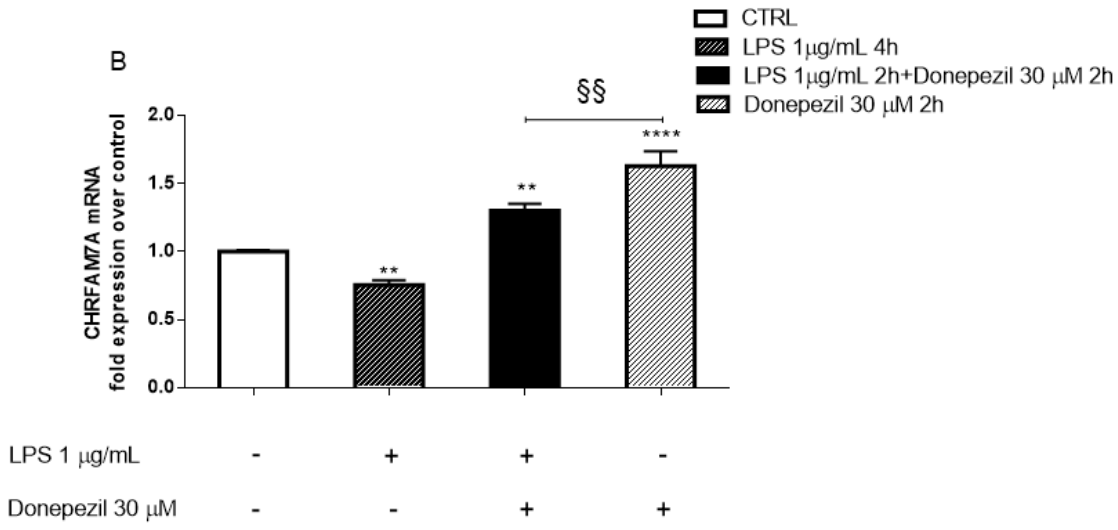

Figure 4.2.3.3: **CHRFAM7A modulation after LPS-Donepezil co-treatment in THP-1 cells** (A) Experimental design of the LPS/Donepezil analysis. (B) The pre-treatment of THP-1 for 2h with 1 μg/mL LPS (dark grey bar) followed by 2h treatment with Donepezil 30 μM showed that Donepezil counteracts the CHRFAM7A transcript down-regulation induced by LPS challenge (black bar vs dark grey bar), resulting in a statistically significant up-regulation compared to the control sample (white bar). Results are expressed as fold expression over the untreated sample (white bar) ± standard deviations, and are the mean of at least three independent experiments. The statistical analysis was performed using ordinary One-way ANOVA followed by Tukey's test; p values<0.005 were considered significant. *statistical significant compared to control (white bar). § statistical significant compared to Donepezil treated cells (hatched grey bar).

LPS treatment is commonly considered as a good paradigm of acute inflammation. In order to investigate whether the Donepezil effect on CHRFAM7A expression could be an indication of an anti-inflammatory effect of the drug, we decided to evaluate the transcriptional response of two inflammatory genes, IL-6 and TNF-α, after Donepezil administration following LPS pre-treatment. LPS strongly induces IL-6 and TNF-α gene expression; for this reason, the experimental design here differed from the protocol of **Fig. 4.2.3F**: we extended the time of Donepezil treatment in order to be sure to measure any possible variation in these inflammatory cytokine genes, as reported in **Fig. 4.2.3.4A**.

After five hours of LPS treatment, the down-regulation of CHRFAM7A transcript is not statistically significant compared to control cells (**Fig. 4.2.3.4 B**: dark grey bar vs white bar), as already reported in Benfante et al., 2011. However, four hours Donepezil treatment induced a significant up-regulation of CHRFAM7A transcript (**Fig. 4.2.3.4B**:

hatched grey bar vs white bar) and the co-treatment determined a significant CHRFAM7A transcript increase over the control (**Fig. 4.2.3.4B**: black bar vs white bar), however significant lower with respect to that induced by Donepezil treatment alone (**Fig. 4.2.3.4B**: black bar vs hatched grey bar).

The TNF-α transcript is dramatically up-regulated after LPS treatment (**Fig. 4.2.3.4C**: dark grey bar vs white bar) but the administration of Donepezil after 1 hour from the LPS challenge significantly reduced TNF-α transcription (**Fig. 4.2.3.4C:** black bar vs dark grey bar). Donepezil alone did not increase TNF- α transcription (**Fig. 4.2.3.4C**: hatched grey bar vs white bar).

The IL-6 transcript is not expressed in untreated THP-1 cells, but LPS treatment induced its expression: the co-treatment LPS-Donepezil determined a slight down-regulation compared to the LPS-treated cells (**Fig. 4.2.3.4D**: black bar vs dark grey bar), however not statistically significant. Nevertheless, all together, this evidence may indicate that Donepezil has an anti-inflammatory effect on THP-1 cells.

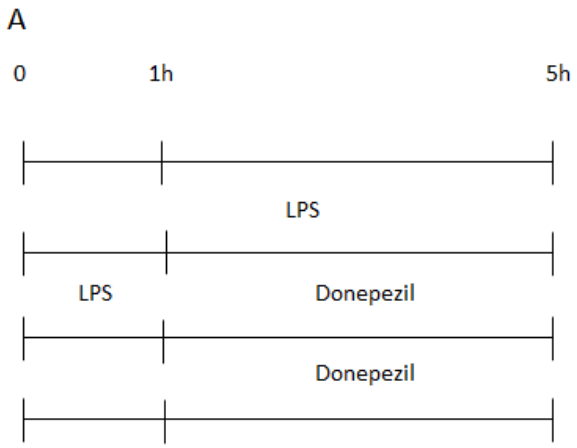

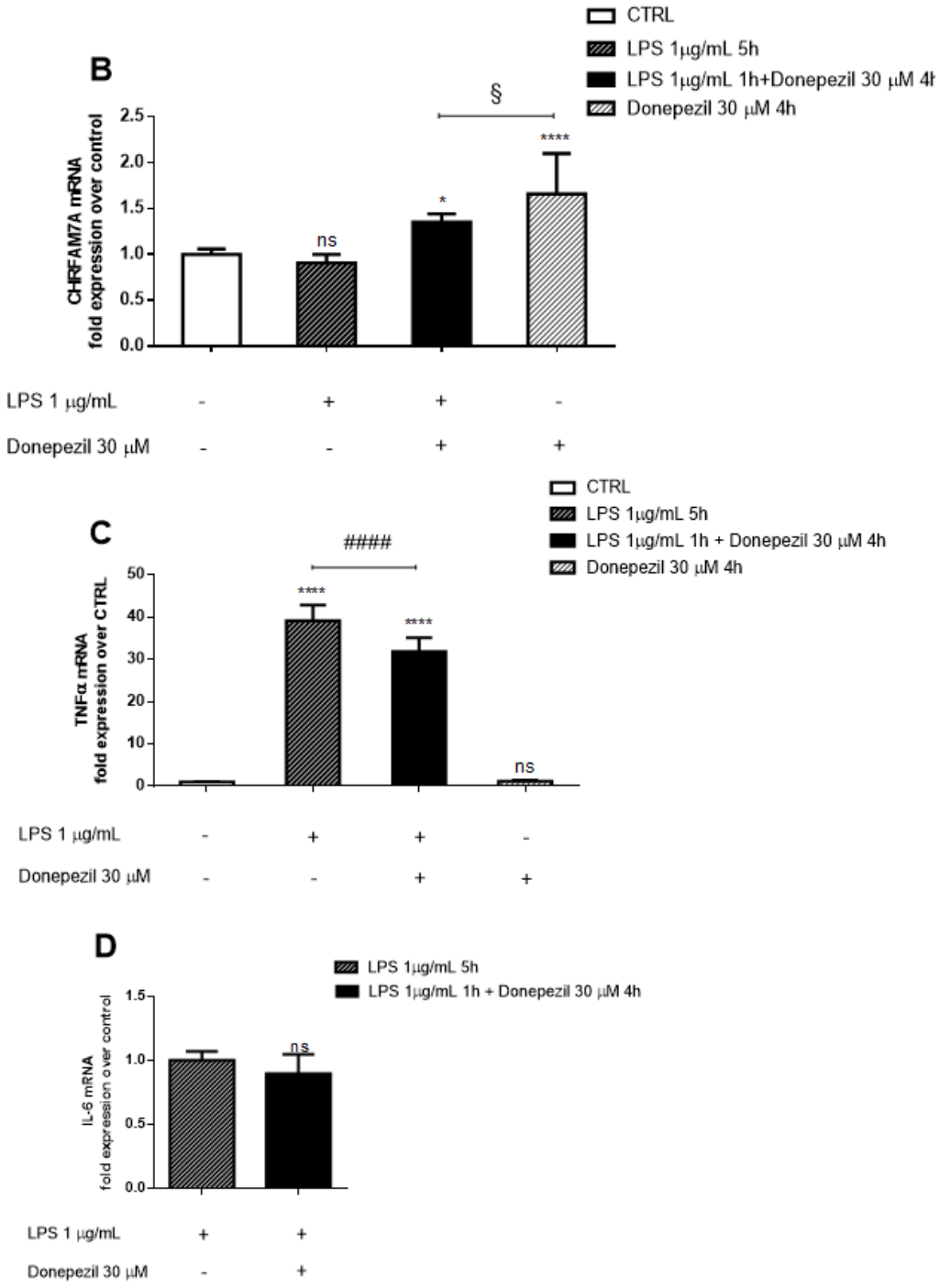

Figure 4.2.3.4: Donepezil counteracts the LPS-mediated pro-inflammatory cytokines expression in THP-1 cells. (A) Experimental design of the LPS/Donepezil analysis performed to investigate the anti-inflammatory effect of Donepezil. (B) Donepezil treatment (4 hrs) after LPS challenge (1 hr) significantly up-regulates CHRFAM7A transcript in THP-1 cell line (black bar vs white bar). (C) Donepezil treatment (4 hrs) after LPS challenge (1 hr) significantly reduces TNF-α transcription (black bar vs grey bar). (D) Donepezil treatment (4 hrs) after LPS challenge (1hr) induces a slight down-regulation of IL-6 transcript (black bar vs grey bar). Results are expressed as fold expression over the untreated sample (white bar) ± standard deviations, and

are the mean of at least three independent experiments. The statistical analysis was performed using ordinary One-way ANOVA followed by Tukey's test; p values<0.005 were considered significant. *statistical significant compared to control (white bar). § statistical significant compared to Donepezil treated cells (hatched grey bar) # statistical significant compared to LPS treated cells.

To further characterize the molecular mechanism of Donepezil on CHRFAM7A up-regulation, we set up a transcription arrest experiment by means of Polymerase II inhibitor DRB treatment, in order to evaluate if the up-regulation of CHRFAM7A transcript after Donepezil treatment is due to a transcriptional or a post-transcriptional mechanism, for example by increasing CHRFAM7A mRNA stability. After three hours of Donepezil challenge, THP-1 cells were treated with 75 µM DRB and collected at 1, 2, and 4 hours of treatment. CHRFAM7A transcript level was evaluated by quantitative Real-Time PCR and compared to that of untreated THP-1 cells (**Fig. 4.2.3.5**).

In the absence of Donepezil, we confirmed that CHRFAM7A transcript half-life measured is approximately 120 minutes (Benfante et al., 2011); Donepezil pre-treatment did not affect CHRFAM7A mRNA stability (**Fig. 4.2.3.5**: white squares vs black dots), indicating that Donepezil does not increase CHRFAM7A expression *via* a post-transcriptional mechanism, but rather suggesting that a regulation occurs at the level of transcription. For control purpose, we also measured CHRFAM7A transcript level of DRB-untreated and DMSO-treated cells (DRB vehicle), in order to exclude changes due to the vehicle (data not shown).

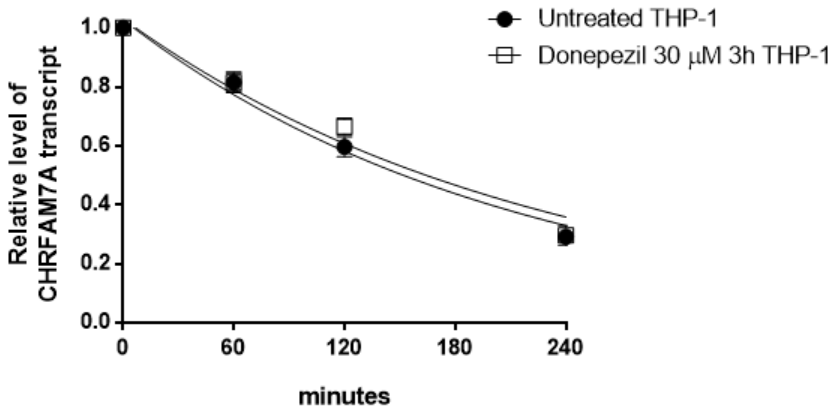

Figure 4.2.5: Transcription arrest analysis on THP-1 treated for 3h with 30 µM Donepezil: no significant changes were observed between the untreated (black circles) and Donepezil-treated (white squares)

samples at 1h, 2h or 4h DRB treatment. Results are expressed as fold expression over time 0 sample (set as 1) ± standard deviations and are the mean of at least three independent experiments. The statistical analysis was performed using ordinary one-way ANOVA followed by Tukey's test; p values <0.05 were considered significant.

4.2.4. Donepezil treatment on human primary macrophages modulates CHRNA7 and CHRFAM7A transcript

The THP-1 cell line usually represents a good *in vitro* model to predict monocytes behaviour. However, the low level of expression of CHRNA7 transcript did not allow to investigate the CHRNA7 gene response to Donepezil treatment. For this reason and in order to better define the *in vivo* response, we decided to repeat the treatment on human primary macrophages obtained by differentiation with M-CSF of human primary monocytes of four different healthy donors. The experiment was performed in collaboration with professor Massimo Locati and doctor Lorenzo Drufuca at the Università degli Studi di Milano.

We followed the protocol described in Fig. 4.2.4C in the presence of 20 µM Donepezil final concentration. Macrophages of the four donors were treated with Donepezil for three hours; qPCR analysis revealed an up-regulation of both CHRNA7 (Fig. 4.2.4A) and CHRFAM7A (Fig. 4.2.4B) transcripts with respect to untreated cells in all donors, although not statistically significant, probably due to the high variability in CHRNA7 and CHRFAM7A basal expression in the human samples (**Fig. 4.2.4A, B**). Indeed, interestingly, one of the donors, indicated as donor C in **Fig. 4.2.4A**, revealed extremely low CHRFAM7A expression level, so we decided to exclude it from the statistical analysis: it is likely that the donor C has only one allele carrying the CHRFAM7A gene.

In order to confirm and expand the findings of the previous experiments about Donepezil effect on the Cholinergic Anti-Inflammatory Pathway, macrophages were pre-treated for 1h with 1 µg/mL LPS followed by 3 hours of Donepezil challenge, as reported in **Fig. 4.2.4C**.

In accordance with the preliminary results reported in the introduction of this thesis, CHRNA7 transcript was up-regulated by LPS treatment (**Fig. 4.2.4D**: dark grey bar vs white bar). Donepezil seemed to synergize the effect of LPS, as we could observe a further

significant up-regulation of CHRNA7 transcript in macrophages co-treated with LPS and Donepezil (**Fig. 4.2.3D**: black bar vs dark grey bar).

The CHRFAM7A transcript level followed the same modulation observed in THP-1 cells: the LPS treatment alone determined a CHRFAM7A down-regulation (**Fig. 4.2.4E**: dark grey bar vs white bar), while the LPS-Donepezil co-treatment induced an up-regulation (black bar vs white bar), which is slight less than to that induced by the Donepezil challenge alone (hatched grey bar vs white bar), indicating that also in an *in vivo* model, Donepezil counteracts LPS effect on CHRFAM7A expression.

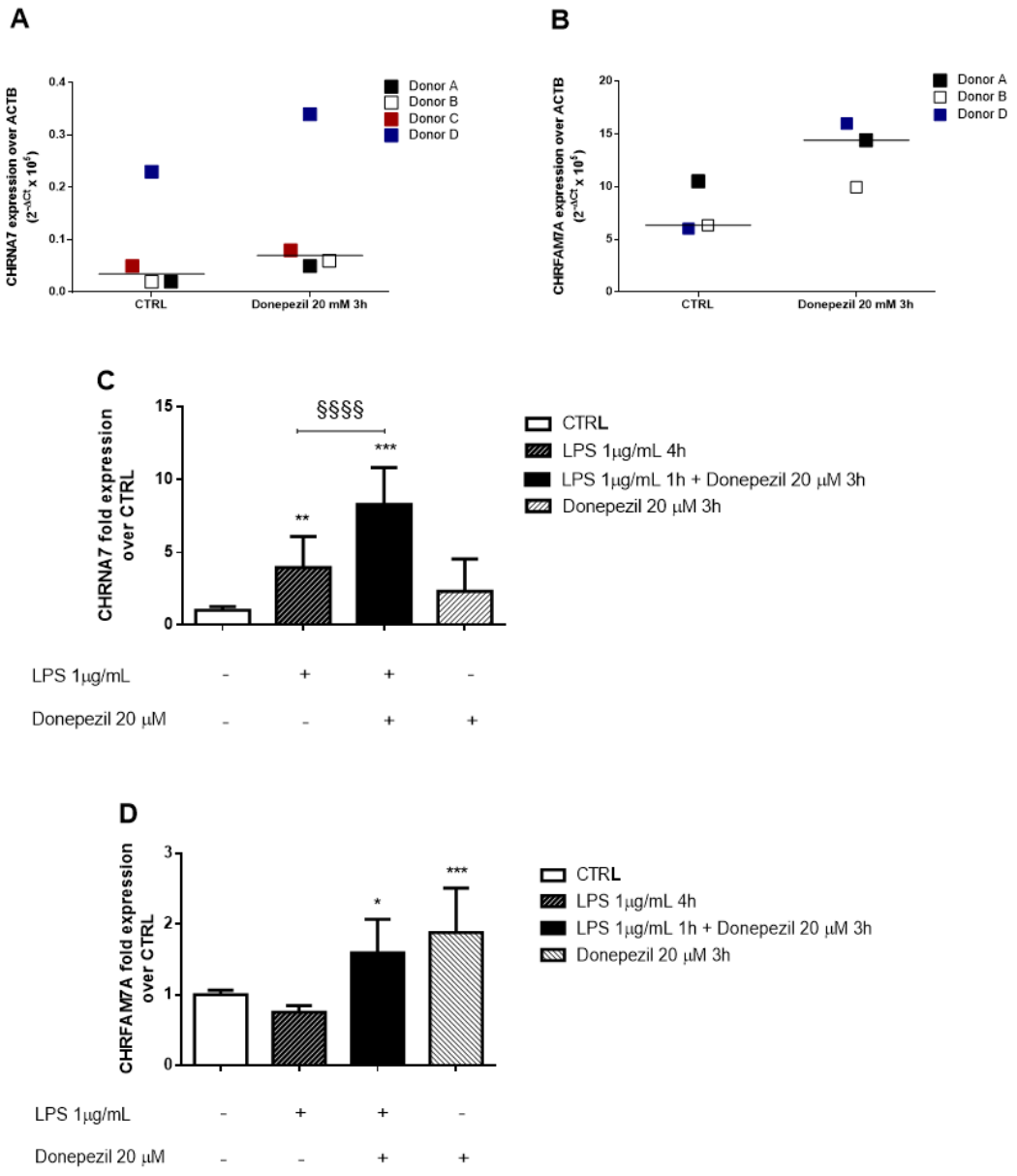

Figure 4.2.4: **Donepezil modulates CHRNA7 and CHRFAM7A expression in human primary macrophages**. (A) Donepezil treatment (20 μM, 3h) on primary human macrophages determined an up-regulation of CHRNA7 transcript, however not statistically significant. (B) Donepezil treatment (20 μM, 3h) on human primary macrophages determined an up-regulation of CHRFAM7A transcript, however not statistically significant. The data were obtained by means of quantitative Real-time PCR by normalization on the endogenous standard ACTB and are expressed as $2^{-\Delta Ct}$ x 10^5. Each point (circles for untreated cells and squares for Donepezil-treated macrophages) represents one donor. The untreated sample and Donepezil-treated sample of the same donor has the same colour. The black line corresponds to the median value. The

statistical analysis was performed using non-parametric T-test and p<0.005 were considered significant. (C) Experimental design of the LPS/Donepezil analysis on human primary macrophages. (D) CHRNA7 and (E) CHRFAM7A modulation after 1h pre-treatment with 1 µg/mL LPS followed by 3h 20 µM Donepezil. The statistical analysis was performed using one-way ANOVA followed by Tukey's test with; p values <0.05 were considered significant. *statistical significant with respect to untreated cells (white bar); § statistical significant with respect to Donepezil treated cells (hatched grey bar).

4.2.5. Donepezil treatment up-regulates CHRFAM7A and down-regulates CHRNA7 gene in SH-SY5Y cell model

The AChEI Donepezil has demonstrated anti-inflammatory properties, but its principal therapeutic effect is exerted in the CNS, where it inhibits the degradation of ACh and potentiate the cholinergic transmission.

For this reason, given the expression of both CHRNA7 and CHRFAM7A in SH-SY5Y neuroblastoma cells, we decided to evaluate the effect of Donepezil in this cell model.

In line with the THP-1 treatment optimization, we treated SH-SY5Y cells with 30 µM Donepezil for 3 hours and 6 hours.

Intriguingly, in the neuroblastoma cell line, we observed a statistical significant down-regulation of CHRNA7 (**Fig. 4.2.5A**: dark grey bat vs black bar) and an up-regulation of CHRFAM7A (**Fig. 4.2.5B**: hatched grey bar and dark grey bar vs black bar) transcript. The CHRNA7 down-regulation is statistically significant only at 6 hours of treatment, whereas CHRFAM7A transcript level compared to control cells is significantly higher both at 3h and 6h of treatment, with a fold expression similar to that observed in Donepezil-treated THP-1 cells.

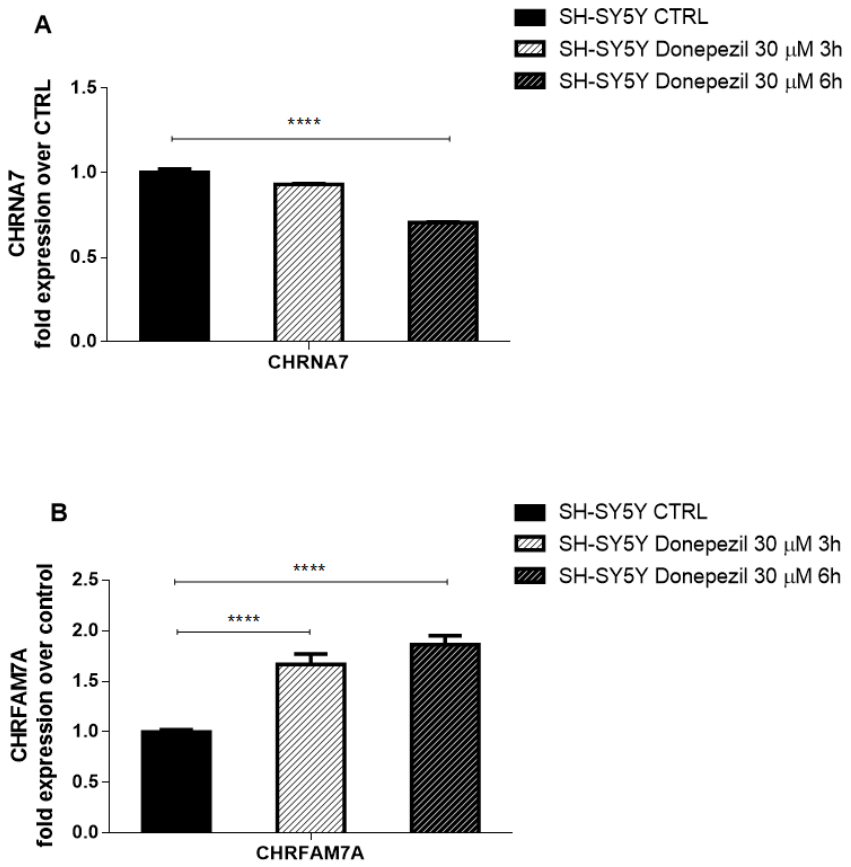

Figure 4.2.5: Donepezil modulates CHRNA7 and CHRFAM7A expression in SH-SY5Y cells. 3 hours and 6 hours 30 μM Donepezil treatment on SH-SY5Y cells induced a down-regulation of (A) CHRNA7 transcript and an up-regulation of (B) CHRFAM7A transcript. The results are the mean of three independent experiments and are expressed as fold increase over the untreated sample according to the $2^{-\Delta\Delta Ct}$ method. The statistical analysis was performed using one-way ANOVA followed by Tukey's; p values <0.05 were considered significant.

4.2.6. Summary

In this part of the project, we have investigated the possible CHRFAM7A expression alteration in human neuronal and immune tissues obtained by Alzheimer's disease patients. Moreover, we have investigated the effect of the acetylcholinesterase inhibitor Donepezil on CHRFAM7A and CHRNA7 expression. Overall, we have concluded that:

- CHRFAM7A is up-regulated in both hippocampal and PBMCs tissues of AD patients compared to controls.
- Donepezil up-regulates CHRFAM7A expression in THP-1 cells through a transcriptional mechanism.
- Donepezil counteract the LPS-mediated down-regulation of CHRFAM7A in THP-1 cells.
- Donepezil up-regulates CHRNA7 and CHRFAM7A in human primary macrophages.
- In SH-SY5Y cells, the drug induces a concomitant down-regulation of CHRNA7 and up-regulation of CHRFAM7A.

5. Discussion

The homomeric α7 nicotinic acetylcholine receptor (α7nAChR) (CHRNA7) is widely expressed in the Central Nervous System (CNS) where it plays pivotal role in neurotransmitter release modulation and generation of the action potential, modulating calcium-dependent events (Berg and Conroy, 2002).

Recently, it has been found also in extra-neuronal tissues, including epithelial cells, endothelial cells, fibroblasts, and macrophages (Sharma and Vijayaraghavan, 2002). The α7nAChR expressed by macrophages is implicated in the Cholinergic Anti-Inflammatory Pathway, which provide a central control of systemic inflammation by triggering a vagal cholinergic response that reduces the pro-inflammatory cytokines release. At the center of this process is the macrophage α7nAChR, which responds to ACh and triggers the intra-cellular signaling, culminating in reduced transcription of pro-inflammatory genes (Wang et al., 2003).

In 1998, Gault and collaborators discovered a new gene, later assigned as CHRFAM7A, composed by exons 5-10 of CHRNA7 fused in frame with exons D, C, B and A, belonging to the FAM7A (Chr.15) and ULK4 gene (Chr.3). The chimeric gene maps on chromosome 15q13.3, 1.6 Mb apart from the parental gene and its presence is restricted to humans (Gault et al., 1998).

The CHRFAM7A gene undergoes alternative splicing and is translated into a 45 KDa and 36 KDa proteins, called α7dup proteins, which conserve the entire transmembrane and C-terminal portion of the α7nAChR conventional subunit, but lack the N-terminal domain, including the signal peptide and the ACh binding domain (Villiger et al., 2002). Many studies proved the direct interaction between the duplicated and the conventional subunits and there is also evidence that the α7dup subunits could exert a dominant negative function toward the conventional receptor, segregating it in the Endoplasmic Reticulum or reducing the ACh-dependent calcium current (De Lucas-Cerillo et al., 2011; Araud et al., 2012; Wang et al., 2014).

Given the expression of the α7dup proteins both in the CNS and in almost all the immune cells, this evidence raise the hypothesis that the α7dup subunits could act as a functional modulator of α7nAChR activity in the CNS and immune systems.

In 2011, a study from my laboratory demonstrated that the pro-inflammatory stimulus, represented by LPS treatment, down-regulates CHRFAM7A transcript both in the THP-1 monocytic cell model and in human primary monocytes and macrophages. This down-regulation is driven by the NF-κB transcription factor, as demonstrated by the recovery of its expression level obtained with Parthenolide (NF-κB inhibitor) treatment (Benfante et al., 2011). Moreover, preliminary results on human primary monocytes and macrophages showed that LPS treatment has an opposite effect on CHRNA7 transcript, inducing an up-regulation of CHRNA7 expression.

These results indicated that THP-1, monocytes and macrophages LPS treatment, which represent a paradigm of acute inflammation, determines an alteration in CHRNA7/CHRFAM7A transcript balance, suggesting a functional role for α7dup in the immune response.

This evidence led us to hypothesize a possible model of function for the α7dup protein: our hypothesis was that it can function as an inflammatory sensor influenced by the local inflammatory status. The signaling triggered by LPS or other inflammatory molecules during the early phase of inflammation converges on NF-κB activation and its translocation into the nucleus where it simultaneously represses CHRFAM7A and induces CHRNA7 transcription, although there is no evidence that the CHRNA7 up-regulation observed in human monocytes and macrophages is directly mediated by NF-κB.

A reduced number of α7dup subunits and an increased number of α7 conventional subunits will be translated, with a consequent increased number of α7 functional receptors in the membrane.

The increased number of α7nAChR enhance the anti-inflammatory effect induced by ACh, thus providing the first step in the resolution of inflammation (**Fig. 5.1**).

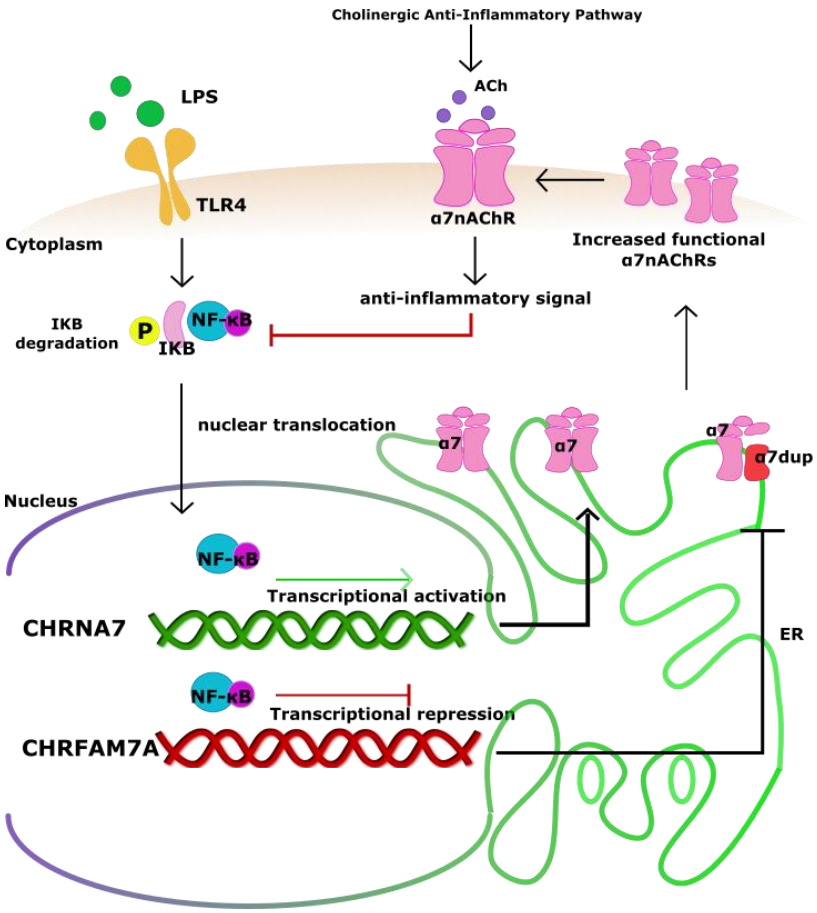

Figure 5.1: Graphical representation of the hypothesized model of function of the α7dup subunit during an acute inflammation process: the signalling triggered by LPS-TLR4 interaction results in NF-κB nuclear translocation. In the nucleus, NF-κB binds CHRNA7 and CHRFAM7A promoter inducing transcriptional activation and repression respectively, thus reducing the number of α7dup subunits retaining the functional α7nAChR in the ER. This process allows an increase in the number of α7 receptors in the cell membrane, thus potentiating the Cholinergic Anti-Inflammatory Pathway response and initiating the resolution phase.

Our goal was to decipher the transcriptional mechanisms driving CHRFAM7A regulation in order to better understand the role of the Cholinergic Anti-Inflammatory Pathway and its possible dysregulation in pathological conditions, including immune system disorders and neurological diseases characterized by inflammatory status.

As a first step, we decided to characterize the CHRFAM7A promoter, in order to better understand its regulation and function. The characterization process included the identification of the TSS and the functional analysis in THP-1 and SH-SY5Y cells. 5'-RACE

analysis performed to identify CHRFAM7A TSS revealed the presence of different alternative and tissue-specific promoters.

In particular, the presence of different TSS for the two splicing isoforms in THP-1 lead us to hypothesize that CHRFAM7A alternative splicing could be driven by alternative promoter expression, as demonstrated for other genes (Ayoubi and Van de Ven, 1996).

On the contrary, in SH-SY5Y cells 5'-RACE analysis identified a unique and different TSS and the only transcript detected is the isoform 1, including exon B. However, the standard PCR analysis, performed with primers designed to specifically detect the transcript from -771 bp and from -447 bp, revealed the presence of these two mRNA also in SH-SY5Y cell model. Nevertheless, the PCR result does not exclude that the transcription can start also and predominantly from the TSS located at -415 bp identified by 5'-RACE analysis. Moreover, standard PCR analysis and Real-Time absolute quantification assay, designed to specifically detect CHRFAM7A isoform 1 and isoform 2, demonstrated the expression of both isoforms in THP-1 and in SH-SY5Y cells, with a higher expression of isoform 1 compared to isoform 2. These results suggested that, whatever is the TSS used in SH-SY5Y cells, the isoform 1, supposedly transcribed from all the TSS identified, is the major CHRFAM7A transcript.

The functional analysis of CHRFAM7A promoter in THP-1 cells, identified a region including strong positive elements sufficient to provide a robust CHRFAM7A expression. The deletion of the AluY sequence found in CHRFAM7A promoter between -1083 and -830 base pairs upstream the ATG codon, determined a dramatic increase in transcriptional activity, suggesting that this sequence can have a negative effect on gene transcription, as reported by other authors: indeed, there are several examples that the presence of Alu sequences in different genes promoters, such as that of the α6 nicotinic acetylcholine receptor (CHRNA6), could drive transcriptional repression (Levine and Manley, 1989; Ebihara et al., 2002).

The region analysed does not correspond to that identified by Costantini and collaborators in 2015 (Constatini et al., 2015), that, by a deeper analysis, is revealed to correspond to CHRFAM7A intron 2. In our opinion, this region is able to provide a basic CHRFAM7A expression (4-fold increase over the empty vector), but lacks all the elements,

which confer to the promoter the higher transcriptional activity (35-fold over the empty vector for the -735 bp/-184 bp deletion construct).

In SH-SY5Y, instead, we could observe a different asset: despite the high level of CHRFAM7A expression, all the deletion construct analysed failed to induce robust transcriptional activity, indicating that this promoter region may either contain strong negative neuro-specific elements or that the 5'-flanking region starting at -735 bp from the ATG in exon B, even if providing a basic transcriptional activity, lacks all the elements necessary for CHRFAM7A expression in neuronal cells.

We then hypothesized that the neuro-specific transcriptional elements could be located in other CHRFAM7A genomic regions. In 2005, Stefen and collaborators identified a neuro-specific enhancer element in the murine *chrna7* intron 4 driving the neuronal expression. The specific location of the enhancer was not identified, but the authors mapped it at the 3' of the deletion breakpoint found in chromosome 15 in a mouse model of Angelman and Prader-Willi syndrome (Stefen et al., 2005).

The recombination event driving the formation of the human CHRFAM7A gene occurred in CHRNA7 intron 4, in correspondence to an Alu sequence. The CHRFAM7A intron 4 is therefore an interesting element, as it contains the recombination point, an Alu element and a region derived from the CHRNA7 intron 4 where a putative neuro-specific enhancer can be present. Interestingly, the analysis of CHRFAM7A intron 4, while not revealing any neuro-specific elements, led us to identify a THP-1-specific negative element, overthrowing CHRFAM7A promoter transcriptional activity. The presence of the AluY element in intron 4 led us to hypothesize a possible role of the repetitive element: indeed, in the last years, several studies demonstrated that these genomic sequences, beforehand considered as "junk DNA", could have pivotal role in regulating crucial molecular process, including transcription, splicing and epigenetic modulation (Ebihara et al., 2002). However, in THP-1 cells, the deletion of the AluY element induced only a partial activity recovery, indicating that the Alu element can have a corollary role in the transcriptional repression exerted by CHRFAM7A intron 4, but that there are also other elements contributing to the tissue-specific repression.

The high complexity of CHRFAM7A transcriptional regulation mechanisms was also confirmed by the casual discovery of a transcription starting from CHRFAM7A intron 5, found in THP-1 and SH-SY5Y cDNA.

Even though THP-1 cells do not express CHRNA7 transcript, making us confident that the transcript analysed was specific for CHRFAM7A gene, we couldn't demonstrate that the putative TSS isn't shared between the CHRNA7 gene and its duplicated form. However, if true, it might implicate the presence of another alternative promoter driving the expression of the shortest CHRFAM7A isoform.

Given the pivotal role played by the α7 nicotinic acetylcholine receptor in the cholinergic anti-inflammatory pathway, and the several evidence that its duplicated form could exert a dominant negative effect toward its function, we were interested in characterizing the CHRFAM7A behaviour in the presence of pro-inflammatory or anti-inflammatory stimuli.

As demonstrated by Benfante et al., both CHRFAM7A transcript and protein are down-regulated by LPS in THP-1 cells and primary human monocytes and macrophages through a transcriptional mechanism reliant on NF-κB transcription factor (Benfante et al., 2011). In this perspective, we decided to better characterize the role of NF-κB, by defining its binding sequence into CHRFAM7A promoter.

We started by analysing a NF-κB consensus sequence predicted by the MatInspector software at -1707 bp from the ATG in exon B. The Chromatin ImmunoPrecipitation (ChIP) analysis revealed that LPS treatment induces a reduction in the Histone 4 acetylation level, confirming that the down-regulation of CHRFAM7A transcript is due to a transcriptional mechanism involving chromatin remodeling. However, no p65, p50 or c-Rel binding was observed. A consequent Electrophoresis Mobility Shift Assay (EMSA) experiment confirmed that the region analysed is not bound by p65, p50 or c-Rel.

Given this evidence, we could hypothesize that (i) NF-κB binds to another cognate sequence into the CHRFAM7A promoter, (ii) the NF-κB subunits involved in the down-regulation are the non-canonical ones, including RelB and p52 or (iii) both the possibilities simultaneously.

As the down-regulation is driven by a transcriptional mechanism, we decided to localize the NF-κB binding sequence, by evaluating the transcriptional activity reduction

of different CHRFAM7A deletion construct after LPS treatment. The three construct, -2122 bp/-184 bp, -1459 bp/-184 bp and -557 bp/-184 bp, underwent a significant activity reduction after 6 hours of LPS challenge, suggesting that the responsive NF-κB sequence is located in the region between -557 bp and -447 bp from the ATG in exon B.

In the last years, increasing evidence has highlighted the link between CHRNA7 expressional or functional dysregulation and development of neuropsychiatric and neurodegenerative disorders.

In particular, Alzheimer's disease (AD) is characterized by a massive loss in cholinergic neurons and recent evidence suggests that most of the biological changes are attributing to a neuro-inflammatory status or even to a systemic inflammatory status (Guan et al., 2002). Moreover, the α7nAChR might play a crucial role in the development of the disease, as it has been demonstrated that it could directly bind to the $A\beta_{42}$ aggregates, which seem to modulate its activation (Wang et al., 2000).

Since its discovery, also the CHRFAM7A gene has become an interesting candidate in the AD research, but, although the numerous studies investigating the effect of CHRFAM7A genotype on AD development risk, little is known about possible CHRFAM7A expressional alteration leading to AD pathogenesis.

We have analysed CHRNA7 and CHRFAM7A gene expression pattern in human post-mortem hippocampal tissues obtained from healthy controls and AD patients: contrary to previous evidence showing no significant changes (Wevers et al., 2000) or even up-regulation (Counts et al., 2007) of CHRNA7 expression in AD brain samples, our results revealed a significant down-regulation of CHRNA7 expression in AD hippocampus compared to controls. This apparent contradiction could be explained by the different brain areas analysed: Counts and collaborators analysed Nucleus Basalis neurons, whereas Wevers et al. analysed neurons obtained from pre-frontal cortex of AD patients. Moreover, it is known that the hippocampal neuronal circuits are necessary for the integrity of memory and learning processes and that cholinergic loss during AD development mainly damages the hippocampal region (Drever et al., 2011). Given this evidence, we found not surprising the down-regulation of CHRNA7 expression in AD samples.

The CHRFAM7A gene is up-regulated in AD hippocampus compared to controls. The up-regulation is however not statistically significant, probably due to the high expressional heterogeneity in the samples analysed. However, we could observe an opposite expression modification of CHRNA7 and CHRFAM7A genes, suggesting that also in AD, as well as in the paradigm of acute inflammation represented by macrophages LPS treatment, the two isoforms undergo opposite regulation.

So far, the possible role of CHRFAM7A gene product as pharmacological target has not been investigated. However, its putative role as dominant negative regulator of the α7 nicotinic receptor makes it an interesting candidate for pharmacological intervention on immune or neurodegenerative diseases, including AD.

The acetylcholinesterase inhibitors (AChEI) drugs are currently used in the therapy for AD and exert a positive but temporary effect on behavioural and cognitive symptoms.

Although the pharmacological effect of AChEI is mainly due to acetylcholine degradation inhibition at cholinergic synapses, recent findings indicated that their ability to trigger the Cholinergic Anti-Inflammatory Pathway by binding the α7nAChR consistently contributes to the therapeutic effect (Tabet, 2006) (**Fig. 5.2**).

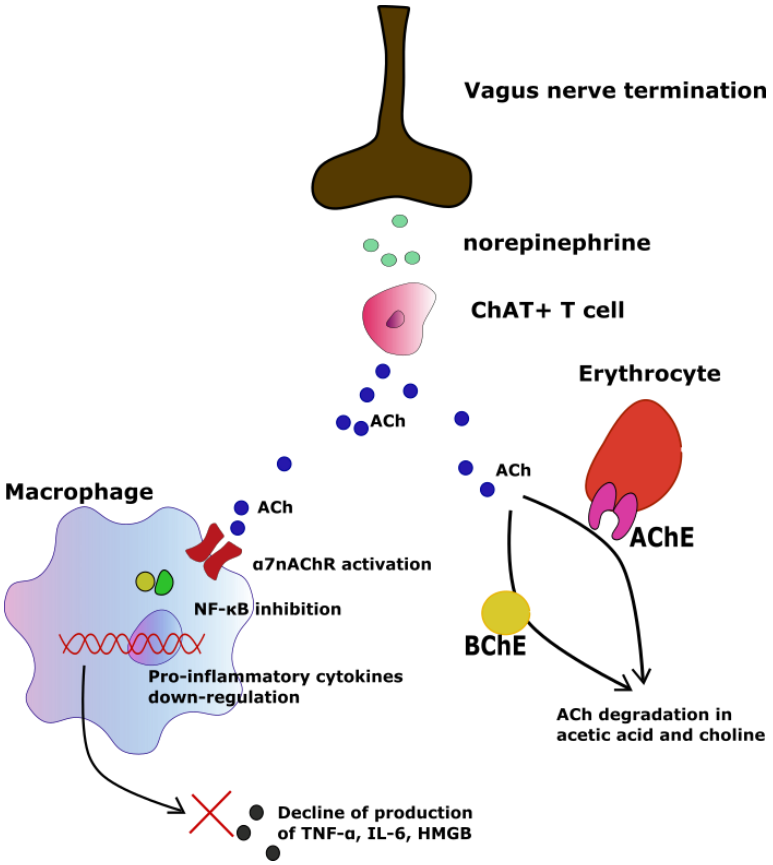

Figure 5.2: schematic representation of the role of AChE and BChE in the Cholinergic Anti-Inflammatory Pathway: the vagus nerve terminations release norepinephrine, which induce the production of ACh, which in turn stimulates the anti-inflammatory response through macrophages' α7nAChR activation. The termination of the anti-inflammatory pathway is granted by degradation of ACh provided by AChE activity associated with the circulating red blood cells and BChE in plasma.

Among the AChEI, Donepezil (Aricept^{TM}) is one of the most effective. It has been classified as a non-competitive selective inhibitor of acetylcholinesterase and, conversely to others AChEI, its mechanism is restricted to AChE and does not involve BChE inhibition. A resume of Donepezil characteristics, compared to other AChEI, is reported in **Table 5.1**.

Group of compounds	Compounds (examples)	Mechanism of inhibition	Inhibition of AChE and BChE	Penetration through Blood Brain	Importance as drug

				Barrier	
Organophosphates	Sarin, Soman, Tabun	irreversible	Equal to AChE and BChE	Good	Low
Carbamates	Pyridogstimine, Neostigmine, Rivastigmine	Pseudo-irreversible	Equal to AChE and BChE	Low	Low
-	Tacrine	Non-competitive	AChE>BChE	Good	Low
-	Galantamine	Competitive	AChE	Good	High
-	Donepezil	Non-competitive	AChE	Good	High
-	Huperzine A	Non-competitive	AChE>>BChE	Good	High

Table 5.1: resume of the main characteristics of AchE inhibitors used in therapy.

In the immune contest, it has been proposed that Donepezil activates the Cholinergic Anti-Inflammatory Pathway by inhibiting peripheral AChE activity and increasing ACh availability. However, Donepezil has been shown to directly bind to α7nAChR, as it exerts anti-inflammatory effect (reducing TNF-α and IL-1 levels) also in microglia cell lines, where no AChE expression was detected (Hwang et al., 2010).

In collaboration with the laboratory of Prof. Carlo Ferrarese at the Università Milano Bicocca, we determined the expression profile of CHRNA7 and CHRFAM7A genes in Peripheral Blood Mononuclear Cells (PBMCs) obtained from healthy controls, AD patients and AD patients treated with the acetylcholinesterase inhibitor Donepezil (Aricept^{TM}).

It has been demonstrated that the α7nAChR protein level is significantly increased in leukocytes of AD patients compared to controls and that the α7nAChR increase inversely correlates with the Mini-Mental State Examination (MMSE) score of the patients, suggesting that α7nAChR blood levels can be used as a marker for AD diagnosis (Chu et al., 2005). Moreover, Conti and collaborators found a significant increase of CHRNA7 mRNA expression in PBMCs of AD patients compared to controls. They also analysed

PBMCs obtained from AD patients treated with Donepezil, but they didn't found any significant differences compared to the untreated patients (Conti et al., 2016).

Our analyses revealed no significant changes in CHRNA7 expression level between the different biological groups, while CHRFAM7A expression is up-regulated in AD PBMCs compared to controls and Donepezil treatment determined a reduction in CHRFAM7A expression compared to the AD-untreated samples. As the antibodies currently used for the identification of the α7 protein are not able to distinguish between the conventional and duplicated form, we can speculate that the significant increment of α7nAChR protein in AD leukocytes observed by Chu et al. is actually mainly determined by CHRFAM7A protein up-regulation.

These studies led us to better characterize the effect of Donepezil specifically on CHRFAM7A gene expression.

Here we demonstrated that Donepezil treatment of THP-1 cells induces the up-regulation of CHRFAM7A mRNA acting at transcriptional level. The drug effect on CHRNA7 gene expression level cannot be measured, as the THP-1 cell model does not express the CHRNA7 transcript.

The CHRFAM7A up-regulation was an unexpected result: given the anti-inflammatory potential of the drug, we expected a down-regulation of the CHRFAM7A transcript, thus inducing an increase in the number of functional α7nAChR in the membrane to potentiate the Cholinergic anti-inflammatory pathway, as also observed in PBMCs of AD patients under Donepezil therapy (Chu et al., 2005; Conti et al., 2016).

It should, however, be taken into consideration that the THP-1 model hardly recapitulate the human monocytic lineage, as several differences in the pattern expression and phenotypic characteristics have been reported. It is possible that the low level of expression of CHRNA7 compared to the primary human monocytes and macrophages, which express both the isoforms, have altered the response to Donepezil. Indeed, it has been demonstrated that Donepezil exerts its anti-inflammatory effects mostly through the direct binding to the α7 receptor. The absence of this receptor in THP-1 cells makes it unlikely that Donepezil up-regulates CHRFAM7A through α7nAChR binding. However, there is evidence that THP-1 cells might have a slight but detectable AChE activity (Thullbery et al., 2005), so that Donepezil effect on CHRFAM7A transcript

could be mediated by AChE inhibition or by other targets, whose activation is not necessary linked to an anti-inflammatory effect observed.

For these reasons, we decided to evaluate the effect of Donepezil treatment on CHRFAM7A expression also in human primary macrophages, which represent a valid model and express also the CHRNA7 gene. The analysis on human macrophages recapitulated the results obtained on THP-1 cells, as we could observe an up-regulation of CHRFAM7A expression, confirming the validity of THP-1 cell model.

Given the results obtained on human macrophages, we hypothesized that CHRFAM7A up-regulation could be a result of a compensatory effect, directed to the restoration of the homeostatic condition after an anti-inflammatory stimulus. Indeed, we showed in THP-1 cell model as well as in human primary macrophages that Donepezil is able to counteract the CHRFAM7A down-regulation exerted by LPS treatment, attenuating the LPS-induced up-regulation of pro-inflammatory cytokines IL-6 and TNF-α.

These results agreed with the recent findings of Arikawa and collaborators, which demonstrated that Donepezil treatment reduces the pro-inflammatory cytokines levels in a murine macrophages cell model stimulated with LPS. The authors also investigated the role of NF-κB in the anti-inflammatory effect exerted by Donepezil, highlighting a reduced LPS-dependent NF-κB nuclear translocation after Donepezil treatment. However, the authors excluded an involvement of the Cholinergic Anti-Inflammatory Pathway in the anti-inflammatory effect of Donepezil, as they observe NF-κB nuclear translocation inhibition after Donepezil treatment also in the presence of the nAChR blocker mecamylamine (Arikawa et al., 2016). Although these results could be in line with our findings, which suggest that Donepezil acts via a α7nAChR-independent route, it is worth noting that the nAChR blocker mecamylamine is not specific for the α7nAChR, leaving open the questions about α7nAChR involvement.

The Donepezil challenge on human primary macrophages, led us to analyse also the CHRNA7 expression response to the drug: intriguingly, Donepezil treatment up-regulated CHRNA7 transcript and the up-regulation is synergized by LPS pre-treatment.

While we could explain the differential effect of LPS upon CHRFAM7A and CHRNA7 transcripts as a compensatory mechanisms directed to the restoration of the homeostatic condition into a physiological perturbation of a healthy system, the effect of Donepezil on

CHRNA7 and CHRFAM7A expression is more complex: a possible explanation is that the drug, in the absence of a specific pathological contest, up-regulates both the transcripts in order to maintain the balance between the pro- and anti-inflammatory forces.

Importantly, in SH-SY5Y cells, we found that Donepezil down-regulates CHRNA7 transcript, while up-regulating CHRFAM7A mRNA. This suggests that in the nervous system Donepezil acts through different routes and that CHRFAM7A gene could have a distinct role from that played in the immune system. Several studies have hypothesized a possible neurotoxic role of α7nAChR up-regulation in neurological disorders, such as AD or HIV-associated Neurocognitive Disorders (HAND), probably due to Ca^{2+}-dependent neuronal apoptosis (Counts et al., 2007; Ballester et al., 2012). In this context, the simultaneous CHRNA7 down-regulation and CHRFAM7A up-regulation exerted by Donepezil treatment in neuronal cell lines may underlie the neuroprotective action of the drug, by reducing α7nAChR function through the potentiation of the dominant negative regulatory effect of CHRFAM7A.

6. Conclusions

Overall, the results achieved in this thesis explored the high complexity of CHRFAM7A transcriptional regulation: as a human-restricted gene and a recent product of the evolutionary history, CHRFAM7A gene is endowed with all the mechanisms contributing to a fine regulation in homeostatic, pathophysiological and pathological conditions:

- CHRFAM7A gene expression is under the control of different tissue-specific regulatory regions in THP-1 monocytic cell model and neuroblastoma SH-SY5Y cell model. The CHRFAM7A 5'-flanking region encompassing -2450 bp and -447 bp from the ATG in exon B is sufficient to drive a robust transcriptional activity in THP-1 cells, allowing us to identify the α7 dup promoter. Contrary, in SH-SY5Y cells the same region did not show transcriptional activity, suggesting that it does not contain neuro-specific elements and confirming the presence of tissue-specific promoters.

- The CHRFAM7A Intron 4 includes a silencer element specific for the THP-1 cell line, as it did not repress the transcriptional activity of the α7 dup promoter in SH-SY5Y cells.

- The CHRFAM7A Intron 5 contains a Transcription Start Site, giving rise to an Open Reading Frame probably encoding the shortest α7 dup splicing isoform.

- The CHRFAM7A gene, which is down-regulated in THP-1 cells after LPS treatment, undergoes chromatin remodeling (reduced H4 acetylation), indicating that LPS mediates CHRFAM7A down-regulation by a mechanisms driven by NF-κB, through a transcriptional route involving epigenetic mechanisms.

- The CHRFAM7A NF-κB consensus sequence is probably located in the region encompassing -557 bp and -447 bp from the ATG in exon B.

Moreover, we have investigated the acetylcholinesterase inhibitor Donepezil effect on CHRFAM7A expression in immune cell model and primary human macrophages:

- In THP-1 cells, CHRFAM7A transcript is up-regulated by the acetylcholinesterase inhibitor Donepezil through a transcriptional mechanism. The drug counteract the down-regulation exerted by LPS thus exerting a possible anti-inflammatory effect. Thanks to the collaboration with professor Locati M. and doctor Drufuca L., we repeated the analysis in human primary macrophages, where we evaluated also Donepezil effect on CHRNA7 transcript. We observed the up-regulation of both CHRNA7 and CHRFAM7A in human macrophages.
- In SH-SY5Y cells Donepezil up-regulates CHRFAM7A, and down-regulates CHRNA7 transcript, suggesting a different mechanism of Donepezil function in the neuroblastoma cell model.

Given the great therapeutic potential of this drug and the little current knowledge about its mechanism of action, we consider that the results provided could contribute to a better characterization of the pharmacological activity of Donepezil.

Acknowledgment

I would like to thank all the people that have contributed to the present work.

In first place, I thank my co-tutor Dr. Roberta Benfante, who is the principal investigator of the project, and my tutors Prof. Grazia Pietrini and Prof. Diego Fornasari. I would also like to express my gratitude to all the collaborators of the present work, Prof. Carlo Ferraresi, and his co-workers, at the Università Milano Bicocca, and Prof. Massimo Locati and Dr. Lorenzo Drufuca, at the Università degli Studi di Milano.

As for the technical help and support, I would like to thank all the laboratory members, Dr. Simona DiLascio, Dr. Debora Belperio and Dr. Silvia Cardani, as well as all past members of the laboratory who have worked on the project, Dr. Fosco Giordano and Dr. Valentina Alari.

Bibliography

Adler, L. E., Olincy, A., Waldo, M., Harris, J. G., Griffith, J., Stevens, K., Flach, K., Nagamoto, H., Bickford, P., Leonard, S., Freedman, R. (1998). Schizophrenia, sensory gating, and nicotinic receptors. *Schizophrenia Bullettin, 24 (2), 189-202*.

Angelov, D., Lenouvel, F., Hans, F., Müller, C. W., Bouvet, P., Bednar, J., Moudrianakis, E. N., Cadet, J., Dimitrov, S. (2004). The histone octamer is invisible when NF-κB binds to the nucleosome. *The Journal of Biological Chemistry, 279 (41), 42374-42382.*

Araud, T., Graw, S., Berger, R., Lee, M., Neveu, E., Bertrand, D., Leonard, S. (2011). The chimeric gene CHRFAM7A, a partial duplication of the CHRNA7 gene, is a dominant negative regulator of the α7nAChR function. *Biochemical Pharmacology, 82 (8), 904-914*.

Arikawa, M., Kakinuma, Y., Noguchi, T., Tokada, H., Sato, T. (2016). Donepezil, an acetylcholinesterase inhibitor, attenuates LPS-induced inflammatory response in murine macrophage cell line RAW 264.7 through inhibition of nuclear factor kappa B translocation. *European Journal of Pharmacology, 789, 17-26*.

Arredondo, J., Chernyavsky, A. I., Jolkovsky, D. L., Pinkerton, K. E., Grando, S. A. (2006). Receptor-mediated tobacco toxicity: cooperation of the Ras/Raf-1/MEK1/ERK and JAK-2/STAT-3 pathways downstream of alpha7 nicotinic receptor in oral keratinocytes. *FASEB Journal, 20 (12), 2093-2101*.

Ayoubi, T. A., Van De Ven, W. J. (1996). Regulation of gene expression by alternative promoters. *FASEB Journal, 10 (4), 453-460*.

Bacchelli, E., Battaglia, A., Cameli, C., Lomartire, S., Tancredi, R., Thomson, S., Sutcliff, J. S., Maestrini, E. (2015). Analysis of CHRNA7 rare variants in autism spectrum disorder susceptibility. *American Journal of Medical Genetics, 167A (4), 715-723*.

Baird, A., Coimbra, R., Dang, X., Eliceiri, B. P., Costantini, T. W. (2016). Up-regulation of the human-specific CHRFAM7A gene in inflammatory bowel disease. *Biochimica and Biophysica acta clinical, 8 (5), 66-71*.

Ballester, L. Y., Capo-Velez, C. M., Garcia-Beltran, W. F., Ramos, F. M., Vazquez-Rosa, E., Rios, R., Mercado, J. R., Melendez, R. I., Lasalde-Dominicci, J. A. (2012). Up-regulation of the neuronal nicotinic receptor α7 by HIV glycoprotein 120: implications for HIV-associated neurocognitive disorders. *Journal of Biological Chemistry, 287 (5), 3079-3086*.

Benfante, R., Antonini, R. A., De Pizzol, M., Gotti, C., Clementi, F., Locati, M., Fornasari, D. (2011). Expression of the α7 nAChR subunit duplicate form (CHRFAM7A) is down-regulated in the monocytic cell line THP-1 on treatment with LPS. *Journal of Neuroimmunology, 230, 74-84*.

Berg, D. K., Conroy, W. G. (2002). Nicotinic α7 receptors: synaptic options and downstream signaling in neurons. *Journal of Neurobiology, 53 (4), 512-523*.

Bernik, T. R., Friedman, S. G., Ochani, M., diRaimo, R., Susarla, S., Czura, C. J., Tracey, K. J. (2002). Cholinergic anti-inflammatory pathway inhibition of tumor necrosis factor during ischemia reperfusion., *Journal of Vascular Surgery, 36 (6), 1231-1236.*

Boettger, M. K., Hensellek, S., Richter, F., Gajda, M., Stöckigt, R., Segond von Banchet, G., Bräuer, R., Schaible, H. (2008). Antinociceptive effects of Tumor necrosis factor α neutralization in a rat model of antigen-induced arthritis. *Arthritis and Rheumatism, 58 (8), 2368-2378*.

Bone, R. C., Grodzin, C. J., Balk, R. A. (1997). Sepsis: a new hypothesis for pathogenesis of the disease process. *Chest, 112 (1), 235-243*.

Borovikova, L., Ivanova, S., Nardi, D., Zhang, M., Yang, H., Ombrellino, M., Tracey, K. J. (2000). Role of vagus nerve signaling in CNI-1493-mediated suppression of acute inflammation. *Autonomic Neuroscience: Basic and Clinical, 85, 141-147.*

Brenner, D. E., Kukull, W. A., van Belle, G., Bowen, J. D., McCormick, W. C., Teri, L., Larson, E. B. (1993). Relationship between cigarette smoking and Alzheimer's disease in a population-based case-control study. *Neurology, 43 (2), 293-296*.

Burghaus, L., Schütz, U., Krempel, U., de Vos, R. A., Jansen Steur, E. N., Wevers, A., Lindstrom, J., Schröder, H. (2000). Quantitative assessment of nicotinic acetylcholine receptor proteins in the cerebral cortex of Alzheimer patients. *Brain Research: Molecular brain Research, 76 (2), 385-388*.

Carson, R., Craig, D., Hart, D., Todd, S., McGuinness, B., Johnston, J. A., O'Neill, F. A., Ritchie, C. W., Passmore, A. P. (2008). Genetic variation in the alpha7 nicotinic acetylcholine receptor is associated with delusional symptoms in Alzheimer's disease. *NeuroMolecular Medicine, 10 (4), 377-384*.

Caufield, M. P., Birdsall, J. M. (1998). International Union of Pharmacology XVII: Classification of muscarinic and acetylcholine receptors. *Pharmacological Reviews, 50 (2), 279-290*.

Changeaux, J. P., Bertrand, D., Corringer, P. J., Dehaene, S., Edelstein, S., Lena, C., Le Novere, N., Marubio, L., Picciotto, M., Zoli, M. (1998). *Brain Research Review, 26, 198-216*.

Chu, L., W., Ma, E. S., Lam, K. K., Chan, M. F., Lee, D., H. (2005). Increased alpha7 nicotine acetylcholine receptor protein levels in Alzheimer's disease patients. *Dementia and Geriatric Cognitive Disorders, 19, 106-112*.

Cogswell, J. P., Godlevski, M. M., Wisely, G. B., Clay, W. C., Leesnitzer, L. M., Ways, J. P., Gray, J. G. (1994). NF-kappa B regulates IL-1 beta transcription through a consensus NF-

kappa B binding site and a non-consensus CRE-like site. *The Journal of Immunology, 153 (2), 712-723*.

Conti, E., Tremolizzo, L., Santarone, M. E., Tironi, M., Radice, I., Zoia, C. P., Aliprandi, A., Salmaggi, A., Dominici, R., Casati, M., Appollonio, I., Ferrarese, C. (2016). Donepezil modulates the endogenous immune response: implication for Alzheimer's disease. *Human Psychopharmacology, 31 (4), 296-303*.

Costantini, T. W., Dang, X., Yurchyshyna, M. V., Coimbra, R., Eliceiri, B., Baird, A. (2015). A human-specific α7-nicotinic acetylcholine receptor gene in human leukocytes: identification, regulation and the consequences of CHRFAM7A expression. *Molecular Medicine, 21, 323-336*.

Counts, S. E., He, B., Che, S., Ikonomovic, M. D., DeKosky, S. T., Ginsberg, S. D., Muffson E. J. (2007). A7 Nicotinic acetylcholine up-regulation in cholinergic basal forebrain neurons in Alzheimer's disease. *Arch. Neuro., 64 (12), 1771-1776*.

Czura, C. J., Yang, H., Amella, C., Tracey, K. J. (2004). HMGB1 in the immunology of sepsis and arthritis. *Advances in Immunology, 84, 181-200*.

Damiano, J. A., Mullen, S. A., Hildebrand, M. S., Bollows, S. T., Lawrence, K. M., Arsov, T., Dibbens, L., Major, H., Dahl, H. H., Mefford, H. C., Darbro, B. W., Scheffer, I. E., Berkovic, S. F. (2015). Evaluation of multiple putative risk alleles within the 15q13.3 region for genetic generalized epilepsy. *Epilepsy Research, 117, 70-73*.

Dang, X., Eliceriri, B. P., Baird, A., Costantini, T. W. (2015). CHRFAM7A: a human-specific α7-nicotinic acetylcholine receptor gene shows differential responsiveness of human intestinal epithelial cells to LPS. *FASEB Journal, 29, 2292-2302*.

Davies, L. C., Jenkins, S. J., Allen, J. E., Taylor, P. R. (2014). Tissue-resident macrophages. *Europe PMC Funders Group (10), 986–995.*

De Jonge, W. I., Van der Zanden, E. P., The, F. O., Bijlsma, M. F., Van Westerloo, D. J., Bennink, R. J., Berthould, H. R., Uematsu, S., Akira, S., Van der Wijngaard, R. M., Boeckxstaens, G. E. (2005). Stimulation of the vagus nerve attenuates macrophage activation by activating the Jak2-STAT3 signaling pathway. *Nature Immunology, 6 (8), 855-851*.

De Lucas-Cerillo, A. M., Maldifassi, M. C., Arnalich, F., Renart, J., Atienza, G., Serantes, R., Cruces, J., Sánchez-Pacheco, A., Andrés-Mateos, E., Montiel, C. (2012). Function of partially duplicated human α7 nicotinic receptor subunit CHRFAM7A gene: potential implications for the cholinergic anti-inflammatory response. *The Journal of Biological Chemistry, 286 (1), 594-606*.

Dempster, E., Toulopoulou, T., McDonand, C., Bramon, E., Walshe, M., Wickham, H., Sham, P. C., Murray, R. M., Collier, D. A. (2006). Episodic memory performance predicted by the 2bp deletion in exon 6 of the "alpha7-like" nicotinic receptor subunit gene. *American Journal of Psychiatry, 163, 1832-1834*.

Drever, B. D., Riedel, G., Platt, B. (2011). The cholinergic system and hippocampal plasticity. *Behavioural Brain Research, 221 (2), 505-514*.

Ebihara, M., Ohba, H., Ohno, S., Yoshikawa, T. (2002). Genomic organization and promoter analysis of the human nicotinic acetylcholine receptor α6 subunit (CHRNA6) gene: Alu and other elements direct transcriptional repression. *Gene, 298, 101-108*.

Egea, J., Buendia, I., Parade, E., Navarro, E., León, R., Lopez, M. G. (2015). Anti-inflammatory role of microglial alpha7 nAChRs and its role in neuroprotection. *Biochemical Pharmacology, 97 (4), 463-472.*

Ek, M., Kurosawa, M., Lundeberg, T., Ericsson, A. (1998). Activation of vagal afferents after intravenous injection of Interleukin-1β: role of endogenous prostaglandins. *The Journal of Neuroscience, 158 (22), 9471-9479*.

Elenkov, I. J., Wilder, R. L., Chrousos, G. P., Vizi, E. S. (2000). The sympathetic nerve- An integrative interface between two supersystems: the brain and the immune system. *Pharmacological reviews, 52 (4), 595-618*.

Elsharkawy, A. M., Oakley, F., Lin, F., Packham, G., Mann, D. A., Mann, J. (2010). The NF-κB p50:p50:HDAC1 repressor complex orchestrates transcriptional inhibition of multiple pro-inflammatory genes. *Journal of Hepatology, 53, 519-527.*

Fehèr, Á., Juhász, A., Rimanóczy, Á., Csibri, È., Kálmán, J., Janka, Z. (2009). Association between a genetic variant of the alpha7 nicotinic acetylcholine receptor subunit and four types of dementia. *Dementia and Geriatric Cognitive Disorders, 28 (1), 56-62*.

Fitzgerald, K. A., Rowe, D. C., Golenbock, D. T. (2004). Endotoxin recognition and signal transduction by the TLR4/MD-2 complex. *Microbes and Infection, 6, 1361-1367*.

Flomen, R. H., Collier, D. A., Osborne, S., Munro, J., Breen, G., StClaire, D., Makoff, A. J. (2006). Association study of CHRFAM7A Copy Number and 2bp deletion polymorphisms with schizophrenia and bipolar affective disorder. *American Journal of Medical Genetics: Neuropsychiatric Genetics, 141B, 571-575*.

Flomen, R. H., Davies, A. F., Di Forti, M., La Cascia, C., Mackie-Ogilvie, C., Murray, R., Makoff, A. (2008). The copy number variant involving part of the α7 nicotinic receptor gene contains a polymorphic inversion. *European Journal of Human Genetics, 16, 1364-1371*.

Flomen, R., Shaikh, M., Walshe, M., Schulze, K., Hall, M., Picchioni, M., Rijsdijk, F., Toulopoulou, T., Kravariti, E., Murray, R. M., Asherson, P., Makoff, A. J., Bramon, E. (2013). Association between the 2-bp deletion polymorphism in the duplicated version of the α7 nicotinic receptor gene and P50 sensory gating. *European Journal of Human Genetics, 21, 76-81*.

Gault, J., Hopkins, J., Berger, R., Drebing, C., Logel, J., Walton, C., Short, M., Vianzon, R., Olincy, A., Ross, R. G., Adler, L. E., Freedman, R., Leonard, S. (2003). Comparison of polymorphisms in the α7 nicotnic receptor gene and its partial duplication in schizophrenic and control subjects. *American Journal of Medical Genetics: Neuropsychiatric Genetics, 123B, 39-49*.

Gault, J., Logel, J., Drebing, C., Berger, R., Hopkins, J., Olincy, A. (1999). Mutation analysis of the_α7 nicotinic acetylcholine receptor gene and its partial duplication in schizophrenia patients. *American Jorunal of Human Genetics,* 65**,** A27.

Gault, J., Robinson, M., Berger, R., Drebing, C., Logel, J., Hopkins, J., Moore, T., Jacobs, S., Meriwether, J., Choi, M., Kim, E., Walton, K., Buiting, K., davis, A., Breese, C., Freedman, R., Leonard, S. (1998). Genomic organization and partial duplication of the human α7 neuronal nicotinic acetylcholine receptor gene (CHRNA7). *Genomics, 52, 173-185*.

Ghia, J. E., Blennerhassett, P., Kumar-Ondiveeran, H., Verdu, E. F., Collins, S. M. (2006). The vagus nerve: a tonic inhibitory influence associated with inflammatory bowel disease in a murine model. *Gastroenterology, 131 (4), 1122-1130*.

Ghia, J. E., Park, A. J., Blennerhassett, P., Khan, W. I., Collins, S. M. (2011). Adoptive transfer of macrophage from mice with depression-like behavior enhances susceptibility to colitis*. Inflammatory Bowel Disease, 17 (7), 1474-1489*.

Goehler, L. E., Gaykema, R., P. A., Hansen, M. K., Anderson, K., Maier, S. F., Watkins, L. R. (2000). Vagal immune-to-brain communication: a visceral chemosensory pathway. *Autonomic Neuroscience: Basic and Clinical, 85, 49-59.*

Guan, Z. Z., Nordberg, A., Mousavi, M., Rinne, J. O., Hellström-Lindahl, E. (2002). Selective changes in the levels of nicotinic acetylcholine receptor protein and of corresponding mRNA species in the brains of patients with Parkinson's disease. *Brain Research, 956 (2), 358-366*.

Hayden, M. S. and Ghosh, S. (2004). Signaling to NF-κB. *Genes and Development, 18, 2195-2224.*

Hebing, I., Mefford, H. C., Sharp, A. J., Guipponi, M., Fichera, M., Franke, A., Muhle, H., De Kovel, C., Barker, C., Von Spiczak, S., Kron, K. L., Steinich, I., Kleefu-Lie, A. A., Leu, C., Gaus, V., Schmitz, B., Klein, K. M., Reif, P. S., Rosenow, F., Weber, Y., Holger, L., Zimprich, F., Urak, L., Fuchs, K., Feucht, M., Genton, P., Thomas, P., Visscher, F., De Haan, G., Møller, R. S., Hjalgrim, H., Luciano, D., Witting, M., Nothnagel, M., Elger, C. E., Nürnberg, P., Romano, C., Malafosse, A., Koeleman, B. P. C., Lindhout, D., Stephani, U., Schreiber, S., Eichler, E. E., Sander, T. (2009). 15q13.3 microdeletions increase risk of idiopathic generalized epilepsy. *Nature Genetics, 41 (2), 160-162*.

Heeschen, C., Jang, J. J., Weis, M., Pathak, A., Kaji, S., Hu, R. S., Tsao, P. S., Johnson, F. L., Cooke, J. P. (2001). Nicotine stimulates angiogenesis and promotes tumour growth and atherosclerosis. *Nature Medicine, 7 (7), 833-839*.

Hong, C. J., Lai, I. C., Liou, L. L., Tsai, S. J. (2004). Association study of the human partially duplicated α7 nicotinic acetylcholine receptor generic variant with bipolar disorder. *Neuroscience Letters, 355, 69-72*.

Huston, J. M., Ochani, M., Rosas-Ballina, M., Liao, H., Ochani, K., Pavlov, V. A., Gallowitsch-Puerta, M., Ashok, M., Czura, C. J., Foxwell, B., Tracey, K. J., Ulloa, L. (2006). *The Journal of Experimental Medicine, 203 (7), 1623-1628.*

Huston, J. M., Wang, H., Ochani, M., Ochani, K., Rosas-Ballina, M., Gollowitsch-puerta, M., Ashok, M., Yang, L., Tracey, K. J., Yang, H. (2008). Splenoctomy protects against sepsis lethality and reduces serum HMGB1 levels. *Journal of Immunology, 181 (5), 3535-3539*.

Hwang, J., Hwang, H., Lee, H. W., Suk, K. (2010). Microglia signaling as a target of Donepezil. *Neuropharmacology, 58 (7), 1122-1129*.

Ishikawa, M., Hashimoto, K. (2010). The role of sigma-1 receptors in the pathophysiology of neuropsychiatric diseases. *Journal of Receptor, Ligand and Channel Research, 3, 25-36*.

Kang, S. M., Tran, A. C., Grilli, M., Leonardo, M.J. (1992). NF-kappaB subunit regulation in non-transformed CD+T lymphocytes. *Science, 256, 1452-1456*.

Karlin, A. (2002). Emerging structure of the nicotinic acetylcholine receptors. *Nature, 3, 102-114*.

Kees, M. G., Pongratz, G., Kees, F., Schölmerich, J., Straub, R. H. (2003). Via β-adrenoceptors, stimulation of extra-splenic sympathetic nerve fibers inhibits lipopolysaccharide-induced TNF secretion in perfused rat spleen. *Journal of Neuroimmunology, 145, 77-85*.

Kunii, Y., Zhang, W., Xu, Q., Hyde, T. M., McFadden, W., Shin, J. H., Deep-Soboslay, A., Ye, T., Li, C., Kleinman, J. E., Wang, K. H., Lipska, B. K. (2015). CHRNA7 and CHRFAM7A mRNAs: co-localized and their expression levels altered in the post-mortem dorsolateral prefrontal cortex in major psychiatric disorders. *American Journal of Psychiatry, 172 (11), 1122-1130*.

LaSalle, J. M., Yasui, D. H. (2009). Evolving role of MeCP2 in Rett syndrome and autism. *Epigenomics, 1 (1), 119-130*.

Lawrence, T., Fong, C. (2010). The resolution of inflammation: anti-inflammatory roles for NF-κB. *The International Journal of Biochemistry and Cell Biology, 42, 519-523.*

Leonard, S., Breese, C., Adams, C., Benhammou, K., Gault, J., Stevens, K., Lee, M., Adler, L., Olincy, A., Ross, R., Freedman, R. (2000). Smoking and schizophrenia: abnormal nicotinic receptor expression. *European Journal of Pharmacology, 393 (1-3), 237-242*.

Leonard, S., Gault, J., Hopkins, J., Logel, J., Vianzon, R., Short, M., Drebing, C., Berger, R., Venn, D., Sirota, P., Zerbe, G., Olincy, A., Ross, R. G., Adler, L. E., Freedman, R. (2002). Association of promoter variants in the alpha7 nicotinic acetylcholine receptor subunit

gene with an inhibitory deficit found in schizophrenia. *Archives of General Psychiatry, 59 (12), 1085-1096*.

Levine, M., Manley, J. L. (1989). Transcriptional repression of eukaryotic promoters. *Cell, 59 (3), 405-408*.

Libermann, T. A., Baltimore, D. (1990). Activation of Interleukin-6 gene expression through the NF-κB transcription factor. *Molecular and Cellular Biology, 10 (5), 2327-2334*.

Lindstrom, J. (1997). Nicotinic acetylcholine receptors in health and disease. *Molecular Neurobiology, 15 (2), 193-222.*

Liu, F., Li, Y., Jiang, R., Nie, C., Zeng, Z., Zhao, N., Huang, C., Shao, Q., Ding, C., Qing, C., Xia, L., Qian, K. (2015). miR-132 inhbits lipopolysaccharide-induced inflammation in alveolar macrophages by the cholinergic anti-inflammatory pathway. *Experiments in Lung Research, 41 (5), 261-269*.

Lu, Y., Yeh, W., Ohashi, P.S. (2008). LPS/TLR4 signal transduction pathway. *Citokines, 42, 145-151.*

Manchia, M., Viggiano, E., Tiwari, A. K., Renou, J., Jain, U., De Luca, V., Kennedy, J. L. (2010). Smoking in adult attention-deficit/hyperactivity disorder: interaction between 15q13 nicotinic genes and Temperament Character Inventory scores. *World Journal of Biological Psychiatry, 11 (2), 506-510*.

Marrero, M. B., Bencherif, M. (2009). Convergence of alpha 7 nicotinic acetylcholine receptor-activated pathways for anti-apoptosis and anti-inflammation: central role for JAK2 activation of STAT3 and NF-kappaB. *Brain Research, 1256, 1-7*.

Marrero, M. B., Lucas, R., Salet, C., Hauser, T. A., Mazurov, A., Lippiello, P. M., Bencherif, M. (2010), An α7 nicotnic acetylcholine receptor-selective agonist reduces weight gain and metabolic changes in a mouse model of diabetes. *Journal of Pharmacological Experimental Therapies, 332 (1), 173-180*.

Marrero, M. B., Papke, R. L., Bhatti, B. S., Shaw, S., Bencherif, M. (2004). The neuroprotective effect of 2-(3-pyridyl)-1-azahicyclo[3.2.2]-nonane (TC-1698), a novel α7 ligand, is prevented through angiotensin II activation of a tyrosine phosphatase. *Journal of Pharmacological Experimental Therapeutics, 309, 16-27.*

Maskrey, B. H., Megson, I. L., Whitfield, P. D., Rossi, A. G. (2010). Mechanisms of resolution of inflammation: a focus on cardiovascular diseases. *Atherosclerosis Thrombosis Vascular Biology in Focus Inflammation, 31, 1001-1006.*

Mazza, J., Rossi, A., Weinberg, J. M. (2010). Innovative uses of tumor necrosis factor alpha inhibitors. *Dermatological Clinics, 28 (3), 559-575*.

McKhan, G., Drachman, D., Folstein, M., Katzman, R., Price, D., Stadlan, E. M. (1984). Clinical diagnosis of Alzheimer's disease. *Neurology, 34 (7), 939-944*.

Medzhitov, R., (2008). Origin and physiological roles of inflammation. *Nature, 454 (7203), 427-435*.

Melchior, L., Bertelesen, B., Debes, N. M., Groth, C., Skov, L., Mikkelsen, J. D., Brøndum-Nielsen, K., Tümer, Z. (2013). Microduplication of the 15q13.3 and Xq21.31 in a family with Tourette syndorme and comorbidities. *American Journal of Medical Genetics: Neuropsychiatric Genetics, 162B (8), 825-831*.

Millar, N. S. (2008). RIC-3: a nicotinic acetylcholine receptor chaperone. *British Journal of Pharmacology, 153, 177-183*.

Mishra, N. C., Rir-sisma-ah, J., Boyd, R. T., Singh, S. P., Gundavarapu, S., Langley, R. J., Razani-Boroujerdi, S., Sopori, M. L. (2010). Nicotine inhibits Fcε RI-induced cysteinyl leukotrienes and cytokine production without affecting mast cell degranulation through α7/α9/α10- nicotinic receptors. *Journal of Immunology, 185 (1), 588-596*.

Morens, D. M., Grandinetti, A., Reed, D., White, L. R., Ross, G. W. (1995). Cigarette smoking and protection from Parkinson's disease: false association or etiological clue? *Neurology, 45 (6), 1041-1051*.

Moretti, M., Zoli, M., George, A. A., Lukas, R. J., Pistillo, F., Maskos, U., Witheaker, P., Gotti, C. (2014). The novel α7β2-nicotinic acetylcholine subtype is expressed in human and mouse basal forebrain: biochemical and pharmacological characterization. *Molecular Pharmacology, 86, 306-317.*

O'Shea, J. M., Perkins, N. D. (2010). Thr435 phosphorylation regulates RelA (p65) NF-κB subunit transactivation, *Biochemical Journal, 426, 345-354.*

Olincy, A., Young, D. A., Freedman, R. (1997). Increased levels of the nicotine metabolite cotinine in schizophrenic smokers compared to others smokers. *Biological Psychiatry, 42 (1), 1-5*.

Olofosson, P., Rosas-Ballina, M., Levine, Y. A., Tracey, K. J. (2012). rethinking inflammation: neural circuits in the regulation of immunity. *Immunological Review, 248 (1), 188-204*.

Ortega-Gómez, A., Peretti, M., Soehnlein, O. (2012). Resolution of inflammation: an integrated review. *EMBO Journal Molecular Medicine, 5, 661-674.*

Patterson, P. H. (2009). Immune involvement in schizophrenia and autism: etiology, pathology and animal models. *Behavioral Brain Research, 204 (2), 313-321*.

Pavlov, V. A., Tracey, K. J. (2004). Neural regulators of innate immune response and inflammation. *Cellular and Molecular Life Science, 61, 2322-2331.*

Pavlov, V. A., Wang, H., Czura, C. J., Friedman, S. G., Tracey, K. J. (2003). The cholinergic anti-inflammatory pathway: a missing link in neuroimmunomodulation. *Molecular Medicine, 9 (5-8), 125-134*.

Pereira, S. G., Oakley, F (2008). Nuclear factor kappaB1: regulation and function. *The internal journal of biochemistry and cell biology, 40, 1425-1430.*

Pettit, D. L., Shao, Z., Yakel, J. L. (2001). Beta-Amyloid (1-42) peptide directly modulates nicotinic receptors in the rat hippocampal slice. *Journal of Neuroscience, 21 (1), RC120*.

Pohanka, M. (2014). Inhibitors of Acetylcholinesterase and Butyrylcholinesterase meet immunity. *International Journal of Molecular Science, 15 (6), 9809-9825*.

Ramos, F. M., Delgado-Velez, M., Ortiz, A. L., Baez-Pagan, C. A., Quesada, O., Lasalde-Dominicci, J. A. (2016). Expression of CHRFAM7A and CHRNA7 in neuronal cells and post-mortem brain of HIV-infected patients: consideration for HIV-associated neurocognitive disorder. *Journal of Neurovirology, 22 (3), 327-335*.

Raux, G., Bonnet-Brilhault, F., Louchart, S., Houy, E., Gantier, R., Levillain, D., Allio, G., Haouzier, S., Petit, M., Martinez, M., Frebourg, T., Thibaut, F., Campion, D. (2002). The 2-base pair deletion in exon 6 of the α-7-like nicotinic receptor subunit gene is a risk factor for the P50 sensory gating deficit. *Molecular Psychiatry, 7, 1006-1011*.

Reale, M., Iarlori, C., Gambi, F., Feliciani, C., Isabella, L., Gambi, D. (2006). The acetylcholinesterase inhibitor, Donepezil, regulates a Th2 bias in Alzheimer's disease patients. *Neuropharmacology, 50 (5), 606-613*.

Riley, B., Williamson, M., Collier, D., Wilkie, H., Makoff, A. (2002). A 3-Mb map of a large segmental duplication overlapping the α7-nicotinic acetylcholine receptor gene (CHRNA7) at human 15q13-q14. *Genomics, 79 (2), 197-209*.

Rosas-Ballina, M., Ochani, M., Parrish, W. R., Ochani, K., Harris, Y. T., Huston, J. M., Chavan, S., Tracey, K. J. (2008). Splenic nerve is required for cholinergic anti-inflammatory pathway control of TNF in endotoxemia. *PNAS, 105 (31), 11008-11013*.

Rosas-Ballina, M., Olofosson, P. S., Ochani, M., Valdès-Ferrer, S. I., Levine, Y. A., Reardon, C., Tusche, M. W., Pavlov, V. A., Andersson, U., Chavan, S., Mak, T. M., Tracey, K. J. (2011). Acetylcholine-synthesizing T cells relay neural signals in a vagus nerve circuit. *Science, 334 (6052), 98-101*.

Rosas-Ballina, M., Tracey, K. J. (2009). Cholinergic control of inflammation, *Journal of Internal Medicine, 265 (6), 663-679*.

Rozycka, A., Dorszewska, J., Steinborn, B., Lianeri, M., Winczewska-Wiktor, A., Sniezawska, A., Wisniewska, K., Jagodzinski, P. P. (2013). Association study of the 2-bp deletion polymorphism in exon 6 of the CHRFAM7A gene with idiopathic generalized epilepsy. *DNA and Cell Biology, 32 (11), 640-647*.

Russo, P., Kisialiou, A., Moroni, R., Pinzi, G., Fini, M. (2015). Effect of genetic polymorphisms (SNPs) in CHRNA7 gene in response to acetylcholinestearse inhbitors (AchEI) in patients with Alzheimer's disease. *Current Drug Targets*.

Saeed, R. W., Varma, S., Peng-Nemeroff, T., Sherry, B., Balakhaneh, D., Huston, J., Tracey, K. J., Al-Abed, Y., Metz, C. N. (2005). Cholinergic stimulation blocks endothelial cell activation and leukocyte recruitment during inflammation. *Journal of Experimental Medicine, 201 (7), 1113-1123*.

Savill, J., Wyllie, A. H., Henson, J. E., Walport, M. J., Henson, P. M., Haslett, C. (1989). Macrophage Phagocytosis of aging neutrophils in inflammation: programmed cell death in the neutrophil leads to its recognition by macrophages*. Journal of Clinical Investigation, 83, 865-875*.

Serbina, N. V., Jia, T., Hohl, T. M. & Pamer, E. G. (2008). Monocyte-mediated defence against microbial pathogens. *Annual Review of Immunology 26, 421–452.*

Serhan, C. N., Savill, J. (2005). Resolution of inflammation: the beginning programs the end. *Nature Immunology, 6 (12), 1191-1197.*

Severance, E. G., Yolken, R. H. (2008). Novel α7 nicotinic receptor isoforms and deficient cholinergic transcription in schizophrenia. *Genes, Brain and Behaviour, 7, 37-45*.

Shaked, I., Meerson, A., Wolf, Y., Avni, R., Greenberg, D., Gilboa-Geffen, A., Soreq, H. (2009). MicroRNA-132 potentiates cholinergic anti-inflammatory signaling by targeting acetylcholinesterase. *Immunity, 31 (6), 965-973*.

Sharma, G., Vijayaraghavan, S. (2002). Nicotinic receptor signaling in nonexcitable cells. *Journal of Neurobiology, 53 (4), 524-534*.

Shaw, S., Bencherif, M., Marrero, M. B. (2002). Janus kinase 2, an early target of alpha7 nicotinic acetylcholine receptor-mediated neuroprotection against Abeta-(1-42) amyloid. *Journal of Biological Chemistry, 277 (47), 44920-44924*.

Shen, H., Kihara, T., Hongo, H., Wu, X., Kem, W. R., Shimohama, S., Akaike, A., Niidome, T., Sugimoto, H. (2010). Neuroprotection by donepezil against glutamate excitotoxicity involves stimulation of α7 nicotinic receptors and internalization of NMDA receptors. *British Journal of Pharmacology, 161, 127-139*.

Shi, C., Pamer, E. G. (2011). Monocyte recruitment during infection and inflammation. *Nature Reviews Immunology*, *11 (11), 762–774*.

Shimohama, S. (2009). Nicotinic receptor-mediated neuroprotection in neurodegenerative disease models. *Biological pharmacology Bullettin, 32 (3), 332-336*.

Shinawi, M., Schaaf, C. P., Bhatt, S. S., Xia, Z., Patel, A., Cheung, S. W., Lanpher, B., Nagl, S., Herding, H. S., Nevinny-Stickel, C., Immken, L. L., Patel, G. S., German, J. R., Beaudet, A. L., Stankiewicz, P. (2009). A small recurrent deletion within 15q13.3 is associated with a range of neurodevelopmental phenotypes. *Nature Genetics, 41 (12), 1269-1271*.

Sica, A., Mantovani, A. (2012). Macrophage plasticity and polarization: in vivo veritas, *Journal of Clinical Investigation, 122 (3), 787-795.*

Siednienko, J., Maratha, A., Yang, S., Mitkiewicz, M., Miggin, S. M., Moynagh, P. N. (2011). The NF-κB subunits RelB and c-Rel negatively regulates TLR3-mediated IFN-β production via induction of the transcriptional repressor protein YY1. *The Journal of Biological Chemistry, 286 (52), 44750-44763*.

Sinkus, M. L., Lee, M. J., Gaut, J., Logel, J., Short, M., Freedman, R., Christian, S. L., Lyon, J., Leonard, S. (2009). A 2-base pair deletion polymorphism in the partial duplication of the α7 nicotinic acetylcholine gene (CHRFAM7A) on chromosome 15q14 is associated with schizophrenia. *Brain research, 1291, 1-11*.

Smirnov, I., Belogurov, A. J., Friboulet, A., Masson, P., Gabibov, A., Renard, P. Y. (2013). Strategies for the selection of catalylic antibodies against organophosphorus nerve agents. *Chemical Biological Interaction, 203 (1), 196-201*.

Soler-Alfonso, C., Carvalho, C. M., Ge, J., Roney, E. K., Bader, P. I., Kolodziejska, K. E., Miller, R. M., Lupski, J. R., Stankiewicz, P., Cheung, S. W., Bi, W., Schaaf, C. P. (2014). CHRNA7 triplication associated with cognitive impairment and neuropsychiatric phenotypes in a three-generation pedigree. *European Journal of Human Genetics, 22 (9), 1071-1076*.

Solntseva, E., I., Kapai, N. A., Popova, O. V., Rogozin, P. D., Skrebitsky, V. G. (2014). The involvment of sigma-1 receptors in donepezil-induced rescue of hippocampal LTP impaired by beta-amyloid peptide. *Brain Research Bulletin, 106, 56-61*.

Stefan, M., Claiborn, K. C., Stasiek, E., Chai, J., Ohta, T., Longnecker, R., Greally, J. M., Nicholls, R. D. (2005). Genetic mapping of putative *Chrna7* and *Luzp2* neuronal transcriptional enhancer due to impact of a transgene-insertion and 6.8 Mb deletion in a mouse model of Prader-Willi and Angelman syndromes. *BMC Genomics, 6 (157), 1-16*.

Stefansson, H., Rujescu, D., Cichon, S., Pietilainen, O.P.H., Ingason, A., Steinberg, S., Fossdal, R., Sigurdsson, E., Sigmundsson, T., Buizer-Voskamp, J.E., Hansen, T., Jakobsen, K.D., Muglia, P., Francks, C., Matthews, P.M., Gylfason, A., Halldorsson, B.V., Gudbjartsson, D., Thorgeirsson, T.E., Sigurdsson, A., Jonasdottir, A., Bjornsson, A., Mattiasdottir, S., Blondal, T., Haraldsson, M., Magnusdottir, B.B., Giegling, I., Moller, H.J., Hartmann, A., Shianna, K.V., Ge, D.L., Need, A.C., Crombie, C., Fraser, G., Walker, N., Lonnqvist, J., Suvisaari, J., Tuulio-Henriksson, A., Paunio, T., Toulopoulou, T., Bramon, E., Di Forti, M., Murray, R., Ruggeri, M., Vassos, E., Tosato, S., Walshe, M., Li, T., Vasilescu, C., Muhleisen, T.W., Wang, A.G., Ullum, H., Djurovic, S., Melle, I., Olesen, J., Kiemeney, L.A., Franke, B., Sabatti, C., Freimer, N.B., Gulcher, J.R., Thorsteinsdottir, U., Kong, A., Andreassen, O.A., Ophoff, R.A., Georgi, A., Rietschel, M., Werge, T., Petursson, H., Goldstein, D.B., Nothen, M.M., Peltonen, L., Collier, D.A., St Clair, D., Stefansson, K. (2008). Large recurrent microdeletions associated with schizophrenia. *Nature, 455, 232-236*.

Stephens, S. H., Logel, J., Barton, A., Franks, A., Schultz, J., Short, M., Dickenson, J., James, B., Fingerlin, T. E., Wagner, B., Hodgkinson, C., Graw, S., Ross, R. G., Freedman, R., Leonard, S. (2009). Association of the 5'-upstream regulatory region of the alpha7

nicotnic acetylcholine receptor subunit gene (CHRNA7) with schizophrenia. *Schizophrenia Research, 109 (1-3), 102-112*.

Stone, J.L., O'Donovan, M.C., Gurling, H., Kirov, G.K., Blackwood, D.H.R., Corvin, A., Craddock, N.J., Gill, M., Hultman, C.M., Lichtenstein, P., McQuillin, A., Pato, C.N., Ruderfer, D.M., Owen, M.J., St Clair, D., Sullivan, P.F., Sklar, P., Purcell, S.M., The International Schizophrenia Consortium (2008). Rare chromosomal deletions and duplications increase risk of schizophrenia. *Nature, 455 (7210), 237-241*.

Sun, S. (2011). Non-canonical NF-κB signailing pathway. *Cell research, 21 (1), 71-85.*

Sun, Y., Li, Q., Gui, H., Xu, D., Yang, Y., Su, D., Liu, X. (2013). MicroRNA-124 mediates the cholinergic anti-inflammatory action through inhbiting the production of pro-inflammatory cytokines*. Cell Research, 23, 1270-1283*.

Swaminathan, S., Shen, L., Kim, S., Inlow, M., West, J. D., Faber, K. M., Foroud, T., Mayeux, R., Saykin, A. J. (2012). Analysis of Copy Number Variation in Alzheimer's disease: the NIA-LOAD/NCRAD family study. *Current Alzheimer Research, 1 (9), 801-814*.

Szafranski, P., Schaaf, C. P., Person, R. E., Gibson, I. B., Xia, Z., Mahadevan, S., Wiszniewska, J., Bacino, C. A., Lalani, S., Potocki, L., Kang, S. H., Patel, A., Cjeung, S., W., Probst, F. J., Graham, B. H., Shinawi, M., Beaudet, A. L., Stankiewicz, P. (2010). Structures and molecular mechanisms for common 15q13.3 micorduplications involving CHRNA7: benign or pathological? *Human Mutations, 31 (7), 840-850*.

Tabet, N. (2006) Acetylcholinesterase inhibitors for Alzheimer's disease: anti-inflammatories in acetylcholine clothing! *Age and Ageing, 35 (6), 336-338*.

Takahashi, H. K., Iwagaki, H., Hamano, R., Yoshino, T., tanaka, N., Nishibori, M. (2006). Effect of nicotine on IL-8-initiated immune response in human monocytes. *Journal of leukocytes Biology, 80 (6), 1388-1394.*

Takata-Takatori, Y., Kume, T., Ohgi, Y., Izumi, Y., Niidome, T., Fujii, T., Sugimoto, H., Akaike, A. (2008). Mechanisms of neuroprotection by donepezil pre-treatment in rat cortical neurons chronically treated with donepezil. *Journal of Neuroscience Research, 86 (16), 3575-3583.*

Tanga, F., Nutile-MacMenemi, N., De-leo, J. A. (2005). The CNS role of Toll Like Receptor 4 in innate neuroimmunity and painful neuropathy. *PNAS, 102 (16), 5856-5861*.

Taylor, P. (1998). Development of acetylcholinesterase inhibitors in the therapy of Alzheimer's disease. *Neurology, 51, S30-S35*.

The, F. O., Boeckxstaens, G. E., Snoek, S. A., Cash, J. L., Bennink, R., Larosa, G. J., Van den Wijngaard, R. M., Greaves, D. R., De Jonge, W. J. (2007). Activation of the cholinergic anti-inflammatory pathway ameliorates postoperative ileus in mice. *Gastroenterology, 133, 1219-1228*.

Thullbery, M. D., Cox, H. D., Schule, T., Thompson, C. M., George, K. M. (2005). Differential localization of acetylcholinesterase in neuronal and non-neuronal cells. *Journal of Cellular Biochemistry, 96 (3), 599-610*.

Tracey, K. J. (2002). The inflammatory reflex. *Nature, 420, 853-859*.

Turner, M. D., Nedjai, B., Hurst, T., Pennington, D. J. (2014). Cytokines and chemokines: At the crossroads of cell signalling and inflammatory disease. *Biochimica and Biophisica Acta - Molecular Cell Research*, *1843 (11), 2563–2582.*

Ulloa, L. (2005). The vagus nerve and the nicotinic anti-inflammatory pathway. *Nature Drug Discovery, 4, 673-684.*

Ulloa, L. (2013). The cholinergic anti-inflammatory pathway meetsmicroRNA. *Cell Research, 23, 1249-1250*.

Van Maanen, M. A., Lebre, M. C., Van der Poll, T., LaRosa, G. J., Elbaum, D., Vervoordeldonk, M. J., Tak, P.P. (2009). Stimulation of nicotnic acetylcholine receptors attenuates collagen-induced arthritis in mice. *Arthritis and rheumatism, 60 (1), 114-122*.

Van Westerloo, D. J. (2010). The vagal immune reflex: a blessing from above. *Wiener medizinische Wochenschrift, 160 (5-6), 112-117.*

Van Westerloo, D. J., Giebelen, I. A., Florquin, S., Bruno, M. J., Larosa, G. J., Ulloa, L., Tracey K. J., Van der Poll, T. (2006). The vagus nerve and nicotinic receptors modulate experimental pancreatitis severity in mice. *Gastoenterology, 130, 1822-1830*.

Vida, G., Peña, G., Deitch, E. A., Ulloa, L. (2011). α7-cholinergic receptor mediates vagal induction of splenic norepinephrine. *Journal of Immunology, 186 (7), 4340-4346*.

Villiger, Y., Szanto, I., jaconi, S., blanchet, C., Buisson, B., Krause, K. H., Bertrand, D., Romand, J. A. (2002). Expression of an α7 duplicate nicotinic acetylcholine receptor-related protein in human leukocytes. *Journal of Neuroimmunology, 126, 86-98*.

Wang, H. Y., Lee, D. H., D'Andrea, M. R., Peterson, P. A., Shank, R. P., Reitz, A. B. (2000). Beta-Amyloid (1-42) binds to the alpha7 nicotinic acetylcholine receptor with high affinity. Implications for Alzheimer's disease pathology. *Journal of Biological Chemistry, 275 (8), 5626-5632*.

Wang, H., Liao, H., Ochani, M., Justiniani, M., Lin, X., Yang, L., Al-Abed, Y., Wang, H., Metz, C., Miller, E., tracey, K. J., Ulloa, L. (2004). Cholinergic agonists inhibit HMGB1 release and improve survival in experimental sepsis. *Nature Medicine, 10 (11), 1216-1221*.

Wang, H., Yu, M., Ochani, M., Amella, C. A., Tanovic, M., Susarla, S., Li, J., Wang, H., Yang, H., Ulloa, L., Al-Abed, Y., Czura, C. K., Tracey, K. J. (2003). Nicotinic acetylcholine receptor α7 subunit is an essential regulator of inflammation. *Nature, 421, 384-388*.

Wang, Y., Xiao, C., Indersmitten, T., Freedman, R., Leonard, S., Lester, H. A. (2014). The duplicated α7 subunits assemble and form functional nicotinic receptors with the full-length α7. *The Journal of Biological Chemistry, 298 (38), 26451-46463*.

Wessels, J., Baer, M., Young, H., Claudio, E., Brown, K., Siebenlist, U., Johnson, P. F. (2004). BCL-3 and NF-κB p50 attenuate Lipopolysaccharide-induced inflammatory response in macrophages. *The Journal of Biological Chemistry, 279 (48), 49995-50003.*

Wevers, A., Burghaus, L., Moser, N., Witter, B., Ortrud K., Steinlein, B., Schutz, U., Achnitz, B., Krempel U., Nowacki S., Pilz, K., Stoodt, J., Lindstrom, J., De Vos, R. A. I., Steur, E., Shroder, R. H. (2000). Expression of nicotinic acetylcholine receptors in Alzheimer's disease: postmortem investigations and experimental approaches. *Behavioral Brain Research, 113, 207-215*.

Wilens, T. E., Decker, M. W. (2007). Neuronal Nicotinic receptor agonists for the treatment of attention-deficit/hyperactivity disorder: focus on cognition. *Biochemical Pharmacology, 74 (8), 1212-1223*.

Yamamoto, M., sato, S., Hemmi, H., Hoshino, K., Kaisho, T., Sanjo, H., Takeuchi., O., Sugiyama, M., Okabe, M., Takeda, K., Akira, S. (2003). Role of the adaptor TRIF in the Myd-88-independent Toll-Like receptor signaling pathway. *Science, 301, 640-643*.

Yasui, D. H., Scoles, H. A., Horike, S., Meguro-Horike, M., Dunaway, K. W., Schroeder, D. I., LaSalle, J. (2011). 15q11.2-13.3 chromatin analysis reveals epigenetic regulation of CHRNA7 with deficiencies in Rett and autism brain. *Human Molecular Genetics, 20 (22), 4311-4323*.

Yoshikawa, H., Kurokawa, M., Ozaki, N., Nara, K., Atou, K., Takada, E., Kamochi, H., Suzuki, N. (2006). Nicotine inhibits the production of pro-inflammatory mediators in human monocytes by suppression of I-kappaB phosphorylation and nuclear-factor-kappaB transcriptional activity through nicotinic acetylcholine receptor alpha7. *Clinical Experimental Immunology, 146 (1), 116-123*.

Zhong, H., May, J., Jimi, E., Ghosh, S. (2002). The phosphorylation status of nuclear NF-kappa B determines its association with CBP/p300 or HDAC1. *Molecular cell, 9, 625-636.*

Zhong, H., Voll, R. E., Ghosh, S., (1998). Phosphorylation of NF-κB p65 by PKA stimulates transcriptional activity by promoting a novel bivalent interaction with the coactivator CBP/p300. *Molecular Cell, 1, 661-671.*